

Université de Montréal

**Novel Non Phospholipid Liposomes with High Sterol Content:  
Development and Characterization**

par  
Zhongkai Cui

Département de chimie  
Faculté des Arts et des Sciences

Thèse présentée à la Faculté des Études supérieures  
en vue de l'obtention du grade de Philosophiae Doctor (Ph. D.)  
en chimie

Octobre 2012

© Zhongkai Cui, 2012

Université de Montréal  
Faculté des études supérieures et postdoctorales

Cette thèse intitulée:

**Novel Non Phospholipid Liposomes with High Sterol Content:  
Development and Characterization**

Présentée par:  
Zhongkai Cui

a été évaluée par un jury composé des personnes suivantes:

Françoise Winnik, présidente-rapporteuse  
Michel Lafleur, directeur de recherche  
Antonella Badia, membre du jury  
Gonzalo Cosa, examinateur externe  
David Morse, représentant du doyen de la FAS

## Résumé

Les liposomes sont des nanovecteurs polyvalents et prometteurs quant à leur utilisation dans plusieurs domaines. Il y a une décennie, un nouveau type de liposome constitué d'amphiphiles monoalkylés et de stérols est né fortuitement dans notre groupe. Ils sont nommés Stérosomes puisqu'ils contiennent une grande proportion de stérols, entre 50 et 70 mol %. Les objectifs de cette thèse sont de développer de nouvelles formulations de Stérosomes ayant des caractéristiques spécifiques et d'acquérir une compréhension plus profonde des règles physicochimiques qui dictent leur comportement de phase. Nous avons spécifiquement examiné le rôle de motifs moléculaires des stérols, de la charge interfaciale et de la capacité à former des liaisons H dans les interactions intermoléculaires menant à l'autoassemblage. Le comportement de phase a été caractérisé par calorimétrie différentielle à balayage (DSC), par spectroscopie infrarouge (IR) et par spectroscopie de résonance magnétique nucléaire du deutérium ( $^2\text{H}$  NMR).

Premièrement, nous avons établi certaines corrélations entre la structure des stérols, leur tendance à former des bicouches fluides en présence d'amphiphile monoalkylé et la perméabilité des grandes vésicules unilamellaires (LUV) formées. La nature des stérols module les propriétés de mélange avec de l'acide palmitique (PA). Les stérols portant une chaîne volumineuse en position C17 sont moins aptes à induire des bicouches fluides que ceux qui ont une chaîne plus simple, comme celle du cholestérol. Un grand ordre de la chaîne alkyle de PA est un effet commun à tous les stérols investigués. Il a été démontré que la perméabilité des LUV peut être contrôlée en utilisant des stérols différents. Cependant, ces stérols n'ont aucun impact significatif sur la sensibilité des Stérosomes au pH. Afin de créer des liposomes qui sont sensibles au pH et qui ont une charge positive à la surface, des Stérosomes composés de stéarylamine et de cholestérol (Chol) ont été conçus et caractérisés. Il a été conclu que l'état de protonation de l'amine, dans ce travail, ou du groupe carboxylique, dans un travail précédent, confère une sensibilité au pH et détermine la charge à la surface du liposome.

Les premiers Stérosomes complètement neutres ont été fabriqués en utilisant un réseau de fortes liaisons H intermoléculaires. Le groupe sulfoxyde est capable de former de fortes liaisons H avec le cholestérol et les molécules d'eau. Une bicouche fluide métastable a été obtenue, à la température de la pièce, à partir d'un mélange équimolaire d'octadécyl méthyl sulfoxyde (OMSO) et de Chol. Ce comportement distinct a permis d'extruder le mélange pour former des LUV à la température de la pièce. Après 30 h, le temps de vie de la phase métastable, des Stérosomes stables et imperméables existaient toujours sous une forme solide. Un diagramme de température-composition a été proposé afin de résumer le comportement de phase des mélanges d'OMSO/Chol.

Finalement, nous avons élaboré des Stérosomes furtifs en incorporant du polyéthylène glycol (PEG) avec une ancre de cholestérol (PEG-Chol) à l'interface de Stérosomes de PA/Chol. Jusqu'à 20 mol % de PEG-Chol peut être introduit sans perturber la structure de la bicouche. La présence du PEG-Chol n'a aucun impact significatif sur la perméabilité de la LUV. L'encapsulation active de la doxorubicine, un médicament contre le cancer, a été réalisée malgré la faible perméabilité de ces LUV et la présence du PEG à l'interface. L'inclusion de PEG a modifié considérablement les propriétés de l'interface et a diminué la libération induite par la variation de pH observée avec des LUV nues de PA/Chol. Cette formulation inédite est potentiellement utile pour l'administration intraveineuse de médicaments.

**Mots-clés:** liposomes, membranes, phase liquide ordonnée, amphiphiles monoalkylés, stérols, cholestérol PEGylé, libération passive, libération contrôlée, encapsulation active, NMR, fluorescence, IR, DSC.

## Abstract

Liposomes are promising and versatile nanocarriers suitable for potential applications in many fields. A decade ago, a new type of liposomes formed from monoalkylated amphiphiles and sterols was born somehow fortuitously in our group. They are referred to as Sterosomes, because they contain a large proportion of sterols, between 50 and 70 mol %. The objectives of the present thesis are to develop novel Sterosome formulations with specific features, and to gain a deeper understanding of the physicochemical rules that dictate their phase behavior. We have specifically examined the role of the molecular features of sterols, of the interfacial charges and of the H-bond capacity in the intermolecular interactions leading to the self-assembly. The phase behavior was characterized by differential scanning calorimetry (DSC), infrared spectroscopy (IR), and nuclear magnetic resonance spectroscopy of deuterium ( $^2\text{H}$  NMR).

First, we have established some correlations between the structure of the sterols, the propensity to form fluid bilayers, and the permeability of the resulting large unilamellar vesicles (LUVs). The nature of the sterol modulates the properties of the mixture with palmitic acid (PA). Sterols bearing a bulky tail chain at C17 are less capable to induce fluid bilayers than those with a non-bulky tail chain, like that of cholesterol. A large ordering of the alkyl chain of PA is an effect exhibited by all of the investigated sterols. It is shown that the permeability of the LUVs can be controlled using different sterols. However, these sterols have no significant impact on the pH-sensitivity of Sterosomes. In order to create liposomes that are pH-sensitive and that have a positive surface charge, Sterosomes composed of stearylamine and cholesterol (Chol) were designed and characterized. It is concluded that the protonation/deprotonation state of the amine (in this work) and carboxylic acid (in previous work) groups confers the pH-sensitivity and determines the surface charge of the liposomes.

The first completely neutral Sterosomes were crafted based on the creation of strong intermolecular hydrogen bond networks. The sulfoxide group was capable of forming strong hydrogen bonds with cholesterol and water molecules. In an equimolar octadecyl methyl sulfoxide (OMSO)/Chol mixture, a metastable fluid bilayer was obtained at room temperature. This distinct phase behavior allowed extruding the mixtures to form LUVs at room temperature. After 30 h, the life-time of the metastable phase, stable and impermeable Sterosomes still existed in the solid form. A temperature–composition diagram was proposed to summarize the phase behavior of OMSO/Chol mixtures.

Finally, a further step was made to prepare “stealth” Sterosomes by incorporating polyethylene glycol (PEG) with a cholesterol anchor (PEG-Chol) at the interface of PA/Chol Sterosomes. Up to 20 mol % PEG-Chol can be introduced without disturbing the bilayer structure. The presence of PEG-Chol had no significant impact on the permeability of the resulting LUVs. Active-loading of an anti-cancer drug, doxorubicin, can be achieved despite the low permeability of these LUVs and the presence of the PEG at the interface. The inclusion of PEG modified considerably the interface properties and decreased significantly the pH-triggered release observed with naked PA/Chol LUVs. This novel formulation is potentially useful for the application of intravenous administration in the drug delivery field.

**Keywords:** liposomes, membranes, liquid-ordered phase, monoalkylated amphiphiles, sterols, PEGylated cholesterol, passive release, controlled release, active loading, NMR, fluorescence, IR, DSC.

# Table of Content

|   |      |
|---|------|
| Résumé.....                             | I    |
| Abstract.....                           | III  |
| List of tables.....                     | IX   |
| List of figures.....                    | X    |
| List of abbreviations and symbols ..... | XIII |
| Acknowledgements.....                   | XVII |

## Chapter 1

|   |          |
|---|----------|
| <b>Introduction.....</b>  | <b>1</b> |
| 1.1 Background knowledge .....  | 2        |
| 1.2 Lamellar self-assemblies of monoalkylated amphiphiles and sterols and the derived liposomes: distinct composition and distinct properties ..... | 4        |
| 1.2.1 Introduction .....  | 5        |
| 1.2.2 Mixtures of monoalkylated amphiphiles and sterols forming bilayers .....  | 6        |
| 1.2.3 Prerequisites for fluid lamellar self-assemblies .....  | 13       |
| 1.2.4 Features of non phospholipid liposomes.....   | 23       |
| 1.2.5 Biological implications and applications of non phospholipid liposomes .....  | 28       |
| 1.2.6 Conclusion.....   | 31       |
| 1.3 Characterization methods in this thesis.....  | 32       |
| 1.3.1. IR spectroscopy .....  | 32       |
| 1.3.2. NMR .....  | 35       |
| 1.4 Description of the thesis sections .....  | 44       |
| 1.5 References .....  | 47       |

## Chapter 2

|   |           |
|---|-----------|
| <b>Influence of the Nature of the Sterol on the Behavior of Palmitic Acid/Sterol Mixtures and Their Derived Liposomes .....</b> | <b>59</b> |
| 2.1 Abstract .....  | 60        |
| 2.2 Introduction.....   | 61        |

|   |    |
|---|----|
| 2.3 Materials and methods .....             | 64 |
| 2.4 Results.....                            | 68 |
| 2.4.1. IR spectroscopy experiments .....    | 68 |
| 2.4.2. NMR experiments .....                | 73 |
| 2.4.3. PA/sterol LUVs .....                 | 78 |
| 2.4.4. Effect of pH on PA/sterol LUVs ..... | 80 |
| 2.5 Discussion .....                        | 82 |
| 2.6 Acknowledgements .....                  | 87 |
| 2.7 References .....                        | 88 |

### **Chapter 3**

#### **Formation of Fluid Lamellar Phase and Large Unilamellar Vesicles with Octadecyl Methyl Sulfoxide/Cholesterol Mixtures..... 93**

|  |     |
|--|-----|
| 3.1 Abstract .....                                       | 94  |
| 3.2 Introduction.....                                    | 95  |
| 3.3 Materials and methods .....                          | 98  |
| 3.3.1 DSC, <sup>2</sup> H NMR, and IR spectroscopy ..... | 99  |
| 3.3.2 Permeability measurements .....                    | 100 |
| 3.4 Results and discussion.....                          | 102 |
| 3.4.1 DSC experiments .....                              | 102 |
| 3.4.2 <sup>2</sup> H NMR experiments.....                | 104 |
| 3.4.3 IR spectroscopy experiments .....                  | 108 |
| 3.4.4 OMSO/Chol temperature–composition diagram .....    | 112 |
| 3.4.5 OMSO/Chol LUVs .....                               | 114 |
| 3.5 Concluding remarks.....                              | 119 |
| 3.6 Acknowledgements .....                               | 121 |
| 3.7 References .....                                     | 122 |

## Chapter 4

### **Formation of pH-Sensitive Cationic Liposomes From a Binary Mixture of Monoalkylated Primary Amine and Cholesterol..... 126**

|  |     |
|--|-----|
| 4.1 Abstract .....   | 127 |
| 4.2 Introduction.....  | 128 |
| 4.3 Materials and methods .....                                    | 130 |
| 4.4 Results and discussion.....                                    | 133 |
| 4.4.1 Thermal phase behavior of SA/Chol mixtures .....             | 133 |
| 4.4.2 Effect of pH on the phase behavior of SA/Chol mixtures ..... | 139 |
| 4.5 Acknowledgements .....   | 148 |
| 4.6 References .....   | 149 |

## Chapter 5

### **Introduction of Interfacial Cholesterol-Anchored Polyethylene Glycol in Sterol-Rich Non Phospholipid Liposomes..... 153**

|   |     |
|---|-----|
| 5.1 Abstract .....                                  | 154 |
| 5.2 Introduction.....                               | 155 |
| 5.3 Materials and methods .....                     | 160 |
| 5.3.1 Materials .....                               | 160 |
| 5.3.2 Mixture preparation.....                      | 161 |
| 5.3.3 <sup>2</sup> H NMR spectroscopy.....          | 161 |
| 5.3.4 <sup>1</sup> H NMR diffusion experiments..... | 162 |
| 5.3.5 LUVs characterization .....                   | 163 |
| 5.3.6 Permeability measurements .....               | 164 |
| 5.3.7 Active loading experiments.....               | 165 |
| 5.4 Results.....                                    | 166 |
| 5.4.1 Characterization of phase behaviors .....     | 166 |
| 5.4.2 Dynamic light scattering and cryo-TEM .....   | 171 |
| 5.4.3 PA/Chol/PEG-Chol LUV permeability .....       | 174 |
| 5.4.4 DOX active loading and release.....           | 175 |
| 5.5 Discussion .....                                | 177 |

|                            |     |
|----------------------------|-----|
| 5.6 Acknowledgements ..... | 182 |
| 5.7 References .....       | 183 |

## **Chapter 6**

|  |            |
|--|------------|
| <b>Conclusions and Future Perspectives .....</b> | <b>190</b> |
| 6.1 New Sterosome formulations .....             | 190        |
| 6.2 Novel discovery and developments.....        | 191        |
| 6.3 Suggestions for future work.....             | 193        |
| 6.4 References .....                             | 196        |

## List of tables

|  |     |
|--|-----|
| Table 1.1. Name and chemical structure of monoalkylated amphiphiles ( $R = C_nH_{2n+1}$ ).<br>.....                                    | 11  |
| Table 1.2. Name and chemical structure of different sterols. ....  | 12  |
| Table 2.1. Characteristics of extruded LUVs for various PA/sterol 3/7 (molar ratio)<br>mixtures. ....                                  | 79  |
| Table 3.1. $^2H$ NMR parameters associated with cholesterol in equimolar<br>OMSO/Chol- $d_5$ mixtures. ....                            | 107 |
| Table 3.2. Hydrodynamic diameter of LUVs $d_{LUVs}$ and initial self-quenching of<br>calcein for various OMSO/Chol LUVs at pH 7.4..... | 115 |
| Table 4.1. $^2H$ NMR parameters associated with cholesterol in equimolar SA/Chol- $d_5$<br>mixtures, at 45 °C.....                     | 138 |
| Table 4.2. Characteristics of extruded LUVs for equimolar SA/Chol mixtures at<br>various pH values <sup>a</sup> .....                  | 142 |
| Table 5.1. Hydrodynamic diameter of PA/Chol/PEG-Chol LUVs $d_{LUVs}$ at various pH<br>values. ....                                     | 172 |

## List of figures

|   |    |
|---|----|
| Figure 1.1. Temperature–composition diagram for PA/Chol system.....   | 8  |
| Figure 1.2. Schematic morphology of deprotonated palmitic acid and cholesterol molecules. ....  | 23 |
| Figure 1.3. Schematic representation of the acyl chain packing and of the in-phase and out-phase modes.....   | 35 |
| Figure 1.4. Different energy levels and resonance lines in solid state $^2\text{H}$ NMR spectroscopy.....   | 36 |
| Figure 1.5. Influence of the orientation of the C–D bond relative to the magnetic field on the quadrupolar interactions and the resulting powder pattern.....   | 38 |
| Figure 1.6. Definition of the angles ( $\theta$ , $\gamma$ , $\alpha$ ), $n$ is the bilayer normal, $a$ is the long (rotation) axis of the molecule and $B$ represents the magnetic field. ....   | 39 |
| Figure 1.7. Illustration of the shapes of $^2\text{H}$ NMR spectra associated with the corresponding phases.....  | 40 |
| Figure 1.8. Schematic representation of stimulated echo sequence. ....  | 44 |
| <br>  |    |
| Figure 2.1. Formula of various investigated sterols.....  | 64 |
| Figure 2.2. Thermotropism of PA- $d_{31}$ in PA- $d_{31}$ /sterol (3/7 molar ratio) mixtures at pH 7.4 and 8.4, probed using the $\nu_{\text{C-D}}$ band position. The sterol in the mixture was dihydrocholesterol, 7-dehydrocholesterol, stigmasterol, or ergosterol. | 70 |
| Figure 2.3. pH dependence of the $\nu_{\text{CO}}$ mode of the PA carboxylic/carboxylate group in PA/dihydrocholesterol mixture (3/7 molar ratio) at room temperature.....  | 71 |
| Figure 2.4. The $\text{CD}_2$ deformation band shape for various PA- $d_{31}$ /sterol mixtures (3/7 molar ratio, 30 °C). ....   | 72 |
| Figure 2.5. $^2\text{H}$ -NMR spectra of PA- $d_{31}$ /dihydrocholesterol mixture, pH 5.5 and 7.4; PA- $d_{31}$ /stigmasterol, pH 7.4 and 8.4 (PA- $d_{31}$ /Sterol 3/7 molar ratio).....   | 74 |
| Figure 2.6. Thermal evolution of the phase composition of the various PA- $d_{31}$ /sterol mixtures (molar ratio of 3/7).....   | 76 |

|  |     |
|--|-----|
| Figure 2.7. Orientational order profile of PA-d <sub>31</sub> alkyl chain, obtained from the lamellar fraction of PA-d <sub>31</sub> /Chol, PA-d <sub>31</sub> /dihydrocholesterol, PA-d <sub>31</sub> /7-dehydrocholesterol, PA-d <sub>31</sub> /stigmastanol, PA-d <sub>31</sub> /stigmasterol, and PA-d <sub>31</sub> /ergosterol mixtures. For all the mixtures, the PA-d <sub>31</sub> /sterol molar ratio was 3/7 and pH was 8.4. .... | 78  |
| Figure 2.8. Passive leakage at room temperature from PA/Chol, PA/dihydrocholesterol, PA/7-dehydrocholesterol, PA/stigmastanol, and PA/stigmasterol LUVs. For all the mixtures, the PA/sterol molar ratio was 3/7 and pH was 7.4. ....  | 80  |
| Figure 2.9. pH-triggered release of calcein from PA/Chol, PA/Dihydrocholesterol (○), and PA/Stigmastanol LUVs.....   | 81  |
| Figure 3.1. Chemical formula of OMSO and cholesterol.....  | 98  |
| Figure 3.2. Thermograms of pure OMSO and of OMSO/Chol mixtures with molar ratio of 7/3, 5/5, 3/7, and 1/9; pH 7.4.....   | 103 |
| Figure 3.3. <sup>2</sup> H NMR spectra of an equimolar OMSO/Chol- <i>d</i> <sub>5</sub> mixture, pH 7.4.....   | 105 |
| Figure 3.4. Kinetics of the crystallization of cholesterol in the metastable liquid ordered phase of an equimolar OMSO/Chol- <i>d</i> <sub>5</sub> mixture at 30 °C. ....  | 108 |
| Figure 3.5. Lipid thermotropism, reported by the ν <sub>C-H</sub> band position from IR spectra, of hydrated OMSO, and of OMSO/Chol mixtures with various composition: 1/9, 3/7, 5/5, and 7/3 (molar ratio), pH 7.4. ....  | 110 |
| Figure 3.6. Lipid thermotropism, reported by the ν <sub>C-H</sub> band position from IR spectra, of an equimolar OMSO/Chol mixture, pH 7.4. ....   | 111 |
| Figure 3.7. Proposed OMSO/Chol temperature–composition diagram.....  | 114 |
| Figure 3.8. Passive calcein leakage from LUVs prepared from an equimolar OMSO/Chol mixture, at pH 7.4 and room temperature. ....   | 116 |
| Figure 3.9. Effect of the external pH on the calcein release, for OMSO/Chol 5/5 and PA/Chol 3/7 LUVs.....  | 118 |
| Figure 4.1. Thermograms of hydrated pure SA and of SA/Chol mixtures of various molar ratios, pH 5.5. ....  | 134 |

|  |     |
|--|-----|
| Figure 4.2. Thermotropism, reported by the $\nu_{C-H}$ band position of the IR spectra, of hydrated SA, and of SA/Chol mixtures with various compositions: 1/9, 3/7, 5/5, 7/3, and 9/1 (molar ratio), pH 5.5. .... | 136 |
| Figure 4.3. $^2H$ NMR spectra of an equimolar SA/Chol- $d_5$ mixture. ....   | 138 |
| Figure 4.4. Thermograms of equimolar SA/Chol mixtures at various pH values. ...  | 139 |
| Figure 4.5. Thermotropism, reported by the $\nu_{C-H}$ band position of the IR spectra, of equimolar SA/Chol mixtures at pH 5.5, 7.5, 9.0, 11 and 12. ....   | 140 |
| Figure 4.6. Passive release of equimolar SA/Chol LUVs, at room temperature, pH 7.5. ....   | 143 |
| Figure 4.7. pH-triggered release of glucose from LUVs obtained from an equimolar SA/Chol mixture. ....   | 145 |
| <br>   |     |
| Figure 5.1. Chemical formula of PA, cholesterol and PEGylated cholesterol. ....  | 159 |
| Figure 5.2. $^2H$ NMR spectra of PA- $d_{31}$ /Chol/PEG-Chol mixtures, pH 8.4 and 5.0. ....  | 168 |
| Figure 5.3. Dependence of the proportion of isotropic phase on the PEG-Chol content in the PA- $d_{31}$ /Chol/PEG-Chol mixtures, at 25 °C and pH 8.4. The PA/sterol ratio remained 3/7. ....                       | 169 |
| Figure 5.4. Variation of the diffusion coefficient of PEG as a function of the PEG-Chol content in the PA- $d_{31}$ /Chol/PEG-Chol LUVs, at 25 °C and pH 8.4. The PA/sterol ratio remained 3/7. ....               | 171 |
| Figure 5.5. Cryo-micrographs of extruded PA/Chol/PEG-Chol LUVs in molar ratio of 30/66/04 pH 8.4/8.4 and pH 5.0/5.0 inside/outside, and in a molar ratio of 30/60/10 pH 8.4/8.4 and 5.0/5.0. ....                  | 173 |
| Figure 5.6. Passive leakage of entrapped calcein from PA/Chol/PEG-Chol 30/66/04 and 30/60/10 (molar ratio) LUVs, measured at room temperature, pH 8.4. ....  | 174 |
| Figure 5.7. Effect of the external pH on the calcein release from PA/Chol/PEG-Chol 30/70/00, 30/66/04 and 30/60/10 LUVs. ....  | 175 |
| Figure 5.8. Passive leakage of actively loaded doxorubicin in PA/Chol/PEG-Chol 30/60/10 (molar ratio) LUVs, measured at room temperature, pH 8.4. ....   | 176 |
| <br>   |     |
| Figure 6.1. Sterosome potential applications in different fields. ....   | 195 |

## List of abbreviations and symbols

|           |  |
|-----------|--|
| $A_Q$     | Static quadrupolar constant  |
| $B_0$     | Static magnetic field  |
| Calcein   | 2,2',2'',2'''-[(3',6'-Dihydroxy-3-oxo-3H-spiro[2-benzofuran-1,9'-xanthene]-2',7'-diyl)bis(methylenenitrilo)]tetraacetic acid |
| Chol      | Cholesterol  |
| CMC       | Critical micelle concentration   |
| $C_mEO_n$ | Polyoxethylene alkylethers   |
| CPC       | Cetylpyridium chloride   |
| CPP       | Critical packing parameter   |
| Cryo-TEM  | Cryogenic transmission electron microscopy   |
| CTAB      | Cetyltrimethylammonium bromide   |
| DeHChol   | 7-dehydrocholesterol   |
| DGL       | Diglyceryl monolaurate   |
| DHChol    | Dihydrocholesterol   |
| DMPC      | 1,2-dimyristoyl-sn-glycero-3-phosphocholine  |
| DOX       | Doxorubicin hydrochloride salt   |
| DSC       | Differential scanning calorimetry  |
| DSPE      | Distearoylphosphatidylethanolamine   |
| EDTA      | Ethylenediaminetetraacetic acid  |

|          |   |
|----------|---|
| EMA      | European Medicines Agency                             |
| ESterol  | Ergosterol  |
| <i>G</i> | Magnetic field gradient                               |
| GM1      | Monosialoganglioside                                  |
| GUVs     | Giant unilamellar vesicles                            |
| IR       | Infrared spectroscopy                                 |
| lo phase | Liquid-ordered phase                                  |
| LUVs     | Large unilamellar vesicles                            |
| lyso-PPC | Lysopalmitoylphosphatidylcholine                      |
| MES      | 2-[N-morpholino]ethanesulfonic acid                   |
| MLVs     | Multilamellar vesicles                                |
| MPS      | Mononuclear phagocyte system                          |
| NAE      | N-acylethanolamine                                    |
| NMR      | Nuclear magnetic resonance                            |
| OMSO     | Octadecyl methyl sulfoxide                            |
| PA       | Palmitic acid   |
| PEG-Chol | Hydroxypolyethyleneglycol cholesteryl ether           |
| POPC     | 1-palmitoyl-2-oleoyl-sn-glycero-3-phosphocholine      |
| POPE     | 1-palmitoyl-2-oleoyl-sn-glycero-3-phosphoethanolamine |
| SA       | Stearylamine  |

|                  |   |
|------------------|---|
| $S_{C-D}$        | Orientational order parameter                                 |
| Schol            | Cholesterol sulfate   |
| $S_{mol}$        | Molecular order parameter                                     |
| SStanol          | Stigmastanol  |
| SSterol          | Stigmasterol  |
| STE              | Stimulated echo   |
| SUVs             | Small unilamellar vesicles                                    |
| $T_1$            | Spin–lattice relaxation time                                  |
| $T_2$            | Spin–spin relaxation time                                     |
| TGL              | Tetraglycerol monolaurate                                     |
| $T_m$            | Melting temperature   |
| Tris             | Tris(hydroxymethyl)aminomethane                               |
| Triton X-100     | polyethylene glycol p-(1,1,3,3-tetramethylbutyl)-phenyl ether |
| Tween            | Polyoxyethylene sorbitan monooleate                           |
| ULVs             | Unilamellar vesicles  |
| 5-FU             | 5-Fluorouracil  |
| $\alpha(F)$ -PA  | $\alpha$ -fluoropalmitic acid                                 |
| $\alpha(OH)$ -PA | $\alpha$ -hydroxypalmitic acid                                |
| $\delta(CD_2)$   | C–D bond scissoring   |
| $\delta(CH_2)$   | C–H bond scissoring   |

|                    |                     |
|--------------------|---------------------|
| $\gamma$           | Gyromagnetic ratio  |
| $\nu_{\text{C-D}}$ | C–D bond stretching |
| $\nu_{\text{C-H}}$ | C–H bond stretching |
| $\omega$           | Larmor frequency    |

## Acknowledgements

First of all, I would like to thank my supervisor Prof. Michel Lafleur for all his support, his help, his availability, and valuable suggestions from the beginning to the end. I appreciate the time he spent on listening to me, and helping me in my projects. Also, I thank him for his kindness, care, patience and cheer for me everyday. I feel honored and fortunate to have had the opportunity to work with him for my Ph.D. His dedication to scientific research, his generous and benevolent mind, positive and optimistic attitude towards life inspire me on the road of science and my life.

I want to thank Prof. André Beauchamp, Ms. Céline Millette, and Ms. Lyne Laurin for their help. I would like to thank the NMR team, Minh Tan Phan Viet, Sylvie Bilodeau and especially Cédric Malveau for his help no matter what time it was. I also want to thank the material characterization and the analysis labs, Karine Venne, Sylvain Essiembre, Alexandra Furtos and Marie-Christine Tang. I am grateful to the members of electronic, glass and mechanical shops.

Special thanks to all group members, without each every single one of you, my life here wouldn't be that enjoyable and joyful. Also, I want to thank Prof. Reber and all members in his group for their open heart, encouragements and kindness. I would like to thank all my friends in Montréal; their help and support made my life here much easier and happier.

I would also like to thank China Scholarship Council and Université de Montréal for my scholarship over the whole Ph.D journey.

Last but not least, I would like to thank my beloved parents. Without their unconditional support and love behind me, it wouldn't be possible for me to accomplish my Ph.D study abroad.

# Chapter 1

## Introduction

Sterol-rich non phospholipid liposomes formed with monoalkylated amphiphiles and sterols were somehow fortuitously born in our group. Palmitic acid (PA) and cholesterol (Chol), in a molar ratio of 30/70, was the very first formulation found to form stable liquid-ordered (lo) phases once PA was unprotonated at high pH ( $\geq 7.5$ ).<sup>1</sup> PA/Chol liposomes displayed a limited permeability and were shown to be pH-sensitive.<sup>2</sup> Those properties make them potential and promising candidates as carriers in many fields, such as drug delivery. Because of their high sterol content, these liposomes were named Sterosomes.

This thesis aims to extend the understanding of the molecular prerequisites for the formation of the lo phase from mixtures of monoalkylated amphiphiles and sterols. The effect of different sterols was studied to establish some correlations between the structure of sterols, the propensity to form a fluid lamellar phase, and the permeability of the resulting large unilamellar vesicles (LUVs). As all the reported Sterosomes, at this point, bear at least one charge. We attempted to develop the first completely neutral formulation, a project that provided us with a deeper understanding related to the contribution of electrostatic interactions in the formation of these lamellar phases. In addition, we designed and created dual functionalized Sterosomes, namely, cationic and pH-sensitive. Finally, we explored the possibility of modifying the

interfacial properties of Sterosomes by grafting a hydrophilic polymer to make them more suitable as drug carriers for intravenous administration.

In this introduction, first we will start briefly with some background knowledge about liposomes. Second, the current state of knowledge associated with the lamellar phases formed from mixtures of monoalkylated amphiphiles and sterols is reviewed. The last part of this introduction focuses on a few techniques utilized in the present work for the characterization of the systems.

## **1.1 Background knowledge**

A nanocarrier is a vehicle of nanoscopic size ( $10^{-9}$  m) attaching, embedding or encapsulating active ingredients to protect them, and/or bring them to targeted sites. Organic and inorganic materials as well as their combinations lead to a rich variety of nanocarriers, such as nanoparticles,<sup>3-5</sup> polymeric micelles,<sup>4, 6</sup> dendrimers<sup>7-10</sup> and liposomes.<sup>11-14</sup> The morphology and physicochemical properties of nanocarriers are found to be very diverse, serving for different applications.

Liposomes are the main subject of this thesis, which will be focused in detail. Liposomes are formed by a single or several bilayers of self-assembled amphiphiles. These bilayers separate the external and the internal environments (both aqueous phases), while their core is hydrophobic. As a consequence, liposomes are able to encapsulate hydrophilic molecules in their entrapped aqueous compartment, and hydrophobic molecules inside their bilayers. Liposomes

can be used in many fields, such as cosmetics,<sup>15</sup> foods,<sup>16, 17</sup> textiles,<sup>18</sup> etc. As pharmaceutical carriers *in vivo*, liposomes evolved from the early classical formulations, via stealth and targeted liposomes, to smart liposomes.<sup>12-14</sup> After intravenous administration, the first physiological barrier to be overcome is the rapid clearance from the blood circulation by the MPS. In order to reach their final destination, liposomes must circulate long enough in the blood stream. Conventional liposomes have very short half-life time in the blood circulation, typically, minutes to a few hours.<sup>19</sup> In order to avoid rapid clearance from the blood stream, one idea is to modify the surface of these conventional liposomes to reduce the binding of opsonins. A steric repulsion can be created at the surface level by grafting flexible and hydrophilic polymers (e.g., PEG and polysaccharides).<sup>20, 21</sup> This polymer shell inhibits opsonization by preventing protein adsorption. Consequently, these "stealth" liposomes have long circulating time in the blood stream.<sup>20, 21</sup>

In the present work, freeze-and-thaw cycles and extrusions have been used to prepare large unilamellar vesicles (LUVs). Freeze-and-thaw cycles are a non-mechanical method leading to the formation of multilamellar vesicles. The extrusion is a mechanical process where the liposomal suspension passes through filters with pores of a well-defined size.

**1.2 Lamellar self-assemblies of monoalkylated amphiphiles and sterols and the derived liposomes: distinct composition and distinct properties**

Zhong-Kai Cui and Michel Lafleur

Ready to be submitted

### 1.2.1 Introduction

Bilayers made of phospholipids and sterols have been studied extensively.<sup>22-27</sup> These self-assemblies are models for eukaryote plasmic membranes, and several interesting findings inferred from these models have influenced our understanding of the physicochemical behavior of membranes, as well as of several biochemical cellular processes. Inspired from biological membranes, these thin, impermeable, and fluid bilayers also constitute valuable nanoscale elements that are useful for technological applications in several fields, including controlled release, targeting,<sup>20, 28, 29</sup> and biosensors.<sup>30, 31</sup> More recently, it has been shown that some mixtures of monoalkylated amphiphiles and sterols can self-assemble to form similar lamellar structures. Typically, monoalkylated amphiphiles or sterols do not form fluid lamellar phases once hydrated individually. Most of the monoalkylated amphiphiles form actually micelles in aqueous environments, while sterols display a very limited solubility. Therefore it was somehow unexpected to find out that, in certain conditions, mixtures of monoalkylated amphiphiles and sterols can form stable fluid bilayers. In the past decade, significant developments have been made, identifying several new systems leading to lamellar self-assemblies and bringing insights into the interactions leading to their formation. It was also shown that these lamellar systems could lead to the formation of unilamellar vesicles, similar to liposomes composed of phospholipids. These vesicles display distinct properties that make them potentially appealing for some applications. The present article reviews the current knowledge relative to these non phospholipid bilayers made of monoalkylated amphiphiles and sterols.

## 1.2.2 Mixtures of monoalkylated amphiphiles and sterols forming bilayers

A fair number of reports indicate or suggest the formation of fluid lamellar phases from monoalkylated amphiphile/sterol mixtures. In most cases, cholesterol is the selected sterol. Different monoalkylated amphiphiles, including zwitterionic, ionic, and neutral ones, have been shown to have the ability to form lamellar phases with sterols.

### 1.2.2.1 Monoalkylated amphiphiles with cholesterol

Lysolecithin (a phospholipid with a phosphocholine head group but bearing a single chain) and cholesterol were the first couple for which the formation of a fluid lamellar phase was reported. Lysolecithin generally forms micelles when hydrated. In 1975, it was shown, using X-ray diffraction, electron spin resonance, and electron microscopy, that lysolecithin derived from egg-yolk lecithin (approximately 80% palmitoyl(C16)lysolecithin and 20% stearoyl(C18)lysolecithin), interacts stoichiometrically with cholesterol to form lamellar structures.<sup>32,33</sup> The formation of a lamellar structure was also reported for the equimolar mixture of 1-palmitoyl-sn-glycerol-3-phosphocholine and cholesterol.<sup>34</sup> The thickness of the resulting bilayer was found to be 4.2 nm. Based on scanning calorimetry and <sup>13</sup>C NMR, it was concluded that the 1:1 molar ratio complex provided an optimal composition because all the lysoPC existed in the fluid lamellar phase without excess of cholesterol. Similarly, a systematic study using <sup>31</sup>P NMR and X-ray scattering showed that mixtures of 1-palmitoyl-2-hydroxy-sn-glycerol-3-phosphocholine/cholesterol form fluid bilayers.<sup>35</sup> The lysoPC self-assembly was progressively

modified upon the addition of cholesterol, from micelles for pure lysoPC to fluid bilayers when the mixture included 70 mol % cholesterol.

Fluid lamellar self-assemblies of palmitic acid (PA) and cholesterol in aqueous environment have been studied systematically by Paré and colleagues.<sup>36</sup> This study reported the phase-composition diagram (Figure 1.1) that shows a region at high temperature where lamellar phase is exclusively formed. The authors concluded that there is a "eutectic-like" composition corresponding to 65–70 mol % cholesterol. The formation of fluid bilayers in the presence of 70 mol % cholesterol was extended to other saturated fatty acids, including myristic acid, stearic acid,<sup>37</sup>  $\alpha$ -hydroxypalmitic acid ( $\alpha$ OH-PA), and  $\alpha$ -fluoropalmitic acid ( $\alpha$ F-PA).<sup>38</sup> The presence of the carboxylic group confers to these bilayers pH-sensitivity. For example, mixtures of cholesterol and unprotonated PA at high pH ( $\geq 7.5$ ) are stable in the lamellar phase. A phase separation occurs, as pH is decreased below 7.5 and PA is protonated. By introducing an electron withdrawn group, such as  $-\text{OH}$  and  $-\text{F}$ , the  $\text{p}K_{\text{a}}$  of palmitic acid derivatives can be modulated, therefore, the stability of the fluid bilayers and of the resulting liposomes can be modulated on the pH scale.<sup>38</sup>

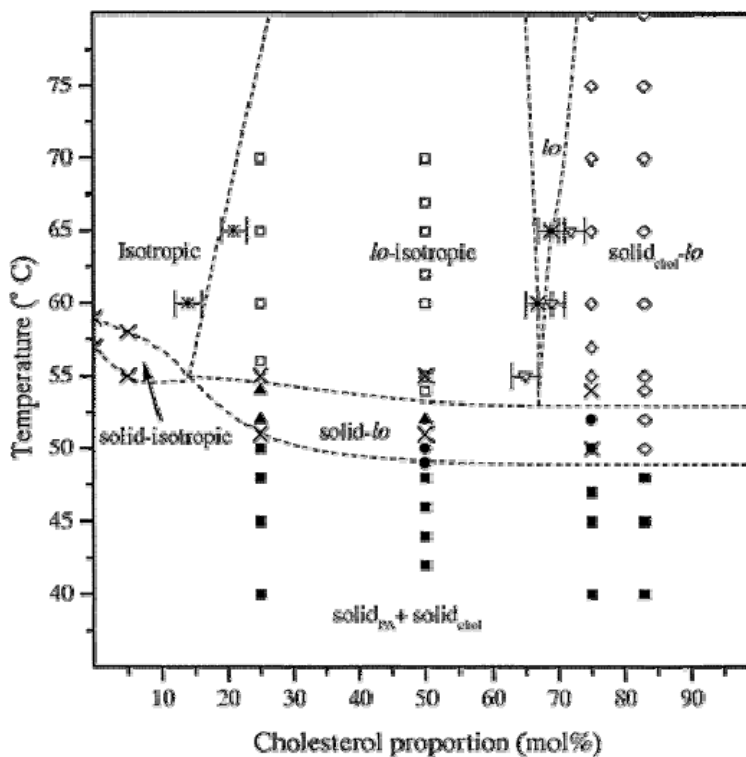


Figure 1.1. Temperature–composition diagram for PA/Chol system.<sup>36</sup>

Alkylated ammonium molecules were also shown to be good candidates for the formation of bilayers with sterols. These amphiphiles lead to the formation of positively charged bilayers. Stable fluid bilayers are formed by equimolar mixtures of stearylamine and cholesterol.<sup>39</sup> At low pH ( $< 9.5$ ), stearylamine is protonated and then bears an ammonium group. The positively charged stearylamine forms stable lamellar phases with cholesterol. However, a phase separation causing the disappearance of the lamellar phase occurs when stearylamine is deprotonated, at  $\text{pH} > 9.5$ . Cetylpyridium chloride (CPC) and cetyltrimethylammonium bromide (CTAB), two cationic detergents exist under micellar form in water.<sup>40</sup> They form stable bilayers with the inclusion of cholesterol.<sup>41-43</sup> Cholesterol induces the transformation of CTAB micelles, to mixed micelles, to bilayers. Beyond 50 mol % of cholesterol, the bilayer reaches the cholesterol solubility limit and cholesterol crystals are observed.

Experimental and computational work by Swamy's group suggests that N-myristoylethanolamine, N-palmitoylethanolamine, and N-stearoylethanolamine can also form lamellar phases in the presence of cholesterol.<sup>44, 45</sup> These amphiphiles showed a chain melting transition that was progressively abolished in the presence of cholesterol. In the equimolar complex, no phase transition was observed. The authors referred to as the formation of a "complex" but no phase characterization was carried out.

The lamellar self-assemblies obtained with hydrated non-ionic surfactants are known as Niosomes.<sup>46-48</sup> Cholesterol is not always essential for bilayer formation in Niosome formulations. For example, synthetic alkyl glycosides<sup>49</sup> and sorbitan esters (Span 20, 40, 60, 80)<sup>50</sup> form vesicles without any cholesterol. The following section focuses on monoalkylated non-ionic surfactants that require cholesterol to form lamellar self-assemblies. Tween 20 and Tween 61 usually form micelles in water, whereas the presence of a minimum amount of 33.3 and 10 mol % cholesterol, respectively, leads to fluid bilayers.<sup>51, 52</sup> For both detergents, the lamellar phases are still observed when the cholesterol content is increased to 50 mol %.<sup>52-56</sup> Tween 21/Chol<sup>55</sup> equimolar mixtures are shown to form lamellar phases. Mixtures of diglyceryl monolaurate (DGL)/Chol and tetraglyceryl monolaurate (TGL)/Chol self-assemble into bilayers once the proportion of cholesterol is minimally 10 and 30 mol %, respectively.<sup>52</sup> Polyoxyethylene alkylethers can also form fluid bilayers in the presence of cholesterol. For example, C<sub>12</sub>EO<sub>2</sub>, C<sub>12</sub>EO<sub>7</sub>, and C<sub>16</sub>EO<sub>2</sub> are reported to exist exclusively in the lamellar phase in the presence of 30, 10, and 25 mol % cholesterol, respectively.<sup>52, 57-59</sup> Recently, it is reported that octadecyl methyl sulfoxide (OMSO) can mix with cholesterol in equimolar proportion, and gives rise to a lamellar phase above its transition temperature.<sup>60</sup>

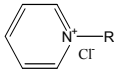
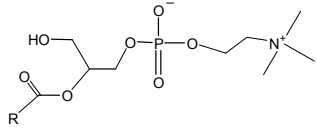
### 1.2.2.2 Sterols

It has been demonstrated that cholesterol is not the only sterol which can induce the formation of lamellar phases with fatty acids. Cholesterol sulfate, dihydrocholesterol, and 7-dehydrocholesterol were also shown to promote the formation of lamellar phases once mixed with palmitic acid and its derivatives.<sup>38, 61, 62</sup> Stigmastanol, stigmasterol, and ergosterol can also lead to the formation of a lamellar structure with palmitic acid but their propensities to induce bilayers is limited.<sup>62</sup> Mixtures of cholesterol sulfate and CPC (70/30 molar ratio) are also found to form stable bilayers between 10 and 70 °C.

### 1.2.2.3 Ternary mixtures

A limited number of studies have examined the behavior of ternary mixtures with two monoalkylated amphiphiles and cholesterol, or one monoalkylated amphiphile and two sterols. Non phospholipid liposomes formed from a ternary mixture of polyoxyethylene alkylether, free fatty acid, and cholesterol have been used commercially as Novasome<sup>®</sup>,<sup>63</sup> Ternary mixtures of Tween 60/SA/Chol were also shown to exist as fluid bilayers.<sup>64</sup> Tween 60 and cholesterol were known to self-assemble in a lamellar phase, and stearylamine was introduced in order to provide the resulting liposomes with a positive surface charge. Ternary mixtures of PA/Chol/Schol were shown to form stable bilayers over a wide range of pH values and temperatures.<sup>61</sup> The combination of the two sterols (a neutral and an anionic one) was an original approach in order to modulate the bilayer stability as a function of pH.

Table 1.1. Name and chemical structure of monoalkylated amphiphiles ( $R = C_nH_{2n+1}$ ).

| Name  | Chemical structure   | n     | Ref              |
|---|--|-------|------------------|
| Myristic acid                                       | RCOOH  | 13    | 37               |
| Palmitic acid (PA)                                  |  | 15    | 36,<br>61,<br>62 |
| Stearic acid  |  | 17    | 37               |
| $\alpha$ -hydroxypalmitic acid<br>( $\alpha$ OH-PA) | RCH(OH)COOH  | 14    | 38               |
| $\alpha$ -fluoropalmitic acid<br>( $\alpha$ F-PA)   | RCH(F)COOH   | 14    |                  |
| Stearylamine (SA)                                   | RNH <sub>2</sub>   | 18    | 39               |
| Cetylpyridium chloride<br>(CPC)                     |   | 16    | 43               |
| Cetyltrimethylammonium<br>bromide (CTAB)            |   | 16    | 41,<br>42        |
| N-myristoylethanolamine                             | RNHCH <sub>2</sub> CH <sub>2</sub> OH  | 14    | 44,<br>45        |
| N-palmitoylethanolamine                             |  | 16    |                  |
| N-stearoylethanolamine                              |  | 18    |                  |
| LysoPC  |    | 16-18 | 32-<br>35        |
| Polyoxyethylene<br>alkylethers                      | RO[CH <sub>2</sub> CH <sub>2</sub> O] <sub>m</sub> H (C <sub>n</sub> EO <sub>m</sub> )   | 16-18 | 52,<br>57-<br>59 |
| Diglyceryl monolaurate<br>(DGL)                     | RCOOCH <sub>2</sub> CH(OH)CH <sub>2</sub> OCH <sub>2</sub> CH(OH)CH <sub>2</sub> OH  | 11    | 52               |
| Tetraglyceryl monolaurate<br>(TGL)                  | RCOOCH <sub>2</sub> CH(OH)CH <sub>2</sub> OCH <sub>2</sub> CH(OH)CH <sub>2</sub> OCH <sub>2</sub> -<br>CH(OH)CH <sub>2</sub> OCH <sub>2</sub> CH(OH)CH <sub>2</sub> OH | 11    |                  |

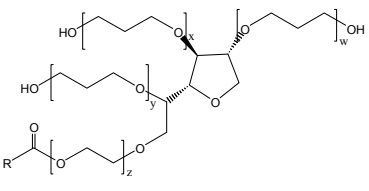
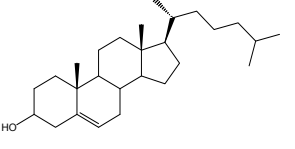
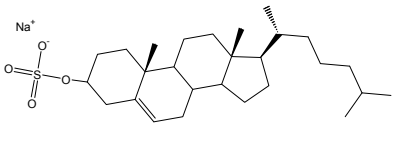
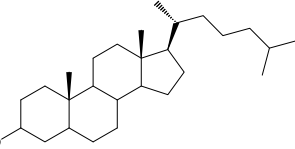
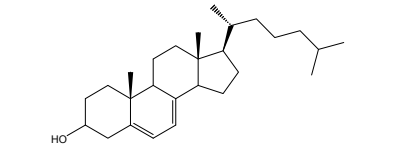
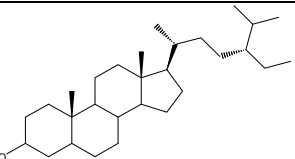
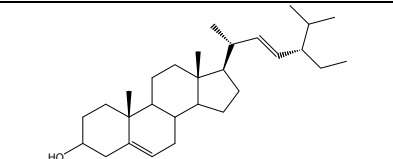
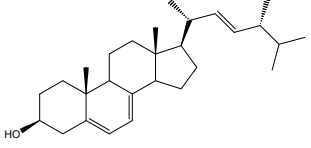
|  |  |    |           |
|--|--|----|-----------|
| Tween 20 ( $w+x+y+z=20$ )              |  | 11 | 52-<br>56 |
| Tween 21 ( $w+x+y+z=4$ )               |  | 17 |           |
| Tween 60; Tween 61<br>( $w+x+y+z=20$ ) |  |    | 18        |
| Octadecyl methyl<br>sulfoxide (OMSO)   | $\text{RSOCH}_3$   |    |           |

Table 1.2. Name and chemical structure of different sterols.

|   |  |
|---|--|
|   |   |
| Cholesterol (Chol)  | Cholesterol sulfate (Schol)  |
|  |  |
| Dihydrocholesterol  | 7-dehydrocholesterol   |
|  |  |
| Stigmastanol  | Stigmasterol   |
|  |  |
| Ergosterol  |  |

### 1.2.3 Prerequisites for fluid lamellar self-assemblies

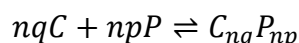
The mixing of the monoalkylated amphiphiles and sterols, and the proper hydration of the interface are two parameters critical for the formation of stable fluid lamellar phases. In this section, factors that impact these parameters are discussed in details. These include the nature of monoalkylated amphiphiles and sterols, the hydrophobic matching, the electrostatic interactions, and the hydrogen bonding.

#### 1.2.3.1 Effect of sterols

Cholesterol is an important biomembrane component that has been studied extensively. It generally exists in large amounts in eukaryotic plasmic membranes, and plays essential roles in membrane functions, including raft formation, cell signaling, and protein sorting.<sup>26, 65-67</sup> One of the most special properties of cholesterol in relation to the phospholipid membrane structure is the formation of a liquid-ordered (lo) lamellar phase, a phenomenon originally introduced by Ipsen et al. in 1987.<sup>24</sup> The lo phase is an intermediate state between the solid-ordered (gel) phase and the liquid-disordered (fluid) phase. The lipid chains are ordered in an almost all-trans form, like in the gel phase. However the bilayers maintain their fluidity, the lateral and rotational diffusions being similar to those observed in the fluid phase.<sup>24, 68</sup> The formation of the lo phase is associated with the ambivalent character of cholesterol. On one hand, because of its shape considerably different than that of phospholipids, it prevents the tight packing of their alkyl chains, and the formation of the gel phase. On the other hand, because of its smooth hydrophobic face, cholesterol rigidifies the neighboring phospholipid alkyl chains. These features lead to fluid

bilayers with ordered alkyl chains. The ordering effect of cholesterol on phospholipid bilayers is well established. The order parameters of the smoothed order profiles of several cholesterol containing systems, including 1-palmitoyl-2-oleoyl-sn-glycero-3-phosphocholine (POPC)/Chol,<sup>69</sup> 1-palmitoyl-2-oleoyl-phosphatidylethanolamine (POPE)/Chol,<sup>70</sup> and dimyristoylphosphatidylcholine (DMPC)/Chol,<sup>71</sup> have high values and demonstrate the restricted intramolecular motions of the lipid alkyl chains. The ordering of the phospholipid chains leads to thicker membranes, and as a consequence, cholesterol incorporated in phospholipid bilayers decreases the permeability of the resulting liposomes. The maximum solubility of cholesterol in phospholipid matrices is typically between 30 and 40 mol %.<sup>72-74</sup> However, this parameter is still somehow a matter of debate because, using alternative preparative methods, it was reported that 66 and 51 mol % cholesterol can be incorporated in phosphatidylcholine and phosphatidylethanolamine bilayers, respectively.<sup>73</sup>

The molecular arrangement in the lo phase is still a controversial topic. Several conceptual models were proposed to explain the cholesterol-phospholipid interactions in the 2D membranes, including the condensed-complex model,<sup>75, 76</sup> the superlattice model,<sup>77, 78</sup> and the umbrella model.<sup>79</sup> The condensed-complex model suggests the reversible formation of stoichiometric cholesterol (*C*)–phospholipid (*P*) complexes, defined in thermodynamics terms.



where, *p* and *q* are prime integers, and *n* is the cooperativity parameter. In a binary mixture of cholesterol and phospholipid, the complex  $C_{nq}P_{np}$  normally coexists either with a phospholipid-rich phase or with a cholesterol-rich phase. At the equivalence molar ratio  $q/(p + q)$ , there is neither an excess of cholesterol nor an excess of phospholipid. This equivalent point is

determined from experimental phase diagrams.<sup>80</sup> For example, reports have confirmed the values of  $q = 1$ ,  $p = 2$ , and a variation of  $n$  from 1 to 10.<sup>76, 81</sup> The superlattice model proposes that cholesterol molecules display, at some critical concentrations, a specific long-ranged order in phospholipid bilayers. It was inferred that for the critical sterol mole proportions of 20.0, 22.2, 25.0, 33.3, 40.0, and 50.0 mol %, regular superlattices are formed by the sterol molecules. At any other given sterol mole fraction, the superlattices coexist with areas where cholesterol is irregularly distributed. The umbrella model proposes that cholesterol molecules are covered by neighboring polar phospholipid head groups to avoid the unfavorable free energy associated with exposing cholesterol to water. Since the hydrophilic part of cholesterol is small (a simple hydroxyl group), the phospholipids organize themselves to form an umbrella to protect cholesterol from interactions with water.

The two-dimensional molecular arrangement of the mixtures of cholesterol and monoalkylated amphiphiles is not known, and the current models proposed for phospholipid-based bilayers do not appear applicable in a straightforward way. For most investigated systems, it was concluded that there is a progressive increase of the lipid proportion existing in the lamellar phase as a function of increasing cholesterol content.<sup>36, 39, 60</sup> It is identified that there is a particular cholesterol proportion for which the system exists exclusively in the  $l_0$  lamellar phase. Increased cholesterol content leads to the appearance of solid cholesterol.<sup>36, 39, 60</sup> In any case there was the identification of critical concentrations of cholesterol that could be associated with superlattice distributions – even though no study has examined a large number of compositions that are involved in such studies.<sup>35, 36, 39, 60</sup> The proportion of monoalkylated amphiphiles, such as fatty acid and fatty amine, in the fluid bilayers make the umbrella model hardly compatible with

these systems. For example, it is practically impossible to picture how 30 mol % of unprotonated PA could provide enough shielding for 70 mol % cholesterol. This proportion is also greatly different than the one reported in the condensed-complex model. Typically, the reported stoichiometry of the complex is 1 cholesterol for 2 phospholipids, and therefore, 4 alkyl chains. This corresponds to 20 mol % cholesterol if one considers cholesterol and single alkyl chains. This value is far from 70 mol % that is commonly determined in the monoalkylated amphiphile/Chol bilayers.

The alkyl chain order of the fluid bilayers prepared from monoalkylated amphiphiles and sterols has been determined for some systems. The mixtures formed with fatty acids have been characterized by  $^2\text{H}$  NMR as some deuterated analogues are commercially available. The orientational order along the palmitic acid chain in the PA/Chol bilayers was typical of a bilayer in the  $l_o$  phase with a plateau region near the polar head group, followed by a rapid decrease of the order going towards the end of the chain.<sup>82, 83</sup> However the measured order parameters were considerably high. For example, it was  $\sim 0.46$  for the plateau of the profile of PA- $\text{d}_{31}$ /Chol bilayers, at 25 °C.<sup>62</sup> It should be mentioned that the maximum order parameter, obtained for an all-trans chain, would be 0.5. Therefore, it is concluded that the alkyl chains of the monoalkylated amphiphiles in these bilayers with a large sterol content display a very high chain order, among the most ordered fluid bilayers ever reported. The smoothed order profiles of the PA/Chol system could be reproduced by molecular simulations for PA/Chol mixtures.<sup>84</sup>

The orientation and dynamics of cholesterol in these bilayers have also been investigated using  $^2\text{H}$  NMR. Cholesterol deuterated at the positions 2,2,4,4,6, on the steroid rings, was

introduced in bilayers formed from a mixture of PA/Chol,<sup>36</sup> OMSO/Chol,<sup>60</sup> CPC/Chol,<sup>43</sup> and SA/Chol.<sup>39</sup> The studies revealed that cholesterol actually experiences similar orientation and dynamics in all these binary mixtures. Cholesterol displays an axially symmetric motion and its long axis is essentially aligned with the bilayer normal. Very limited molecular wobbling is reported. These characteristics are comparable to those previously reported for cholesterol inserted in phospholipid bilayer such as DMPC/Chol,<sup>85, 86</sup> in model mixtures of stratum corneum lipids forming bilayers,<sup>83</sup> and even in human red blood cell membranes<sup>87</sup> and membranes of mycoplasma *Acholeplasma laidlawii* (Strain B).<sup>88</sup> It appears that, despite the limited proportion of amphiphiles to "solubilize" cholesterol in the two-dimensional bilayers, the sterol displays a behavior similar to that in phospholipid-based bilayers.

Several sterols are reported to display an impact on phospholipid bilayers similar to that observed for cholesterol.<sup>26, 71, 89-94</sup> A "universal behavior" of sterols on the hydrophobic thickness and the elastic properties of phospholipid membranes has even been proposed.<sup>89</sup> Similar effects of other sterols were observed on the lamellar self-assemblies but small variations are reported depending on the molecular details of the sterol structure. The ordering effect of other sterols on palmitic acid, as determined by <sup>2</sup>H NMR, was similar to that of cholesterol. The investigated sterols were dihydrocholesterol, 7-dehydrocholesterol, stigmastanol, stigmasterol, and ergosterol.<sup>62</sup> In a binary mixture of PA/sterol 30/70 molar ratio, dihydrocholesterol and 7-dehydrocholesterol displayed an equivalent propensities for the formation of lo bilayers with palmitic acid. However, stigmastanol, stigmasterol, and ergosterol had a limited ability to form lamellar phases with palmitic acid.<sup>62</sup> All of these sterols are neutral and bear a hydroxyl group at the position C3. Stigmastanol, stigmasterol, and ergosterol have branched and unsaturated chains

at the position C17, leading to a bulkier group than the others. These bulky alkyl tail chains may result in a less tight chain packing, leading to reduced intermolecular interactions. Such situation appears to be unfavorable for the formation of fluid lamellar phases. Thus, it is concluded that different sterols have the ability to induce the formation of lo lamellar phases, and that the alkyl tail chain of those sterols has more pronounced effects than the ring network on the stability of the resulting lamellar self-assemblies.

### 1.2.3.2 Hydrophobic match

It was demonstrated that the hydrophobic matching between the alkyl chain of monoalkylated amphiphiles and the hydrophobic section of sterols is essential to form stable bilayers. The self-assembled structures formed by a series of mixtures including cholesterol and a linear saturated fatty acid with various chain length was characterized.<sup>37</sup> It was found that fatty acids with acyl chains of 14–18 carbon atoms led to the formation of lo phase bilayers with cholesterol, whereas the shorter lauric acid (C12) and longer lignoceric acid (C24) did not. Recently computational simulations provided some description at the molecular level of these phase behaviors.<sup>84</sup> On one hand, when bilayers were formed with cholesterol and lauric acid (that was reported too short to form bilayers with cholesterol), it was found that the amphiphilic balance of the free fatty acid would lead to a significant proportion of lauric acid diffusing out of the bilayer, leading to the formation of spherical micelles and to the destabilization of the lamellar structure. On the other hand, the simulations showed that lignoceric acid (that was reported too long to form bilayers with cholesterol) would increase locally the bilayer thickness, creating voids that would unzip the two leaflets of the bilayer.

The majority of the reported monoalkylated amphiphile/sterol systems leading to the formation of fluid bilayers fulfill the hydrophobic match requirement. There are, however, reports of a few systems with shorter alkyl chain that appear to mix with cholesterol and to form fluid lamellar phases. This is the case, for example, of C<sub>12</sub>EO<sub>2</sub>, DGL, and TGL, three non-ionic surfactants bearing a 12 carbon alkyl chain that formed bilayers with 30, 10 and 30 mol % cholesterol.<sup>52</sup> The large size of the head group of C<sub>12</sub>EO<sub>2</sub>, DGL, and TGL appears to bring a specific stability to the resulting lamellar assemblies.

### 1.2.3.3 Electrostatic interactions

Electrostatic interactions favor both lipid mixing and hydration. At this point, most of the binary mixtures of a monoalkylated amphiphile and a sterol that form stable lamellar phases include at least one species with a charge at the head group level. It is proposed that the electrostatic repulsion is reduced by mixing with the other neutral molecules, promoting a homogenous mixture. Usually, a phase separation occurs in either both neutral or both like-charged systems; fatty acid/sterol<sup>95</sup> and SA/Chol<sup>39</sup> systems exemplify this behavior. For PA/Chol mixture, lamellar phases exist when neutral cholesterol is mixed with deprotonated PA at high pH (PA is negatively charged). Solid PA and cholesterol are observed at low pH when both of them are neutral.<sup>95</sup> Conversely, fluid bilayers are formed when negatively charged cholesterol sulfate is mixed with neutral PA, at low pH. Phase-separated species appear at high pH when they both bear a negative charge.<sup>61</sup> In the SA/Chol mixture, stable lamellar phases exist only when SA is protonated (SA is positively charged). Phase separations occur when SA is neutralized.<sup>39</sup> The absence of charges on the neutral bilayers causes the expulsion of water

molecules at the interface, and therefore, reduces the hydration and favors the phase separation. By modulating the bulk pH, one can switch the protonation/deprotonation states of the monoalkylated amphiphiles. Taking the advantage of this pH-dependent phase behavior, pH-sensitive liposomes were successfully developed from PA/sterol<sup>62</sup> and SA/Chol<sup>39</sup> mixtures.

It is also found fluid bilayers are self-assembled when both of the species share an unlike charge, providing electrostatic attraction, and consequently promoting lipid mixing and suitable hydration at the interface. When positively charged CPC is mixed with negatively charged cholesterol sulfate in a molar ratio of 30/70, lo lamellar phases are reported to be stable over the relatively wide range of temperature and pH (10–70 °C, pH 5–9).<sup>43</sup> When positively charged SA is mixed with Schol at low pH, stable lamellar phases are also observed (unpublished data). In the ternary mixture of PA/Chol/Schol (30/28/42 molar ratio), when PA protonated or deprotonated, 70 or ~40 mol % negative charges exist in the system. The electrostatic repulsion can be minimized by the neutral species. Three different lipids were well-mixed and with proper hydration degree, the mixture formed stable fluid bilayers over a wide range of pH.<sup>61, 96</sup>

It was shown that lysoPC, a zwitterionic monoalkylated amphiphiles, could also form bilayers with cholesterol.<sup>35</sup> In this case, it is likely that the presence of the charges at the head group level would favor the hydration of the interface,<sup>97</sup> which stabilizes the lo phase formed with cholesterol.

#### 1.2.3.4 Hydrogen bonds

Hydrogen bonds can also promote lipid mixing and hydration. The stability of fluid bilayers with non-ionic surfactants, such as alkylethers and cholesterol must originate from other type of intermolecular interactions than coulombic interactions, and hydrogen bonds are proposed to play a pivotal role in some systems. In these systems, the polar head group of monoalkylated amphiphiles can act as both donors and acceptors for hydrogen bonds. The hydrogen bonds between the monoalkylated amphiphiles and sterols promote lipid mixing. In parallel, the hydrogen bonds with water molecules enhance the hydration of the interface. Both of the factors have synergistic effects on the formation of *l<sub>o</sub>* phases.

Sulfoxide group is a very good hydrogen bond acceptor that forms hydrogen bonds with hydroxyl groups stronger than those formed with carbonyl group.<sup>98,99</sup> Moreover sulfoxide group interacts strongly with water. OMSO/Chol mixtures can form fluid lamellar phases at room temperature,<sup>60</sup> and it is proposed that these strong hydrogen bonds involving the sulfoxide group and both cholesterol and water molecules contribute to the stability of the bilayers. The behavior of this mixture contrasts with that of the equimolar mixture of PA/Chol at low pH (PA is neutral), which forms, at room temperature, phase separated crystalline forms.<sup>1</sup> It is proposed that the hydrogen bonds between the carbonyl group of PA and cholesterol and water are not strong enough to drive good lipid mixing and proper hydration. It must be pointed out that OMSO/Chol fluid bilayers are in fact metastable at room temperature and there is a progressive solidification of the components over 30 hours. Experimental and computational results also demonstrated that hydrogen bonds are one of the important factors in the stabilization of the fluid lamellar phases

obtained from mixtures of N-acylethanolamines/Chol. Two hydrogen bonds are proposed to be particularly important: the one between the hydroxyl group of cholesterol and the amide carbonyl of N-acylethanolamine, and the one between the hydroxyl groups of N-acylethanolamine and the hydrogen of the hydroxyl group on cholesterol.<sup>100</sup> For non-ionic surfactants, such as alkyl glycerol ether ( $C_nG_m$ ) and alkylesters ( $C_nEO_m$ ) systems, there are multiple hydrogen bond possibilities with cholesterol and water molecules,<sup>51</sup> and this contribution is believed to promote the formation of lo lamellar phases.

#### 1.2.3.5 Molecular morphology and critical packing parameter

The amphiphile morphology plays a critical role in determining the geometry of their self-assemblies. This concept has led to a model developed by Israelachvili,<sup>101, 102</sup> that defines a critical packing parameter (CPP).

$$CPP = \frac{v}{I_c a_0}$$

where  $v$  is the volume of the hydrocarbon chain,  $I_c$ , the critical hydrophobic chain length, and  $a_0$ , the area of the hydrophilic head group. It has been shown that a calculated CPP value between 0.5 and 1 indicates that the amphiphile is likely to form lamellar phases. Values below 0.5 (indicating a large contribution from the hydrophilic head group area relative to the hydrophobic section) are typical for amphiphiles self-assembling into micelles. A CPP above 1 (indicating a large contribution from the hydrophobic group volume relative to the polar head group) would result in the formation of inverted micelles. Even though the CPP values are somewhat difficult to identify with high precision in an absolute manner, the model is a useful tool for predicting the morphology of self-assemblies, in a semi-quantitative manner.

In order to form bilayers, the overall CPP of the system should be around 1. The CPP of cholesterol is estimated to 1.08, based on its volume ( $605 \text{ \AA}^3$ ), length ( $15.2 \text{ \AA}$ ), and hydrophilic area ( $37 \text{ \AA}^2$ ). Generally, the CPP values for detergent are 0.5 or below. It can be assumed that the geometrical parameters of the component of a mixture are additive.<sup>103, 104</sup> Consequently, it is predicted that mixing of the cone-shape cholesterol and inverted cone-shape detergent leads to an overall CPP compatible with the formation of a lamellar phase (Figure 1.2). The overall CPP was calculated to be around 1 when 65–75 mol % cholesterol was mixed with PA; such mixtures lead in fact to a lamellar phase.<sup>36</sup>

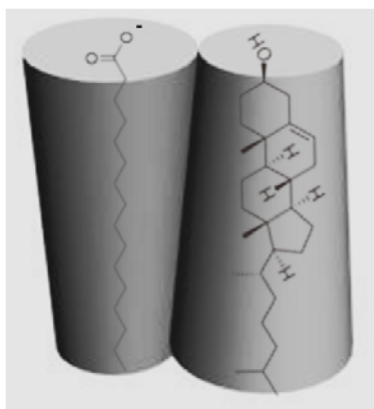


Figure 1.2. Schematic morphology of deprotonated palmitic acid and cholesterol molecules.

#### 1.2.4 Features of non phospholipid liposomes

The formation of fluid bilayers by mixtures of monoalkylated amphiphiles and sterols offers the possibility to prepare unilamellar vesicles. Such structures could be successfully obtained using different methods, and the resulting liposomes have been shown to possess some distinct properties.

#### 1.2.4.1 Formation methods

Multilamellar vesicles are formed spontaneously when the powdered amphiphiles are hydrated.<sup>2</sup> It is possible to extrude the multilamellar dispersion to prepare large unilamellar vesicles (LUVs), using standard extrusion techniques. LUVs were prepared, for instance, from PA/sterols<sup>2, 62</sup> (30/70), OMSO/Chol<sup>60</sup> (50/50), CPC/Schol<sup>43</sup> (30/70), CPC/Chol (50/50), SA/Chol<sup>39</sup> (50/50) mixtures. The extrusion technique displays some advantages. The size of the resulting vesicles is fairly uniform, and can be easily controlled by the pore size of the filter.<sup>2</sup> This method can be easily scaled up for commercial developments. Alternative methods were used for unilamellar liposome preparations. CTAB/Chol LUVs were prepared using the DELOS-SUSP method. This method is particularly suitable for the preparation of LUVs that include a water-insoluble compound such as cholesterol.<sup>42</sup> Briefly, a supersaturated cholesterol solution in acetone is mixed with CO<sub>2</sub> supercritical fluid. This homogenized solution is then mixed with the surfactant upon depressurization; cholesterol and surfactant molecules self-assemble into vesicles. Sonication has also been used for unilamellar vesicle preparation, especially in the case of Niosomes.<sup>47, 53, 55, 58</sup> This method is straightforward but leads to difficulties in obtaining uniform size of vesicles and in scale-up.

#### 1.2.4.2 Encapsulation, stability & permeability

It was demonstrated that the liposomes prepared from monoalkylated amphiphile/sterol systems can encapsulate solutes in a manner analogous to phospholipid-based liposomes. At this point, only passive loading has been investigated with the LUVs prepared from monoalkylated

amphiphile/sterol mixtures. For example, the encapsulation capacity of PA/Chol LUVs with diameter varying from 50 to 200 nm was determined to be 1.4 to 3.4 L/mol.<sup>2</sup> Those values are similar to those measured for phospholipid vesicles.<sup>105, 106</sup> These LUVs were made from a monoalkylated amphiphile, and therefore this effectively decreases the encapsulation capacity expressed in molar terms comparing with phospholipid liposomes, as these molecules bear two hydrophobic chains. Solute trapping is also reported for LUVs prepared from equimolar mixtures of Tween 61/Chol, C<sub>12</sub>EO<sub>2</sub>/Chol, and TGL/Chol, and the entrapment efficiency is 21%, 4%, and 5%, respectively. It was proposed that the short 12-carbon alkyl chain leads to weak interactions with cholesterol, and more deformable liposomes. The formation of tube-shaped aggregates instead of spherical liposomes would be a critical factor in the low entrapment efficiency observed for mixtures of cholesterol with C<sub>12</sub>EO<sub>2</sub> and TGL.

The size of the LUVs composed of several monoalkylated amphiphile/sterol systems is found to be very stable. No significant size changes were observed at least for a month for PA/Chol,<sup>2</sup> OMSO/Chol,<sup>60</sup> and SA/Chol<sup>39</sup> liposomes, at room temperature and pH ~7.5. Particularly, OMSO/Chol vesicles were stable over a wide pH range (2–12), nearly without size change and with very limited permeability. A similar behavior is reported for PA/Chol/Schol liposomes.<sup>61, 96</sup>

The permeability of liposomes prepared from several monoalkylated amphiphile/sterol mixtures has been characterized,<sup>2, 38, 39, 43, 61, 62, 96</sup> and it was determined to be very limited. For example, the passive release of entrapped glucose from PA/Chol led to a leakage of only 10% after 30 days,<sup>2</sup> and about 90% of the entrapped glucose was released from SA/Chol LUVs over

the same period.<sup>39</sup> This passive permeability compares advantageously to that of phospholipid-based liposomes: for example, more than 90% of encapsulated glucose leaked out from phosphatidylcholine liposomes containing between 40 and 50 mol % cholesterol within 10 days.<sup>2</sup><sup>107</sup> Similarly, after 600 days (near two years), ~70% of calcein was still trapped in the PA/Chol liposomes.<sup>38</sup> LUVs prepared from the ternary PA/Chol/Schol mixture were shown to sustain a pH gradient 100 times longer than POPC/Chol ones.<sup>96</sup> It has been proposed that the high content sterol incorporated in the non phospholipid liposomes was the main reason for the limited permeability. It was shown that these bilayers in the lo phase display a very high chain order (see 1.3.3.1), leading to thick bilayers and very low permeability.

#### 1.2.4.3 Functionalized liposomes

Up to now, pH-sensitive liposomes are the main class of functionalized liposomes that were designed with the monoalkylated amphiphile/sterol systems. As described above, the electrostatic intermolecular interactions are of prime importance in the formation of lo lamellar phase with mixtures of monoalkylated amphiphiles and sterols. The stability of these bilayers and consequently the stability of the resulting liposomes can be modulated by using a pH responsive amphiphile such as fatty acids or fatty amines. Because coulombic interactions can be modulated by both the sterol and the monoalkylated amphiphile, a very versatile family of pH-sensitive liposomes was created.<sup>2, 38, 39, 62</sup> First, the direction of the pH change leading to stimulated release can be controlled. For example, the release from PA/Chol LUVs can be triggered by a pH decrease (protonation of PA),<sup>62</sup> whereas the release is induced by a pH increase in the case of PA/Schol LUVs (when PA is deprotonated).<sup>61</sup> Cationic and pH-sensitive liposomes could be

designed from a mixture of stearylamine and cholesterol.<sup>39</sup> The fluid lamellar phase is stable only when stearylamine is charged, i.e., at pH lower than its  $pK_a$ , whereas stearylamine and cholesterol exist under a solid form when stearylamine is neutral. Second, because the release is induced by the change in the protonation state of the fatty acid, it was shown possible to fine-tune the pH triggering the content release by including monoalkylated amphiphiles with different  $pK_a$ . For example, the  $pK_a$  of PA can be modulated by the insertion of an electron-withdrawing group at the  $\alpha$  of the carboxylic function group; the  $pK_a$  of PA,  $\alpha$ -hydroxypalmitic acid, and  $\alpha$ -fluoropalmitic acid under the monomeric form is 4.8, 3.8, and 2.6, respectively.<sup>38</sup> As a consequence, the extent of release from liposomes at low pH can be modulated by these different fatty acids. At pH 4.5, after 24 h, PA/Chol LUVs are completely empty, more than 20% release is observed for  $\alpha$ OH-PA/Chol LUVs at pH 4.5, and practically no release is observed for  $\alpha$ F-PA/Chol LUVs. Similarly cholesteryl hemisuccinate, a molecule carrying a carboxylic function, can be introduced in Tween 20/Chol niosomes to provide pH-sensitivity.<sup>56</sup> The protonation of polar head groups of cholesteryl hemisuccinate at lower pH leads to the destabilization of the LUVs and the release of their content.

### 1.2.5 Biological implications and applications of non phospholipid liposomes

The investigations of the fluid lamellar phase obtained from monoalkylated amphiphiles and sterols led to the development of novel nanovectors that exhibit distinct properties as well as a better understanding of the physicochemical rules of their self-assembly. One can ponder whether such lamellar structures made of simple and abundant biomolecules could be found in biological systems. At this point, there is no clear indication that nature is using these systems. However, some potential biological implications of these systems have been suggested.

Skin is the major organ protecting the body from dehydration, chemicals, and mechanical stress. The stratum corneum, the outmost layer of the skin, is a key element of the skin barrier. It is formed of coenocytes, keratin-filled cells, glued together with lipids. The lipid phase contains actually very little phospholipid, and is mainly composed of ceramides, cholesterol, and free fatty acids.<sup>108, 109</sup> This unusual lipid composition for a biological membrane is associated with an unusual structure as the lipid phase includes a large fraction of solid or crystalline lipids.<sup>109</sup> It has been proposed that the lipidic phase of the stratum corneum is formed of small crystalline domains embedded in a fluid lipid matrix.<sup>110-112</sup> At this point, the lipids that would participate in this fluid matrix have not been identified. In light of their considerable concentration in the stratum corneum, it has been suggested that this fluid lipid phase is mainly formed by fatty acids and cholesterol.<sup>37</sup> A study on the phase behavior of model stratum corneum mixture made of nonhydroxyl palmitoyl ceramide, palmitic acid, and cholesterol, revealed that when the mixture was challenged with heat, fluid domains enriched in cholesterol and palmitic acid were formed,<sup>113</sup> suggesting a preferential interaction between these two species.

It was shown that a lo lamellar phase was formed by mixtures of lysoPC and cholesterol.<sup>35</sup> These are two components of the red blood cell membranes. The putative formation of domains of cholesterol and lysoPC could ensure the presence of an appropriate amount of lysoPC in these cellular membranes. This monoalkylated amphiphile is prone to leave membranes. An excessive proportion of lysoPC is however detrimental to the bilayer structure. Therefore the formation of lo phase domains could therefore be involved in the control of the lysoPC content in membranes. The LysoPC content is critical in the control of the hemolysis caused by certain agents (e.g., alcohols) and in the activity of cholesterol oxidase.<sup>114</sup> Therefore its content in the bilayer should be regulated and the formation of domains with cholesterol is a phenomenon that should be investigated.

N-acylethanolamines naturally exist in the membranes of plants and animals, and they are involved in vital biological processes, such as responses to injury, to dehydration, and to myocardial infarction. N-acylethanolamines are produced in membranes from the enzymatic degradation of N-acylphosphatidylethanolamines, when the organism suffers stress.<sup>115, 116</sup> They have anti-inflammatory effect, relieve pain sensation, they are endogenous ligands for cannabinoid receptors, and they were proposed to have pro-apoptotic activity.<sup>117-120</sup> N-arachidonylethanolamine reduces the fertilizing capacity of the sperm.<sup>121</sup> At this point, there is no indication of specific interaction with sterols. But considering that they are found in membranes where cholesterol is also present, and it is shown that they can together form stable self-assemblies, their putative interactions should be carefully examined.

From the application point of view, non phospholipid liposomes obtained from monoalkylated amphiphiles and sterols are promising alternatives to other formulation including conventional liposomes because they are stable, they can be made at low cost, and they are easy to handle, transport, and store. Such formulations are already used in cosmetics by L'Oréal. Their niosomes showed reduced toxicity compared to emulsions, and improved the delivery of active ingredients for promoting skin hydration.<sup>59</sup> Niosomes formed from Tween 60/Chol/SA mixtures were tested *in vitro* as vector for indomethacin, a non-sterol anti-inflammatory drug known to inhibit platelet aggregation. It was shown that liposomal indomethacin was more than two times efficient to inhibit platelet aggregation than the free drug.<sup>64</sup> Non phospholipid liposomes have been also examined as adjuvant of vaccine delivery.<sup>122</sup> Tetanus toxoid encapsulated in Novasomes<sup>®</sup> exhibited higher levels of anti-tetanus toxoid IgG2a and IgG2b than when adsorbed to aluminum phosphate. It was concluded that non phospholipid liposomes may be alternative to aluminum adjuvants for human vaccines. In the food industry, ascorbic acid (vitamin C) is added to foods because of its reducing and antioxidant properties. It retards enzymatic browning, protects certain compounds from oxidation, inhibits nitrosamine formation, etc. However, free ascorbic acid is generally not stable in these milieus. It was reported that encapsulation of vitamin C in liposomes with acidic internal pH can improve considerably its stability in real food matrices.<sup>123</sup> A recent study showed that the encapsulation of ascorbic acid in PA/Chol/Schol liposomes can protect vitamin C from an oxidizing milieu (in the presence of Iron(III)), and its degradation rate in such a milieu is reduced by a factor of ~20 000 compared to the free ascorbic acid.<sup>96</sup>

### 1.2.6 Conclusion

Since liposomes were first developed around 1980s, the development and use of this type of nanocarriers have made considerable progress. Given their distinct properties, liposomes made of monoalkylated amphiphiles and sterols display a great potential in several application fields. There is now a relatively good understanding of the physicochemical rules of the self-assembly of these molecular species, allowing scientists to design functional non phospholipid liposomes. These non phospholipid liposomes are made of molecules which are fairly easy to obtain, handle, transport, and store. It is expected that these studies will open the door to applications in various fields including pharmaceuticals, cosmetics, food industry, and agriculture.

## 1.3 Characterization methods in this thesis

Many characterization methods have been used in the present thesis. Most of their applications are relatively straightforward. I decided to restrict the technical section, and to present specific aspects of the data interpretation inferred from IR and NMR spectroscopy.

### 1.3.1. IR spectroscopy

Infrared spectroscopy (IR) provides information relative to the vibrational energies of chemical bonds. The vibrational modes include stretching, deformation, rocking, wagging, twisting, etc. The time scale of these molecular vibrations is typically  $\sim 10^{13} \text{ s}^{-1}$ . IR spectroscopy is a common, powerful, and convenient tool to study lipids and membranes. First, several functional groups of phospholipid molecules can be distinguished and studied structurally in a single experiment. For example, information relative to saturated or unsaturated chains can be obtained from the C–H stretching bands whereas the interface can be investigated from the C=O and PO<sub>4</sub> vibrations associated with the polar heads. Second, it is versatile from a sample point of view. Samples in different physical states (solids, solutions, dispersions, etc) can be examined. Finally, it requires a limited amount of sample.<sup>124</sup>

The C–H stretching vibrations are found in the spectral region between 3100 and 2800  $\text{cm}^{-1}$ . Normally, the CH<sub>2</sub> asymmetric and symmetric stretching modes, at  $\sim 2920$  and  $\sim 2850 \text{ cm}^{-1}$  respectively, are the most intense bands in lipid spectra.<sup>124-126</sup> Their exact frequencies are sensitive to the trans–gauche isomerization of the alkyl chain, and therefore, their position is

useful for the identification of lipid phases with different conformational order. Because the asymmetric band is usually partially overlapped with other vibrational modes, such as CH<sub>3</sub> asymmetric stretching band at  $\sim 2956\text{ cm}^{-1}$  and the intense O–H stretching band of water centered at  $\sim 3400\text{ cm}^{-1}$ , the band at  $2850\text{ cm}^{-1}$  corresponding to the C–H symmetric stretching mode, is more commonly used for the phase characterization.<sup>124, 125</sup> It is also possible to determine the  $T_m$  of a membrane. The position of the CH<sub>2</sub> stretching modes shifts to higher frequencies from the gel to fluid phase as the hydrocarbon chains become more disordered.<sup>124</sup> Typically, in the solid phase the frequency is below  $2850\text{ cm}^{-1}$ , as the hydrocarbon chains are tightly packed and in an all-trans form. When several gauche isomers exist, the frequency shifts to above  $2853\text{ cm}^{-1}$ , such as in the liquid-disordered phase.<sup>125-127</sup> The frequency of this mode is found at  $\sim 2851\text{ cm}^{-1}$  for lo phases.<sup>61, 126</sup> Cholesterol induces less ordered chains than those in the gel phase, and more ordered chains compared to the liquid-disordered phase, resulting in those intermediate values. For highly ordered monoalkylated amphiphiles, such as for PA and CPC in solid phases,<sup>43, 61, 128</sup> the C–H symmetric stretching mode is usually below  $2849\text{ cm}^{-1}$ . The frequency shifts to above  $2853\text{ cm}^{-1}$  when PA and CPC exist as micelles.<sup>43, 61, 128</sup>

When the protons are substituted by deuteriums, the methyl and methylene stretching modes are shifted to lower frequencies due to the vibrational isotope effect. The C–D stretching frequencies are approximately in the range of  $2300\text{--}2000\text{ cm}^{-1}$ , a spectral region generally free of interference. The asymmetric and symmetric of C–D stretching modes are found at  $\sim 2194$  and  $\sim 2090\text{ cm}^{-1}$ , respectively.<sup>124, 125</sup> These bands are also sensitive to the conformations of the alkyl chains. For mixtures of monoalkylated amphiphiles and cholesterol, in the lo phase, the

frequency of the C–D symmetric stretching is  $\sim 2091\text{ cm}^{-1}$ . In the solid and fluid phases, the frequencies are below  $2089\text{ cm}^{-1}$  and above  $2094\text{ cm}^{-1}$ , respectively.<sup>36, 95</sup>

The correlation field splitting of the methylene deformation bands is useful for the characterization of the hydrocarbon chain packing.<sup>129, 130</sup> The methylene deformation band is observed at  $1468\text{ cm}^{-1}$  for  $\text{CH}_2$  and at  $1088\text{ cm}^{-1}$  for  $\text{CD}_2$ . For chains packed in an orthorhombic symmetry (Figure 1.3), these modes split into two components due to the vibrational coupling between neighborhood chains. Typically, two components located at  $1472$  and  $1464\text{ cm}^{-1}$  are observed for the  $\text{CH}_2$  groups, while they appear at  $1091$  and  $1086\text{ cm}^{-1}$  for  $\text{CD}_2$  groups. The interchain coupling occurs only when the oscillators have similar frequencies.<sup>129, 131</sup> Therefore, vibrational coupling of the methylene modes can only exist between isotopically alike chains.<sup>129</sup> The splitting is maximal when the coupling involves 100 molecules or more, and it decreases progressively for smaller domains. When the maximum splitting is observed for a mixture of hydrogenated (or deuterated) species, it can be concluded that a phase separation leads to domains with orthorhombic chain packing that include at least 100 molecules. When a single component is observed for the methylene deformation, there is less information because it could be due to a different chain packing symmetry, to the formation of a fluid phase, or to a mixing of the hydrogenated and deuterated chains. The lo phase displays a single component but indeed, a single component is not specific to the lo phase.

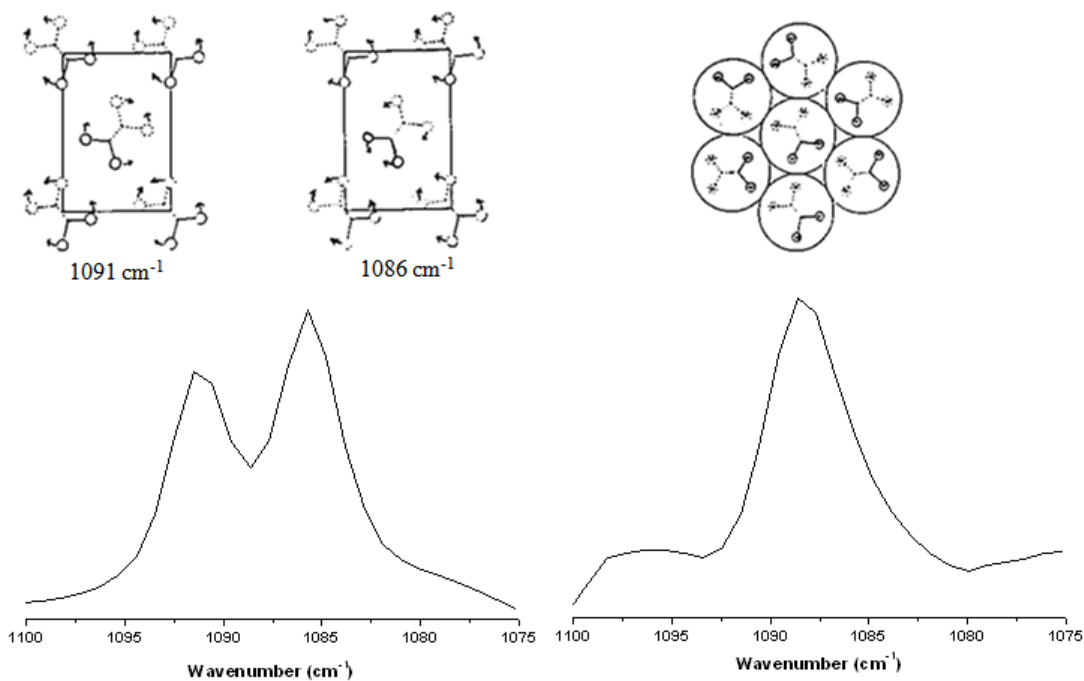


Figure 1.3. Schematic representation of the acyl chain packing and of the in-phase and out-phase modes giving rise to the splitting in the case of orthorhombic packing. The bands corresponding to the  $\text{CD}_2$  deformation mode are also reproduced.

### 1.3.2. NMR

Solid-state deuterium NMR was used to characterize the phase behavior of mixtures with monoalkylated amphiphiles and sterols. Proton pulsed-field-gradient NMR was used in chapter 5 for the diffusion measurements of PEG molecules in the PA/Chol/PEG-Chol LUVs.

#### 1.3.2.1 $^2\text{H}$ NMR

Nuclear magnetic resonance spectroscopy of deuterium ( $^2\text{H}$  NMR) is a powerful tool to study membrane systems as it provides characteristic signals for various phases, from solid to

isotropic liquid. Nuclear resonance in solids is sensitive to different interactions: the chemical shift anisotropies, dipolar interactions and quadrupolar interactions. The spin ( $I$ ) of deuterium is 1, thus quadrupolar interactions are involved. They are associated with electrostatic interactions between the quadrupolar moment of the nucleus and the surrounding gradient of electric field. For  $I = 1$ , there are three Zeeman energy levels corresponding to three orientations of the magnetic moment relative to the magnetic field (characterized by the quantum numbers  $m_I = +1$ , 0, and  $-1$ ). According to the selection rule, two single-quantum nuclear spin transitions between adjacent spin energy levels are allowed (Figure 1.4). Taking only into account Zeeman interactions, these two transitions would involve the same energy, and would give rise to a single absorption band. In  $^2\text{H}$  NMR, the quadrupolar coupling modifies slightly the level energy, and as a consequence, the transitions  $m_I = +1 \rightarrow 0$  and  $m_I = 0 \rightarrow -1$  do not involved the same energy, and therefore, a doublet is observed.

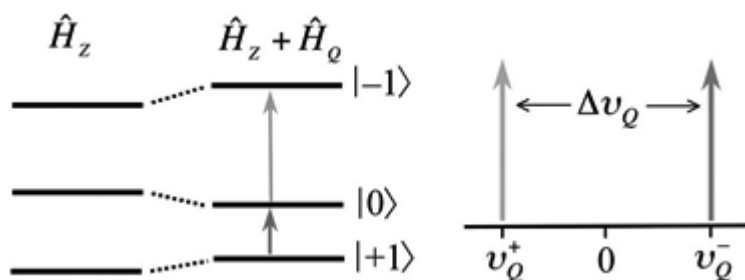


Figure 1.4. Different energy levels and resonance lines in solid state  $^2\text{H}$  NMR spectroscopy.

These strong quadrupolar interactions determine the shape of the spectra, and lead to a signal that can be spread over more than 100 kHz. Therefore, the associated time scale of the experiment is approximately  $10^{-5}$  s.<sup>126</sup> Motions slower than this time scale are in the slow regime,

and do not affect the magnitude of the quadrupolar interactions. Motions faster than the time scale are in the fast regime, and lead to the averaging of the quadrupolar interactions. In a C–D bond, the electric field gradient is along the bond because of the electronegativity difference between the two nuclei. It is also axially symmetric. Therefore, the magnitude of the quadrupolar splitting is sensitive to the orientation of C–D bonds relative to the magnetic field. The quadrupolar splitting,  $\Delta\nu$ , is associated with the average orientation of the C–D bond relative to the magnetic field.  $\Delta\nu$  can be expressed as the following equation:

$$\Delta\nu = \frac{3}{2}A_Q \left\langle \frac{3\cos^2\Phi - 1}{2} \right\rangle \quad (1.1)$$

where  $A_Q$  is the static quadrupolar constant (170 kHz for aliphatic, 175 kHz for olefinic<sup>85</sup> and 193 kHz for aromatic C–D bonds<sup>132</sup>) and  $\Phi$  is the angle between the magnetic field and the C–D bond at the origin of the electric field gradient. When the molecules are in a solid phase, they are virtually immobile. As a consequence, the fixed orientation of the C–D bond relative to the magnetic field defines  $\Delta\nu$ . When  $\Phi$  equals  $0^\circ$ ,  $\Delta\nu$  has the maximum value, i.e.  $\frac{3}{2}A_Q$ . For a C–D bond oriented at the magic angle, i.e.  $54.7^\circ$ ,  $\Delta\nu$  becomes zero and a singlet is observed. When  $\Phi = 90^\circ$ ,  $\Delta\nu$  is  $-\frac{3}{4}A_Q$ . (Figure 1.5)

In a powder, the probability of a C–D bond oriented parallel to the magnetic field is relatively low. Therefore, the intensity of the corresponding doublet is low. The probability of the C–D bonds perpendicular to the magnetic field rises to the maximum, and hence the intensity of the resulting doublet is maximal. The random distribution in a powder gives rise to different orientations and to different doublets superimposed together to give a broad powder pattern. (Figure 1.5 and 1.7)

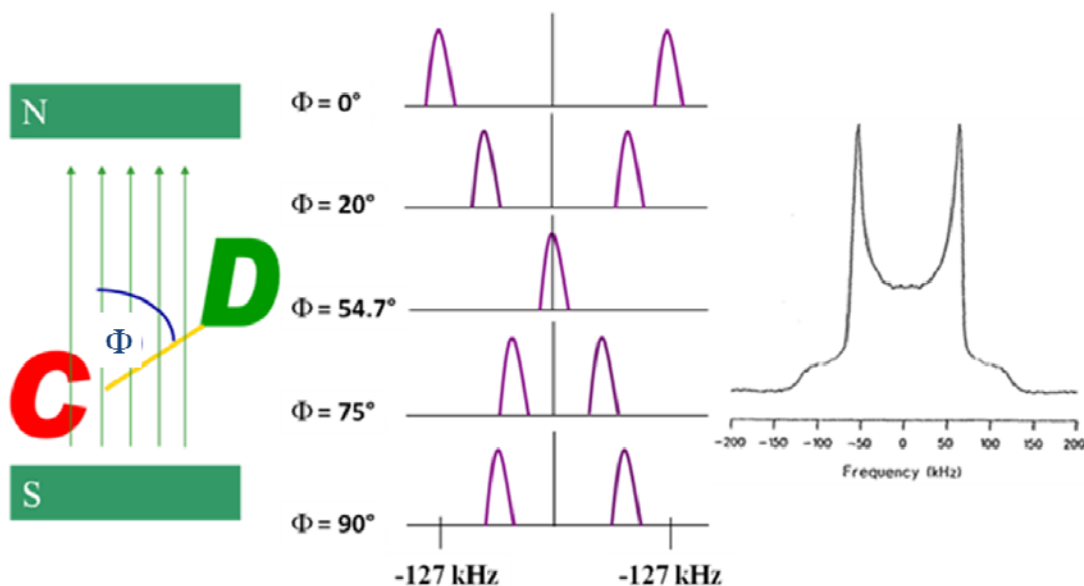


Figure 1.5. Influence of the orientation of the C–D bond relative to the magnetic field on the quadrupolar interactions and the resulting powder pattern.

In a fluid bilayer, molecules are mobile. On the NMR time scale, three main axially symmetric motions are involved: (1) the rotation along the long axis of the molecule; (2) the fluctuations of the whole molecule with respect to the bilayer normal; and (3) trans–gauche isomerization within the alkyl chain. Considering these three different motions, the quadrupolar splitting can be expressed as follows:

$$\Delta\nu = \frac{3}{2}A_Q \left( \frac{3 \cos^2 \theta - 1}{2} \right) \left\langle \frac{3 \cos^2 \gamma - 1}{2} \right\rangle \left\langle \frac{3 \cos^2 \alpha - 1}{2} \right\rangle = \frac{3}{2}A_Q \left( \frac{3 \cos^2 \theta - 1}{2} \right) S_{mol} S_{C-D} \quad (1.2)$$

Where  $\theta$  is the angle between the bilayer normal ( $n$ ) and the magnetic field ( $B$ ),  $\gamma$  is the angle between the bilayer normal and the long axis of the molecule ( $a$ ),  $\alpha$  is the angle between the C–D bond and the long axis of the molecule (Figure 1.6). The terms associated to motions (2) and (3) are represented by  $S_{mol}$  (molecular order parameter) and  $S_{C-D}$  (orientational order parameter),

respectively. In the  $l_0$  phase, the hydrocarbon region of the bilayer is not isotropic. The segment of the chains near the interface is more ordered compared to the segment towards the middle of the bilayer. Therefore, there is a decrease of order parameters along the chain, from the head group to its end; this is referred to as the order profile. Typically, several overlapping powder patterns, associated with the order gradients along the deuterated chains, are observed in the spectrum (Figure 1.7). Near the interface, the order does not vary considerably and this segment of the profile is referred to as the plateau region. Generally, decreasing the temperature and the incorporation of cholesterol in phospholipid bilayers, increase the order of the chains. The maximum value of the orientational order parameter is 0.5 as  $\alpha$  is  $90^\circ$  for an all-trans chain.

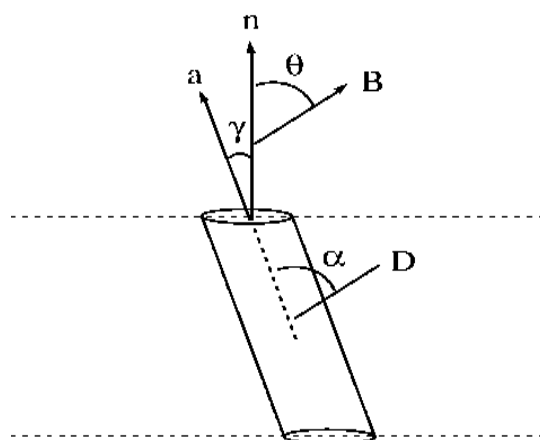


Figure 1.6. Definition of the angles ( $\theta$ ,  $\gamma$ ,  $\alpha$ ),  $n$  is the bilayer normal,  $a$  is the long (rotation) axis of the molecule and  $B$  represents the magnetic field.

In the case of a solution or a micellar suspension, fast motions lead to a rapid and isotropic reorientation of the C–D bonds. As a result, the quadrupolar interactions are completely averaged out. Only a sharp peak is observed in the spectrum (Figure 1.7).

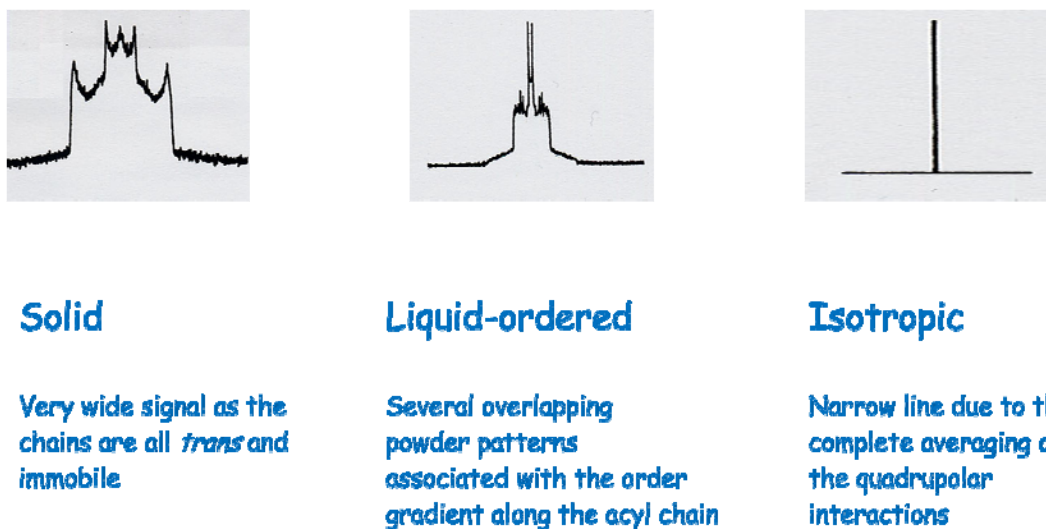


Figure 1.7. Illustration of the shapes of  $^2\text{H}$  NMR spectra associated with the corresponding phases.

Therefore the quadrupolar splittings of a deuterated alkyl chain reflect both the structure and the dynamics of the labeled groups. Because of the advantages of this unique technology, solid state  $^2\text{H}$  NMR is widely used for the structural and dynamical characterization of model, and biological membranes.<sup>86, 132-135</sup>

In the present thesis, PA- $d_{31}$  and deuterated Chol- $d_5$  at position 2,2,4,4,6 were used. The smoothed order of PA- $d_{31}$  can be derived from  $^2\text{H}$  NMR spectra. Briefly, the “de-Paked” spectra are obtained using a mathematical algorithm presented elsewhere.<sup>82, 136</sup> This iterative method extracts the NMR spectrum typical of an oriented system from the powder spectrum; this transformation facilitates the identification of the various doublets. Assuming a monotonic decrease of the order along the alkyl chains, each deuterium molecule is assigned to a quadrupolar splitting. In chapter 2, the smoothed order profiles of PA- $d_{31}$  were obtained for bilayers with different sterols.

For the  $^2\text{H}$  NMR experiments with deuterated cholesterol, the C–D bond was attached on the steroid rigid ring of cholesterol. Consequently, the angle  $\alpha$  (Figure 1.5) is constant, and  $S_{\text{C-D}}$  is essentially associated with this fixed orientation of the C–D bond relative to the long axis of the molecule. If  $\alpha$  is known, it is possible to determine  $S_{\text{mol}}$  from the experimental values of  $\Delta\nu$ , measured at  $\theta = 90^\circ$  (the most intense doublet) – see Equation 1.2. A calculated  $S_{\text{mol}}$  close to 1 indicates that the cholesterol axis of rotation is parallel to the bilayer normal, and there is very little wobbling of cholesterol in the bilayer (i.e.,  $\gamma$  is close to  $0^\circ$ ). In chapter 3 and 4, this model was applied to extract  $S_{\text{mol}}$  for cholesterol inserted in various bilayers, and therefore, to gain information relative to its orientation in the bilayer.

The spin-lattice relaxation time  $T_1$  is a very important parameter in NMR spectroscopy. The relaxation process associated with  $T_1$  involves an energy transfer from the spins to the surroundings. The spin-lattice relaxation originates from the local magnetic fields fluctuating at a frequency close to the resonance frequency of the transition. Generally, the tumbling motion of molecules determines the local field fluctuations. If the molecular tumbling matches the transition frequency,  $T_1$  is short. However, if the molecular tumbling leads to magnetic field fluctuations too slow or too fast relative to the resonance frequency, the energy transfer is inefficient, and consequently,  $T_1$  is long. In solid phases, the tumbling motion of molecules is practically absent, and therefore,  $T_1$  is long relative to the fluid phases. Thus, by controlling the intersequence delay, the contribution of a solid phase in spectra can be modulated. When a long intersequence delay is used (5 times  $T_1$  of the slow relaxation solid component), enough time is provided for the spin-lattice relaxation of the molecules in all the present phases (solid, lo, and/or isotropic phases, if there is any), and therefore, all the molecules contribute in the spectrum. When the intersequence

delay is short relative to  $T_1$  of the slow relaxation solid component, only the fast relaxing molecules in the fluid phase (molecules with short  $T_1$ ) relax and contribute to the spectrum. Taking the advantage of different  $T_1$  of cholesterol in solid and lo phases, the solidification of cholesterol was quantified in OMSO/Chol mixtures by controlling the intersequence delays (Chapter 3).

### 1.3.2.2 Diffusion NMR

The proton pulsed-field-gradient NMR spectroscopy is a widely used, convenient, and noninvasive technique using  $^1\text{H}$  signal to assess self-diffusion of molecules in solution and suspension.<sup>137, 138</sup> A magnetic field gradient is employed to generate a linear dependence between the position of the nuclei along a given axis and their precession frequency.

The stimulated echo sequence developed by Tanner<sup>139</sup> in 1970 was used in this thesis to evaluate the self-diffusion in suspensions. This sequence is composed of three  $90^\circ$  pulses along  $x$  axis and two gradient pulses along  $z$  axis (Figure 1.8). The first step is to apply a  $90^\circ$  pulse to place the magnetization in the  $xy$  plane. Thereafter, a short pulse of magnetic field gradient is applied to encode spin positions along the direction of the applied magnetic field gradient. Applying a magnetic field gradient along the axis parallel to the main field, the correlation of the precession frequency of a spin and its position along the axis can be expressed as follows:

$$\omega = \gamma(B_0 + G_z z) \quad (1.3)$$

where  $\omega$  is the Larmor frequency (radians/s),  $\gamma$  is the gyromagnetic ratio ( $\text{rad T}^{-1} \text{s}^{-1}$ ),  $B_0$  (T) is the strength of the static magnetic field,  $G_z$  is the magnetic field gradient (typically the unit for gradient is Gauss/cm, 1 T = 10 000 Gauss), and  $z$  is the position along the axis.

The application of the second  $90^\circ$  pulse flips the magnetization along the axis  $-z$ . The spin magnetization is stored along the  $-z$  direction during the delay period, ranging from a few milliseconds to a few seconds. The third  $90^\circ$  pulse brings the spin magnetization back to the  $xy$  plane. The second and third  $90^\circ$  pulse has an equivalent effect on reversing the direction of precession as a  $180^\circ$  pulse. This strategy prevents an undesired contribution of spin-spin relaxation. The second gradient pulse, identical to the first, is applied to decode the spins, counteracting the phase shift induced by the first gradient pulse. The influence of the two gradient pulses is not identical for the molecules that have moved during the interval  $\Delta$ . The molecular diffusion results in an incomplete refocusing of the magnetization, and therefore, a reduced intensity of the NMR signal. The diffusion coefficients can be obtained by fitting the variation of the echo intensity as a function of the gradient strength ( $G$ ) using the following equation:

$$\ln(S/S_0) = -(G\gamma\delta)^2 D(\Delta - \delta/3) \quad (1.4)$$

where  $S$  and  $S_0$  are the integrated echo intensities with and without a field gradient,  $\gamma$  is the gyromagnetic ratio of the investigated nucleus,  $\delta$  is the trapezoidal gradient pulse and  $\Delta$  is the interpulse delay.

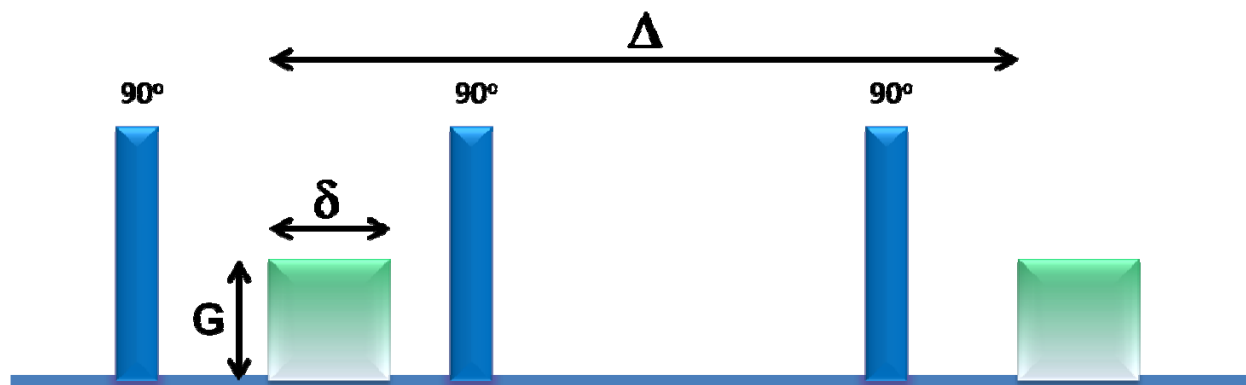


Figure 1.8. Schematic representation of stimulated echo sequence.

The echo attenuation is related to the mean displacement of the molecules along the axis of the applied gradient. This technique measures diffusion over the millisecond to second time scale. The diffusion coefficient measured using this method is an average mobility of the spin system over the whole sample. The stimulated echo pulse sequence is preferable for systems with longitudinal relaxation time longer than transverse relaxation time ( $T_1 > T_2$ ).  $T_1$  of macromolecules is typically longer than  $T_2$ ,<sup>140</sup> and consequently, this suitable sequence was used to measure the diffusion coefficient of PEG in the present thesis.

## 1.4 Description of the thesis sections

In the present thesis, the physicochemical behavior of self-assemblies of monoalkylated amphiphiles and sterols and various properties of the liposomes resulting from these mixtures were studied.

In chapter 2, the goal was to investigate whether the formation of  $l_0$  phases with monoalkylated amphiphiles was a peculiar feature of cholesterol, or if other sterols would exhibit the same behavior. By changing the molecular details of the sterols, we could provide a better understanding of the sterol features leading to Sterosomes formation. Different sterols (cholesterol, dihydrocholesterol, 7-dehydrocholesterol, stigmastanol, stigmasterol and ergosterol) were selected for the studies of the phase behavior of binary mixtures with palmitic acid. The passive release of the resulting liposomes as a function of time and the pH-triggered leakage were also characterized.

In chapter 3, the possibility to form completely neutral liposomes from a monoalkylated amphiphile mixed with cholesterol was examined. OMSO was chosen as the amphiphile, because the sulfoxide group is capable to form strong hydrogen bonds. First, the phase behavior of OMSO/Chol mixtures with various compositions was characterized by DSC, IR, and  $^2\text{H}$  NMR. This effort led to establishing the phase diagram of the mixture. Second, the formation of liposomes was carried out through extrusion and the permeability was evaluated.

In chapter 4, we report the design of dual functionalized (pH-sensitive and cationic) Sterosomes based on all the prerequisites identified for the  $l_0$  phase formation. Stearylamine was selected because the amine group could provide a positive charge at low pH, and its deprotonation might cause the destabilization of the self-assembly. The conditions leading to  $l_0$  phase formation with binary mixtures of stearylamine and cholesterol were identified, and vesicles were formed by extrusion. The pH-sensitivity of resulting liposomes was studied by measuring the release of encapsulated glucose.

In chapter 5, we wanted to develop a new formulation of Sterosomes with a long circulation life time in the blood stream, a feature that is critical for their use as drug nanocarriers for intravenous therapies. The strategy is to insert PEGylated cholesterol in the PA/Chol bilayers. First, the possibility and the amount of incorporation of PEG-Chol were studied. Second, the stability and the permeability of the resulting liposomes were assessed. Finally, the possibility of active-loading a real anti-cancer drug, doxorubicin, in this unique formulation was examined.

In chapter 6, perspectives and suggestions for future work are discussed.

## 1.5 References

1. Ouimet, J.; Croft, S.; Paré, C.; Katsaras, J.; Lafleur, M., Modulation of the polymorphism of the palmitic acid/cholesterol system by the pH. *Langmuir* **2003**, *19*, 1089-1097.
2. Bastiat, G.; Oligier, P.; Karlsson, G.; Edwards, K.; Lafleur, M., Development of non-phospholipid liposomes containing a high cholesterol concentration. *Langmuir* **2007**, *23*, 7695-7699.
3. Hillaireau, H.; Couvreur, P., Nanocarriers' entry into the cell: relevance to drug delivery. *Cell. Mol. Life Sci.* **2009**, *66*, 2873-2896.
4. Husseini, G. A.; Pitt, W. G., Micelles and nanoparticles for ultrasonic drug and gene delivery. *Adv. Drug Delivery Rev.* **2008**, *60*, 1137-1152.
5. Azarmi, S.; Roa, W. H.; Löbenberg, R., Targeted delivery of nanoparticles for the treatment of lung diseases. *Adv. Drug Delivery Rev.* **2008**, *60*, 863-875.
6. Miller, T.; Hill, A.; Uezguen, S.; Weigandt, M.; Goepferich, A., Analysis of Immediate Stress Mechanisms upon Injection of Polymeric Micelles and Related Colloidal Drug Carriers: Implications on Drug Targeting. *Biomacromolecules* **2012**, *13*, 1707-1718.
7. Tomalia, D. A.; Baker, H.; Dewald, J.; Hall, M.; Kallos, G.; Martin, S.; Roeck, J.; Ryder, J.; Smith, P., A new class of polymers: starburst-dendritic macromolecules. *Polym. J.* **1985**, *17*, 117-132.
8. Manchun, S.; Dass, C. R.; Sriamornsak, P., Targeted therapy for cancer using pH-responsive nanocarrier systems. *Life Sci.* **2012**, *90*, 381-387.
9. Esfand, R.; Tomalia, D. A., Poly(amidoamine) (PAMAM) dendrimers: from biomimicry to drug delivery and biomedical applications. *Drug Discov. Today* **2001**, *6*, 427-436.
10. Menjoge, A. R.; Kannan, R. M.; Tomalia, D. A., Dendrimer-based drug and imaging conjugates: design considerations for nanomedical applications. *Drug Discov. Today* **2010**, *15*, 171-185.
11. Bangham, A. D.; Horne, R. W., Negative staining of phospholipids and their structural modification by surface-active agents as observed in the electron microscope. *J. Mol. Biol.* **1964**, *8*, 660-668.

12. Sawant, R. R.; Torchilin, V. P., Liposomes as 'smart' pharmaceutical nanocarriers. *Soft Matter* **2010**, *6*, 4026-4044.
13. Immordino, M. L.; Dosio, F.; Cattel, L., Stealth liposomes: review of the basic science, rationale, and clinical applications, existing and potential. *Int. J. Nanomed.* **2006**, *2006*, 297-315.
14. Torchilin, V. P., Recent advances with liposomes as pharmaceutical carriers. *Nat. Rev. Drug Discov.* **2005**, *4*, 145-160.
15. Papakostas, D.; Rancan, F.; Sterry, W.; Blume-Peytavi, U.; Vogt, A., Nanoparticles in dermatology. *Arch. Dermatol. Res.* **2011**, *303*, 533-550.
16. Fathi, M.; Mozafari, M. R.; Mohebbi, M., Nanoencapsulation of food ingredients using lipid based delivery systems. *Trends Food Sci. Technol.* **2012**, *23*, 13-27.
17. Taylor, T. M.; Weiss, J.; Davidson, P. M.; Bruce, B. D., Liposomal nanocapsules in food science and agriculture *Crit. Rev. Food Sci. Nutr.* **2005**, *45*, 587-605.
18. Barani, H.; Montazer, M., A review on applications of liposomes in textile processing. *J. Liposome Res.* **2008**, *18*, 249-262.
19. Woodle, M. C.; Lasic, D. D., Sterically stabilized liposomes. *Biochim. Biophys. Acta* **1992**, *1113*, 171-199.
20. Huynh, N. T.; Roger, E.; Lautram, N.; Benoit, J. P.; Passirani, C., The rise and rise of stealth nanocarriers for cancer therapy: passive versus active targeting. *Nanomed.* **2010**, *5*, 1415-1433.
21. Moghimi, S. M.; Hunter, A. C.; Murray, J. C., Long-circulating and target-specific nanoparticles: Theory to practice. *Pharmacol. Rev.* **2001**, *53*, 283-318.
22. McMullen, T. P. W.; McElhaney, R. N., New aspects of the interaction of cholesterol with dipalmitoylphosphatidylcholine bilayers as revealed by high-sensitivity differential scanning calorimetry. *Biochim. Biophys. Acta* **1995**, *1234*, 90-98.
23. Vist, M. R.; Davis, J. H., Phase equilibria of cholesterol/dipalmitoylphosphatidylcholine mixtures: deuterium nuclear magnetic resonance and differential scanning calorimetry. *Biochemistry* **1990**, *29*, 451-464.
24. Ipsen, J. H.; Karlström, G.; Mouritsen, O. G.; Wennerström, H.; Zuckermann, M. J., Phase equilibria in the phosphatidylcholine-cholesterol system. *Biochim. Biophys. Acta* **1987**, *905*, 162-172.

25. Thewalt, J. L.; Bloom, M., Phosphatidylcholine: cholesterol phase diagrams. *Biophys. J.* **1992**, *63*, 1176-1181.
26. Mouritsen, O. G.; Zuckermann, M. J., What's so special about cholesterol? *Lipids* **2004**, *39*, 1101-1113.
27. Bloom, M.; Mouritsen, O. G., The evolution of membranes. *Can. J. Chem.* **1988**, *66*, 706-712.
28. Drummond, D. C.; Noble, C. O.; Hayes, M. E.; Park, J. W.; Kirpotin, D. B., Pharmacokinetics and in vivo drug release rates in liposomal nanocarrier development. *J. Pharm. Sci.* **2008**, *97*, 4696-4740.
29. Danhier, F.; Feron, O.; Preat, V., To exploit the tumor microenvironment: Passive and active tumor targeting of nanocarriers for anti-cancer drug delivery. *J. Control. Release* **2010**, *148*, 135-146.
30. Reimhult, E.; Baumann, M. K.; Kaufmann, S.; Kumar, K.; Spycher, P. R., Advances in nanopatterned and nanostructured supported lipid membranes and their applications. In *Biotechnology and Genetic Engineering Reviews, Vol 27*, Harding, S. E., Ed. Nottingham Univ Press: Nottingham, 2010; Vol. 27, pp 185-216.
31. Bally, M.; Bailey, K.; Sugihara, K.; Grieshaber, D.; Voros, J.; Stadler, B., Liposome and Lipid Bilayer Arrays Towards Biosensing Applications. *Small* **2010**, *6*, 2481-2497.
32. Purdon, A. D.; Hsia, J. C.; Pinteric, L.; Tinker, D. O.; Rand, R. P., Lysolecithin-cholesterol interaction. A spin-resonance and electron-micrographic study. *Can. J. Biochem.* **1975**, *53*, 196-206.
33. Rand, R. P.; Pangborn, W. A.; Purdon, A. D.; Tinker, D. O., Lysolecithin and cholesterol interact stoichiometrically forming bimolecular lamellar structures in the presence of excess water, of lysolecithin or cholesterol. *Can. J. Biochem.* **1975**, *53*, 189-95.
34. Ramsammy, L. S.; Brockerhoff, H., Lysophosphatidylcholine-cholesterol complex. *J. Biol. Chem.* **1982**, *257*, 3570-4.
35. Gater, D. L.; Seddon, J. M.; Law, R. V., Formation of the liquid-ordered phase in fully hydrated mixtures of cholesterol and lysopalmitoylphosphatidylcholine. *Soft Matter* **2008**, *4*, 263-267.
36. Paré, C.; Lafleur, M., Formation of liquid ordered lamellar phases in the palmitic acid/cholesterol system. *Langmuir* **2001**, *17*, 5587-5594.

37. Ouimet, J.; Lafleur, M., Hydrophobic match between cholesterol and saturated fatty acid is required for the formation of lamellar liquid ordered phases. *Langmuir* **2004**, *20*, 7474-7481.
38. Phoeung, T.; Aubron, P.; Rydzek, G.; Lafleur, M., pH-triggered release from nonphospholipid LUVs modulated by the pKa of the included fatty acid. *Langmuir* **2010**, *26*, 12769-12776.
39. Cui, Z.-K.; Bouisse, A.; Cottenye, N.; Lafleur, M., Formation of pH-sensitive cationic liposomes from a binary mixture of monoalkylated primary amine and cholesterol. *Langmuir* **2012**, *28*, 13668-13674.
40. Bhat, M.; Gaikar, V. G., Characterization of interaction between butylbenzene sulfonates and cetyl pyridinium chloride in a mixed aggregate system. *Langmuir* **2000**, *16*, 1580-1592.
41. Cano-Sarabia, M.; Angelova, A.; Ventosa, N.; Lesieur, S.; Veciana, J., Cholesterol induced CTAB micelle-to-vesicle phase transitions. *J. Colloid Interface Sci.* **2010**, *350*, 10-15.
42. Cano-Sarabia, M.; Ventosa, N.; Sala, S.; Patino, C.; Arranz, R.; Veciana, J., Preparation of uniform rich cholesterol unilamellar nanovesicles using CO<sub>2</sub>-expanded solvents. *Langmuir* **2008**, *24*, 2433-2437.
43. Phoeung, T.; Morfin Huber, L.; Lafleur, M., Cationic detergent/sterol mixtures can form fluid lamellar phases and stable unilamellar vesicles. *Langmuir* **2009**, *25*, 5778-5784.
44. Ramakrishnan, M.; Kenoth, R.; Kamlekar, R. K.; Chandra, M. S.; Radhakrishnan, T. P.; Swamy, M. J., N-Myristoylethanolamine–cholesterol (1:1) complex: first evidence from differential scanning calorimetry, fast-atom-bombardment mass spectrometry and computational modelling. *FEBS Lett.* **2002**, *531*, 343-347.
45. Ramakrishnan, M.; Tarafdar, P. K.; Kamlekar, R. K.; Swamy, M. J., Differential scanning calorimetric studies on the interaction of N-acylethanolamines with cholesterol. *Curr. Sci.* **2007**, *93*, 234-238.
46. Uchegbu, I. F.; Vyas, S. P., Non-ionic surfactant based vesicles (niosomes) in drug delivery. *Int. J. Pharm.* **1998**, *172*, 33-70.
47. Rajera, R.; Nagpal, K.; Singh, S. K.; Mishra, D. N., Niosomes: A Controlled and Novel Drug Delivery System. *Biol. Pharm. Bull.* **2011**, *34*, 945-953.
48. Azeem, A.; Anwer, M. K.; Talegaonkar, S., Niosomes in sustained and targeted drug delivery: some recent advances. *J. Drug Target.* **2009**, *17*, 671-689.

49. Kiwada, H.; Nakajima, I.; Matsuura, H.; Tsuji, M.; Kato, Y., Application of synthetic alkyl glycoside vesicles as drug carriers. III. Plasma components affecting stability of the vesicles. *Chem. Pharm. Bull.* **1988**, *36*, 1841-6.
50. Yoshioka, T.; Sternberg, B.; Florence, A. T., Preparation and properties of vesicles (niosomes) of sorbitan monoesters (Span 20, 40, 60 and 80) and a sorbitan triester (Span 85). *Int. J. Pharm.* **1994**, *105*, 1-6.
51. Uchegbu, I. F.; Florence, A. T., Non-ionic surfactant vesicles (Niosomes): Physical and pharmaceutical chemistry. *Adv. Colloid Interface Sci.* **1995**, *58*, 1-55.
52. Manosroi, A.; Wongtrakul, P.; Manosroi, J.; Sakai, H.; Sugawara, F.; Yuasa, M.; Abe, M., Characterization of vesicles prepared with various non-ionic surfactants mixed with cholesterol. *Colloid Surf., B* **2003**, *30*, 129-138.
53. Carafa, M.; Marianecchi, C.; Lucania, G.; Marchei, E.; Santucci, E., New vesicular ampicillin-loaded delivery systems for topical application: characterization, in vitro permeation experiments and antimicrobial activity. *J. Control. Release* **2004**, *95*, 67-74.
54. Carafa, M.; Marianecchi, C.; Rinaldi, F.; Santucci, E.; Tampucci, S.; Monti, D., Span (R) and Tween (R) neutral and pH-sensitive vesicles: Characterization and in vitro skin permeation. *J. Liposome Res.* **2009**, *19*, 332-340.
55. Di Marzio, L.; Marianecchi, C.; Petrone, M.; Rinaldi, F.; Carafa, M., Novel pH-sensitive non-ionic surfactant vesicles: comparison between Tween 21 and Tween 20. *Colloid Surf.* **2011**, *82*, 18-24.
56. Carafa, M.; Di Marzio, L.; Marianecchi, C.; Cinque, B.; Lucania, G.; Kajiwara, K.; Cifone, M. G.; Santucci, E., Designing novel pH-sensitive non-phospholipid vesicle: Characterization and cell interaction. *Eur. J. Pharm. Sci.* **2006**, *28*, 385-393.
57. Vandegriff, K. D.; Wallach, D. F. H.; Winslow, R. M., Encapsulation of hemoglobin in non-phospholipid vesicles. *Artif. Cells Blood Substit. Immobil. Biotechnol.* **1994**, *22*, 849-854.
58. ElBaraka, M.; Pecheur, E. I.; Wallach, D. F. H.; Philippot, J. R., Non-phospholipid fusogenic liposomes. *Biochim. Biophys. Acta*, **1996**, *1280*, 107-114.
59. Handjani-Vila, R. M.; Ribier, A.; Rondot, B.; Vanlerberghie, G., Dispersions of lamellar phases of non-ionic lipids in cosmetic products. *Int. J. Cosmet. Sci.* **1979**, *1*, 303-14.

60. Cui, Z.-K.; Bastiat, G.; Lafleur, M., Formation of fluid lamellar phase and large unilamellar vesicles with octadecyl methyl sulfoxide/cholesterol mixtures. *Langmuir* **2010**, *26*, 12733-12739.
61. Bastiat, G.; Lafleur, M., Phase behavior of palmitic acid/cholesterol/cholesterol sulfate mixtures and properties of the derived liposomes. *J. Phys. Chem. B* **2007**, *111*, 10929-10937.
62. Cui, Z.-K.; Bastiat, G.; Jin, C.; Keyvanloo, A.; Lafleur, M., Influence of the nature of the sterol on the behavior of palmitic acid/sterol mixtures and their derived liposomes. *Biochim. Biophys. Acta* **2010**, *1798*, 1144-1152.
63. Singh, A.; Malviya, R.; Sharma, P. K., Novasome-a breakthrough in pharmaceutical technology a review article. *Adv. Biol. Res.* **2011**, *5*, 184-189.
64. Pillai, G. K.; Salim, M. L. D., Enhanced inhibition of platelet aggregation in-vitro by niosome-encapsulated indomethacin. *Int. J. Pharm.* **1999**, *193*, 123-127.
65. Vance, D. E.; Van den Bosch, H., Cholesterol in the year 2000. *Biochim. Biophys. Acta*, **2000**, *1529*, 1-8.
66. Simons, K.; Ikonen, E., Cell biology - How cells handle cholesterol. *Science* **2000**, *290*, 1721-1726.
67. Mouritsen, O. G., The liquid-ordered state comes of age. *Biochim. Biophys. Acta*, **2010**, *1798*, 1286-1288.
68. Almeida, P. F. F.; Vaz, W. L. C.; Thompson, T. E., Lateral diffusion in the liquid phases of dimyristoylphosphatidylcholine/cholesterol lipid bilayers: a free volume analysis. *Biochemistry* **1992**, *31*, 6739-6747.
69. Lafleur, M.; Cullis, P. R.; Bloom, M., Modulation of the orientational order profile of the lipid acyl chain in the  $L\alpha$  phase. *Eur. Biophys. J.* **1990**, *19*, 55-62.
70. Paré, C.; Lafleur, M., Polymorphism of POPE/cholesterol system: a  $^2\text{H}$  nuclear magnetic resonance and infrared spectroscopic investigation. *Biophys. J.* **1998**, *74*, 899-909.
71. Urbina, J. A.; Pekarar, S.; Le, H. B.; Patterson, J.; Montez, B.; Oldfield, E., Molecular order and dynamics of phosphatidylcholine bilayer membranes in the presence of cholesterol, ergosterol and lanosterol: a comparative study using  $^2\text{H}$ -,  $^{13}\text{C}$ - and  $^{31}\text{P}$ -NMR spectroscopy. *Biochim. Biophys. Acta* **1995**, *1238*, 163-176.
72. Bach, D.; Wachtel, E., Phospholipid/cholesterol model membranes: formation of cholesterol crystallites. *Biochim. Biophys. Acta*, **2003**, *1610*, 187-197.

73. Huang, J.; Buboltz, J. T.; Feigenson, G. W., Maximum solubility of cholesterol in phosphatidylcholine and phosphatidylethanolamine bilayers. *Biochim. Biophys. Acta* **1999**, *1417*, 89-100.
74. Ibarguren, M.; Alonso, A.; Tenchov, B. G.; Goñi, F. M., Quantitation of cholesterol incorporation into extruded lipid bilayers. *Biochim. Biophys. Acta* **2010**, *1798*, 1735-1738.
75. Radhakrishnan, A.; Anderson, T. G.; McConnell, H. M., Condensed complexes, rafts, and the chemical activity of cholesterol in membranes. *Proc. Natl. Acad. Sci. U. S. A.* **2000**, *97*, 12422-12427.
76. Radhakrishnan, A.; McConnell, H. M., Condensed Complexes of Cholesterol and Phospholipids. *Biophys. J.* **1999**, *77*, 1507-1517.
77. Chong, P. L. G., Evidence for regular distribution of sterols in liquid crystalline phosphatidylcholine bilayers. *Proc. Natl. Acad. Sci. U. S. A.* **1994**, *91*, 10069-10073.
78. Huang, J. Y., Exploration of molecular interactions in cholesterol superlattices: Effect of multibody interactions. *Biophys. J.* **2002**, *83*, 1014-1025.
79. Huang, J.; Feigenson, G. W., A Microscopic Interaction Model of Maximum Solubility of Cholesterol in Lipid Bilayers. *Biophys. J.* **1999**, *76*, 2142-2157.
80. McConnell, H. M.; Radhakrishnan, A., Condensed complexes of cholesterol and phospholipids. *Biochim. Biophys. Acta*, **2003**, *1610*, 159-173.
81. Radhakrishnan, A.; McConnell, H. M., Electric field effect on cholesterol-phospholipid complexes. *Proc. Natl. Acad. Sci. U. S. A.* **2000**, *97*, 1073-1078.
82. Lafleur, M.; Fine, B.; Sternin, E.; Cullis, P. R.; Bloom, M., Smoothed orientational order profile of lipid bilayers by <sup>2</sup>H-nuclear magnetic resonance. *Biophys. J.* **1989**, *56*, 1037-1041.
83. Fenske, D. B.; Thewalt, J. L.; Bloom, M.; Kitson, N., Model of stratum corneum intercellular membranes: <sup>2</sup>H NMR of macroscopically oriented multilayers. *Biophys. J.* **1994**, *67*, 1562-1573.
84. Hadley, K. R.; McCabe, C., A simulation study of the self-assembly of coarse-grained skin lipids. *Soft Matter* **2012**, *8*, 4802-4814.
85. Dufourc, E. J.; Parish, E. J.; Chitrakorn, S.; Smith, I. C. P., Structural and dynamical details of cholesterol-lipid interaction as revealed by deuterium NMR. *Biochemistry* **1984**, *23*, 6062-6071.

86. Marsan, M. P.; Muller, I.; Ramos, C.; Rodriguez, F.; Dufourc, E. J.; Czaplicki, J.; Milon, A., Cholesterol orientation and dynamics in dimyristoylphosphatidylcholine bilayers: A solid state deuterium NMR analysis. *Biophys. J.* **1999**, *76*, 351-359.
87. Kelusky, E. C.; Dufourc, E. J.; Smith, I. C. P., Direct observation of molecular ordering of cholesterol in human erythrocyte membranes. *Biochim. Biophys. Acta* **1983**, *735*, 302-304.
88. Monck, M. A.; Bloom, M.; Lafleur, M.; Lewis, R. N. A. H.; McElhaney, R. N.; Cullis, P. R., Evidence for two pools of cholesterol in the *Acholeplasma laidlawii* strain B membrane: a deuterium NMR and DSC study. *Biochemistry* **1993**, *32*, 3081-3088.
89. Henriksen, J.; Rowat, A. C.; Brief, E.; Hsueh, Y. W.; Thewalt, J. L.; Zuckermann, M. J.; Ipsen, J. H., Universal behavior of membranes with sterols. *Biophys. J.* **2006**, *90*, 1639-1649.
90. Endress, E.; Bayerl, S.; Prechtel, K.; Maier, C.; Merkel, R.; Bayerl, T. M., The effect of cholesterol, lanosterol, and ergosterol on lecithin bilayer mechanical properties at molecular and microscopic dimensions: a solid-state NMR and micropipet study. *Langmuir* **2002**, *18*, 3293-3299.
91. Hsueh, Y. W.; Gilbert, K.; Trandum, C.; Zuckermann, M.; Thewalt, J., The effect of ergosterol on dipalmitoylphosphatidylcholine bilayers: A deuterium NMR and calorimetric study. *Biophys. J.* **2005**, *88*, 1799-1808.
92. Kodama, M.; Shibata, O.; Nakamura, S.; Lee, S.; Sugihara, G., A monolayer study on three binary mixed systems of dipalmitoyl phosphatidyl choline with cholesterol, cholestanol and stigmasterol. *Colloids Surf., B* **2004**, *33*, 211-226.
93. Ollila, O. H. S.; Rog, T.; Karttunen, M.; Vattulainen, I., Role of sterol type on lateral pressure profiles of lipid membranes affecting membrane protein functionality: comparison between cholesterol, desmosterol, 7-dehydrocholesterol and ketosterol. *J. Struct. Biol.* **2007**, *159*, 311-323.
94. de Meyer, F.; Smit, B., Effect of cholesterol on the structure of a phospholipid bilayer. *Proc. Natl. Acad. Sci. U. S. A.* **2009**, *106*, 3654-3658.
95. Ouimet, J.; Croft, S.; Pare, C.; Katsaras, J.; Lafleur, M., Modulation of the polymorphism of the palmitic acid/cholesterol system by the pH. *Langmuir* **2003**, *19*, 1089-1097.
96. Carbajal, G.; Cui, Z.-K.; Lafleur, M., Non phospholipid liposomes with high sterol content display a very limited permeability. *Sci. China Chemistry* **2013**, *56*, 40-47.

97. Rand, R. P.; Parsegian, V. A., Hydration forces between phospholipid bilayers. *Biochim. Biophys. Acta* **1989**, *988*, 351-376.
98. Wang, N.-N.; Li, Q.-Z.; Yu, Z.-W., Hydrogen bonding interactions in three 2-mercaptoethanol system: an excess infrared spectroscopic study. *Appl. Spectrosc.* **2009**, *63*, 1356-1362.
99. Abraham, M. H.; Platts, J. A., Hydrogen bond structural group constants. *J. Org. Chem.* **2001**, *66*, 3484-3491.
100. Swamy, M. J.; Tarafdar, P. K.; Kamlekar, R. K., Structure, phase behaviour and membrane interactions of N-acyl ethanolamines and N-acyl phosphatidylethanolamines. *Chem. Phys. Lipids* **2010**, *163*, 266-279.
101. Israelachvili, J. N.; D.J., M.; B.W., N., Theory of self-assembly of hydrocarbon amphiphiles into micelles and bilayers. *J. Chem. Soc., Faraday Trans.* **1976**, *72*, 1525-1568.
102. Israelachvili, J., Intermolecular and surface forces. In *Intermolecular and surface forces, 2th edition*, Israelachvili, J., Ed. Academic Press inc.: London, 1991.
103. Chen, Z.; Rand, R. P., The influence of cholesterol on phospholipid membrane curvature and bending elasticity. *Biophys. J.* **1997**, *73*, 267-276.
104. Lafleur, M.; Bloom, M.; Eikenberry, E. F.; Gruner, S. M.; Han, Y.; Cullis, P. R., Correlation between lipid plane curvature and lipid chain order. *Biophys. J.* **1996**, *70*, 2747-2757.
105. Hope, M. J.; Bally, M. B.; Webb, G.; Cullis, P. R., Production of large unilamellar vesicles by a rapid extrusion procedure. Characterization of size distribution, trapped volume and ability to maintain a membrane potential. *Biochim. Biophys. Acta* **1985**, *812*, 55-65.
106. Cullis, P. R.; Mayer, L. D.; Bally, M. B.; Madden, T. D.; Hope, M. J., Generating and loading of liposomal systems for drug-delivery applications. *Adv. Drug Delivery Rev.* **1989**, *3*, 267-282.
107. Demel, R. A.; Kinsky, S. C.; Kinsky, C. B.; Van Deenen, L. L. M., Effects of temperature and cholesterol on the glucose permeability of liposomes prepared with natural and synthetic lecithins. *Biochim. Biophys. Acta* **1968**, *150*, 655-665.
108. Ponec, M.; Weerheim, A.; Kempenaar, J.; Mommaas, A. M.; Nugteren, D. H., Lipid composition of cultured human keratinocytes in relation to their differentiation. *J. Lipid Res.* **1988**, *29*, 949-61.

109. Bouwstra, J. A.; Ponec, M., The skin barrier in healthy and diseased state. *Biochim. Biophys. Acta* **2006**, *1758*, 2080-2095.
110. Kitson, N.; Thewalt, J. L., Hypothesis: the epidermal permeability barrier is a porous medium. *Acta Derm. Venereol. Suppl.* **2000**, *208*, 12-15.
111. Forslind, B.; Norlén, L.; Engblom, J., A structural model for the human skin barrier. *Prog. Coll. Pol. Sci.* **1998**, *108*, 40-46.
112. Forslind, B., A domain mosaic model of the skin barrier. *Acta Derm. Venereol.* **1994**, *74*, 1-6.
113. Brief, E.; Kwak, S.; Cheng, J. T. J.; Kitson, N.; Thewalt, J.; Lafleur, M., The phase behaviour of equimolar mixture of *N*-palmitoyl *D*-erythro-sphingosine, cholesterol and palmitic acid, a mixture with optimized hydrophobic matching. *Langmuir* **2009**, *25*, 7523-7532.
114. Lange, Y.; Ye, J.; Steck, T. L., Activation of membrane cholesterol by displacement from phospholipids. *J. Biol. Chem.* **2005**, *280*, 36126-36131.
115. Dimarzo, V.; Fontana, A.; Cadas, H.; Schinelli, S.; Cimino, G.; Schwartz, J. C.; Piomelli, D., Formation and inactivation of endogenous cannabinoid anandamide in central neurons. *Nature* **1994**, *372*, 686-691.
116. Schmid, H. H. O.; Schmid, P. C.; Natarajan, V., The N-acylation-phosphodiesterase pathway and cell signalling. *Chem. Phys. Lipids* **1996**, *80*, 133-142.
117. Facci, L.; Daltoso, R.; Romanello, S.; Buriani, A.; Skaper, S. D.; Leon, A., Mast cells express a peripheral cannabinoid receptor with differential sensitivity to anandamide and palmitoylethanolamide. *Proc. Natl. Acad. Sci. U. S. A.* **1995**, *92*, 3376-3380.
118. Calignano, A.; Rana, G. L.; Giuffrida, A.; Piomelli, D., Control of pain initiation by endogenous cannabinoids. *Nature* **1998**, *394*, 277-281.
119. Lambert, D. M.; Vandevoorde, S.; Jonsson, K. O.; Fowler, C. J., The palmitoylethanolamide family: A new class of anti-inflammatory agents? *Curr. Med. Chem.* **2002**, *9*, 663-674.
120. Rodriguez de Fonseca, F.; Navarro, M.; Gomez, R.; Escuredo, L.; Nava, F.; Fu, J.; Murillo-Rodriguez, E.; Giuffrida, A.; LoVerme, J.; Gaetani, S.; Kathuria, S.; Gall, C.; Piomelli, D., An anorexic lipid mediator regulated by feeding. *Nature* **2001**, *414*, 209-212.
121. Schuel, H.; Goldstein, E.; Mechoulam, R.; Zimmerman, A. M.; Zimmerman, S., Anandamide (arachidonylethanolamide), a brain cannabinoid receptor agonist, reduces sperm

fertilizing capacity in sea urchins by inhibiting the acrosome reaction. *Proc. Natl. Acad. Sci. U. S. A.* **1994**, *91*, 7678-7682.

122. Gupta, R. K.; Varanelli, C. L.; Griffin, P.; Wallach, D. F. H.; Siber, G. R., Adjuvant properties of non-phospholipid liposomes (Novasomes(R)) in experimental animals for human vaccine antigens. *Vaccine* **1996**, *14*, 219-225.

123. Wechtersbach, L.; Poklar, N.; Cigić, B., Liposomal stabilization of ascorbic acid in model systems and in food matrices. *LWT Food Sci. and Technol.* **2012**, *45*, 43-49.

124. Mantsch, H. H.; McElhaney, R. N., Phospholipid phase transitions in model and biological membranes as studied by infrared spectroscopy. *Chem. Phys. Lipids* **1991**, *57*, 213-226.

125. Casal, H. L.; Mantsch, H. H., Polymorphic phase behaviour of phospholipid membranes studied by infrared spectroscopy. *Biochim. Biophys. Acta* **1984**, *779*, 381-401.

126. Kodati, R. V.; Lafleur, M., Comparaison between orientational and conformational orders in fluid lipid bilayers. *Biophys. J.* **1993**, *64*, 163-170.

127. Umemura, J.; Cameron, D. G.; Mantsch, H. H., A fourier transform infrared spectroscopic study of the molecular interaction of cholesterol with 1,2-dipalmitoyl-sn-glycero-3-phosphocholine. *Biochim. Biophys. Acta* **1980**, *602*, 32-44.

128. Wong, T. C.; Wong, N. B.; Tanner, P. A., A fourier transform IR study of the phase transitions and molecular order in the hexadecyltrimethylammonium sulfate/water system. *J. Coll. Interf. Sci.* **1997**, *186*, 325-331.

129. Snyder, R. G.; Strauss, H. L.; Cates, D. A., Detection and measurement of microaggregation in binary mixtures of esters and of phospholipid dispersions. *J. Phys. Chem.* **1995**, *99*, 8432-8439.

130. Snyder, R. G., Vibrational correlation splitting and chain packing for the crystalline n - alkanes. *J. Chem. Phys.* **1979**, *71*, 3229-3235.

131. Cameron, D. G.; Casal, H. L.; Gudgin, E. F.; Mantsch, H. H., The gel phase of dipalmitoyl phosphatidylcholine an infrared characterisation of the acyl chain packing. *Biochim. Biophys. Acta* **1980**, *596*, 463-467.

132. Seelig, J., Deuterium magnetic resonance: theory and application to lipid membranes. *Q. Rev. Biophys.* **1977**, *10*, 353-418.

133. Vist, M. R.; Davis, J. H., Phase equilibria of cholesterol/dipalmitoylphosphatidylcholine mixtures:  $^2\text{H}$  nuclear magnetic resonance and differential scanning calorimetry. *Biochemistry* **1990**, *29*, 451-464.
134. Davis, J. H., Deuterium magnetic resonance study of the gel and liquid crystalline phases of dipalmitoyl phosphatidylcholine. *Biophys. J.* **1979**, *27*, 339-358.
135. Dufourc, E. J.; Smith, I. C. P.; Jarrell, H. C., A  $^2\text{H}$ -NMR analysis of dihydrosterculoyl-containing lipids in model membranes : structural effects of a cyclopropane ring. *Chem. Phys. Lipids* **1983**, *33*, 153-177.
136. Sternin, E.; Bloom, M.; MacKay, A. L., De-Pake-ing of NMR spectra. *J. Magn. Reson.* **1983**, *55*, 274-282.
137. Soderman, O.; Stilbs, P., NMR-studies of complex surfactant systems. *Prog. Nucl. Magn. Reson. Spectrosc.* **1994**, *26*, 445-482.
138. Leal, C.; Rognvaldsson, S.; Fossheim, S.; Nilssen, E. A.; Topgaard, D., Dynamic and structural aspects of PEGylated liposomes monitored by NMR. *J. Coll. Interf. Sci.* **2008**, *325*, 485-493.
139. Tanner, J. E., Use of the stimulated echo in NMR diffusion studies. *J. Chem. Phys.* **1970**, *52*, 2523-2526.
140. Blümich, B., *NMR imaging of materials*. Oxford University Press ed.; New York, 2000; p 541.

## Chapter 2

# **Influence of the Nature of the Sterol on the Behavior of Palmitic Acid/Sterol Mixtures and Their Derived Liposomes**

Zhong-Kai Cui, Guillaume Bastiat, Chester Jin, Amir Keyvanloo, and Michel Lafleur

Reprinted with permission from

*Biochimica et Biophysica Acta*, 2010, **1798**, 1144–1152

Copyright © 2010 Elsevier B.V.

Keywords: Palmitic acid; Sterol; Liquid-ordered phase; Liposome; Permeability; pH-sensitive

## **2.1 Abstract**

The phase behavior of mixtures formed with palmitic acid (PA) and one of the following sterols (dihydrocholesterol, ergosterol, 7-dehydrocholesterol, stigmasterol and stigmastanol), in a PA/sterol molar ratio of 3/7, has been characterized by IR and  $^2\text{H}$  NMR spectroscopy at different pH. Our study shows that it is possible to form liquid-ordered (lo) lamellar phases with these binary non-phospholipid mixtures. The characterization of alkyl chain dynamics of PA in these systems revealed the large ordering effect of the sterols. It was possible to extrude these systems, using standard extrusion techniques, to form large unilamellar vesicles (LUVs), except in the case of ergosterol-containing mixture. The resulting LUVs displayed a very limited passive permeability consistent with the high sterol concentration. In addition, the stability of these PA/sterol self-assembled bilayers was also found to be pH-sensitive, therefore, potentially useful as nanovectors. By examining different sterols, we could establish some correlations between the structure of these bilayers and their permeability properties. The structure of the side chain at C17 of the sterol appears to play a prime role in the mixing properties with fatty acid.

## 2.2 Introduction

Cholesterol (Chol) and saturated linear fatty acid can form fluid lamellar phases with cholesterol content between 65, and 70 mol %.<sup>1-4</sup> The fatty acid in the resulting phase displays a very high chain order, likely because of the high cholesterol content, while both cholesterol and fatty acid display a fast rotational mobility, on the <sup>2</sup>H NMR time scale ( $\sim 10^{-5}$  s). Therefore a liquid-ordered (lo) phase, analogous to those formed by phospholipid/sterol systems (e.g.,<sup>5-7</sup>) was proposed. A very low thermal expansion coefficient has been predicted for these bilayers, a property that could be associated to the small size of the hydrophilic part of the molecular constituents.<sup>4</sup> The cholesterol content in these fluid bilayers is considerably higher than the reported cholesterol solubility in phospholipid bilayers.<sup>8</sup> Despite the high cholesterol content, the fatty acid/cholesterol systems can be extruded, using standard methods, to form large unilamellar vesicles (LUVs).<sup>4</sup> These LUVs showed a permeability that is much more limited than that found for phospholipid/Chol systems. Because the state of protonation of the fatty acid affects the stability of these bilayers, palmitic acid (PA)/Chol LUVs are pH-sensitive and this property can be exploited to induce pH-triggered release of the content, a characteristic that can be useful for controlled release of drugs.

It has been shown that it was also possible to prepare these high sterol-content non-phospholipidic liposomes with cholesterol sulphate.<sup>9</sup> At this point, the understanding of the molecular prerequisites leading to the formation of these fluid bilayers, prepared from a high proportion of cholesterol and a monoacylated amphiphiles, is limited. It has been found that hydrophobic matching between the length of the acyl chain fatty acid and that of the long axis of

cholesterol is required to form stable bilayers.<sup>3</sup> It is postulated that this matching maximizes the interactions between the two molecular species, preventing a phase separation that would lead to the destabilization of the fluid bilayers. At the interfacial level, the electrostatic interactions appear to be a critical parameter for the stability of the fluid bilayers. In the presence of cholesterol, it was shown that the fluid lamellar phases were more stable when large fraction of the carboxylic groups were unprotonated.<sup>1, 2</sup> The substitution of cholesterol by cholesterol sulphate changed drastically this behavior.<sup>9</sup> In the presence of cholesterol sulphate, fluid bilayers were stable at low pH, when PA was protonated, and became unstable at high pH, upon deprotonation of PA.

In the present paper, we examine whether the formation of fluid bilayers with palmitic acid is a general behavior shared by several sterol molecules or if it is a peculiar property of cholesterol, and cholesterol sulphate. It has been shown that several sterols share a common impact on the properties of phospholipid bilayers.<sup>10-20</sup> For example, several sterols were shown to rigidify the phospholipid acyl chains, even though the extent of the rigidification depends on the molecular details of the sterol structure. Similarly the induction of the liquid-ordered phase appears to be a feature shared by several sterols. On the basis of these similarities observed for phospholipid bilayers, a "universal behavior" of sterol has been recently proposed.<sup>13</sup> We have examined the phase behavior of mixtures of palmitic acid with 5 different sterols: dihydrocholesterol, ergosterol, 7-dehydrocholesterol, stigmasterol and stigmasterol; their structures are presented in Figure 2.1. All these investigated sterols are neutral, have a hydroxyl group at the position 3, and methyl groups are present at positions C10, and C13. Their dimensions are comparable and they are classified as membrane-active sterol.<sup>21</sup> Cholesterol,

dihydrocholesterol and 7-dehydrocholesterol bear the same alkyl side chain at C17 whereas ergosterol and stigmasterol include a trans double bond at C22–C23 and a methyl or ethyl group at C24. Differences are also observed at the steroid skeleton level. Cholesterol and stigmasterol have a double bond between C5 and C6. The ring network is completely saturated for dihydrocholesterol and stigmasterol whereas 2 conjugated C=C bonds are present at C5–C6 and C7–C8 in 7-dehydrocholesterol and ergosterol. Ergosterol is the main sterol in fungal membranes whereas stigmasterol is a predominant plant sterol. 7-dehydrocholesterol is a cholesterol precursor. The phase behavior of these mixtures was characterized by IR and  $^2\text{H}$  NMR spectroscopy. The comparison of the behavior of these different mixtures provides additional insights into the rules dictating the formation of self-assembled fluid bilayers with high sterol content. In addition we have examined the possibility to form LUVs with the mixtures forming fluid lamellar phases and we have characterized their permeability in order to establish a relationship between the structure of these bilayers and their permeability properties. The characterization of the influence of the molecular details of the sterol molecules on the properties of these non-phospholipid bilayers also brings, by extension, insights into their influence on phospholipid bilayers and biological membranes.

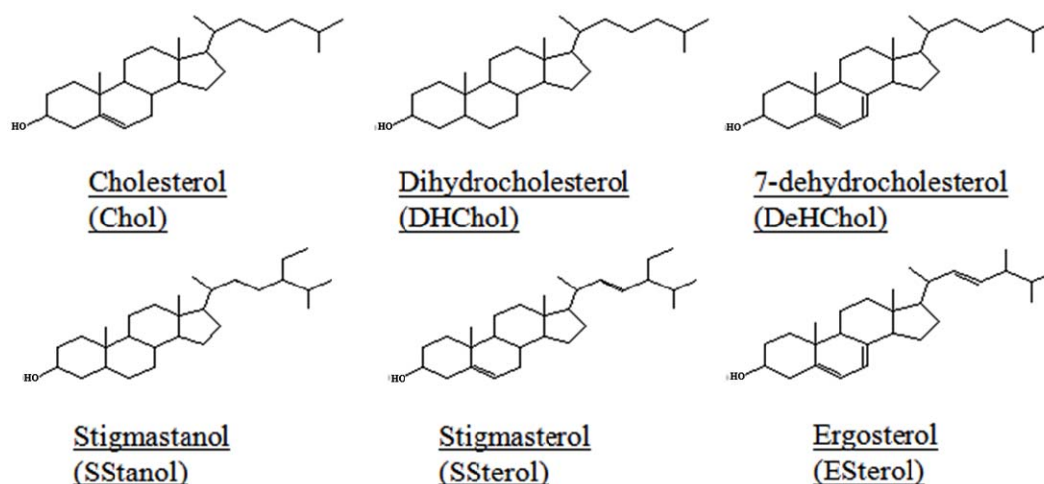


Figure 2.1. Formula of various investigated sterols.

## 2.3 Materials and methods

Cholesterol (>99%), dihydrocholesterol (95%), ergosterol (75%), 7-dehydrocholesterol (>85%), stigmasterol (95%), stigmastanol (95%) PA (99%), tris(hydroxymethyl)aminomethane (TRIS) (99%), 2-[N-morpholino]ethanesulfonic acid (MES) (>99%), ethylenediaminetetraacetic acid (EDTA) (99%), NaCl (>99%), Triton X-100 (99%), deuterium-depleted water (>99.99%) were supplied by Sigma Chemical Co. (St. Louis, MO, USA). Deuterated palmitic acid (PA-d<sub>31</sub>) (98.9%) was supplied from CDN Isotopes (Pointe-Claire, QC, Canada). Calcein (high purity) has been obtained from Molecular Probes (Eugene, OR, USA). Sephadex G-50 Medium was purchased from Pharmacia (Uppsala, Sweden). Methanol (spectrograde) and benzene (high purity) were obtained from American Chemicals Ltd. (Montreal, QC, Canada), and BDH Inc. (Toronto, ON, Canada), respectively. All solvents and products were used without further purification.

Mixtures of PA and sterol were prepared by dissolving weighed amounts of the solids in a mixture of benzene/methanol 95/5 (v/v). The solutions were then frozen in liquid nitrogen and lyophilized for at least 16 hours to allow complete sublimation of the organic solvent. For the  $^2\text{H}$  NMR and IR experiments, PA was replaced by PA- $\text{d}_{31}$ . In this study, all the mixtures had a PA/sterol molar ratio of 3/7 because its ratio was shown to lead to fluid lamellar phases with cholesterol and cholesterol sulphate.<sup>2, 9</sup> The freeze-dried lipid mixtures were hydrated with an MES/TRIS buffer (TRIS 50 mM, MES 50 mM, NaCl 10 mM, EDTA 5 mM) providing a buffered range between pH 5 and 9. The buffer was prepared with deuterium-depleted water for IR spectroscopy and  $^2\text{H}$  NMR samples. The final lipid concentration was 30 mg/mL for IR spectroscopy and  $^2\text{H}$  NMR experiments. The suspensions were subjected to five cycles of freezing-and-thawing (from liquid nitrogen temperature to 75 °C) and vortexed between successive cycles, to ensure a good hydration of the samples. After hydration, the pH was measured and readjusted, if necessary, by the addition of HCl or NaOH diluted solution.

The IR spectra were recorded on a Thermo Nicolet 4700 spectrometer, equipped with a KBr beam splitter and a DTGS-L-alanine detector. Briefly, an aliquot of the sample was placed between two  $\text{CaF}_2$  windows separated by a 5  $\mu\text{m}$ -thick Teflon ring. This assembly was inserted in a brass sample holder, whose temperature was controlled using Peltier thermopumps. Each spectrum was the result of 60 scans with a nominal  $2\text{ cm}^{-1}$  resolution Fourier transformed using a triangular apodization function. The temperature was varied from low to high, with 2 °C steps and a 5 min-incubation period prior to the data acquisition. The reported band positions correspond to the centers of gravity calculated from the top 5% of the band.

The  $^2\text{H}$  NMR spectra were recorded on a Bruker AV-400 spectrometer, using a Bruker static probe equipped with a 10 mm coil. A quadrupolar echo sequence was used with a  $90^\circ$  pulse of 6.1  $\mu\text{s}$  and an interpulse delay of 26  $\mu\text{s}$ . About 1 mL of the sample was transferred into a home-made Teflon holder after hydration. The recycling time was 60 s. In absence of a slow-relaxation component, namely a solid phase, the recycling delay was reduced to 0.3 s. Typically 4000 FID were co-added. The temperature was regulated using a Bruker VT-3000 controller. The characteristic fluid-phase spectra were dePaked using an iterative method.<sup>22</sup> However the recorded spectra of PA/ergosterol and PA/stigmasterol mixtures, at pH 8.4, were typical of partially oriented samples and the dePaked spectra exhibit unphysical negative amplitudes. In these cases, the regularization dePakeing algorithm was used.<sup>23</sup> The smoothed order profiles were extracted from the dePaked spectra using an established procedure.<sup>24</sup> This approach assumes a monotonic decrease of orientation order along the alkyl chain, from the head group toward its end. The quadrupolar splitting of the terminal  $\text{CD}_3$  was, however, measured directly on the dePaked spectra as it was always well resolved. The orientational order parameters,  $S_{\text{C-D}}$ , were calculated from these splittings. The proportions of the different phases could be estimated from the  $^2\text{H}$  NMR spectra. The solid phase proportions were obtained from the area integrations prior to and after the subtraction of the solid spectral component. When present, the isotropic phase proportion was similarly estimated from the area integrations prior to and after the elimination of the narrow central peak. The remaining area was associated with the lo phase.

The permeability of the LUVs was measured using a standard procedure based on the self-quenching property of calcein at high concentration.<sup>25,26</sup> LUVs loaded with calcein (80 mM) were prepared from PA/sterol mixtures in the previously described MES/TRIS buffer, pH 7.4 to

obtain a final lipid concentration of 20 mM. The LUVs were prepared by extrusion using a handheld Liposofast extruder (Avestin, Ottawa, Canada). The dispersions were passed 15 times through two stacked polycarbonate filters (100 nm-pore size) at  $\sim 75$  °C. Calcein-containing LUVs were separated at room temperature from free calcein by gel permeation chromatography, using Sephadex G-50 Medium (column diameter: 1.5 cm, length: 25 cm, equilibrated with an iso-osmotic MES/TRIS buffer (MES 50 mM, TRIS 50 mM, NaCl 130 mM, EDTA 5 mM, pH 7.4). The collected vesicle fraction was diluted 100 times and these stock LUVs suspensions were incubated at a given temperature. Fluorescence intensities were recorded on a SPEX Fluorolog spectrofluorometer and the excitation and emission wavelengths were 490 and 513 nm and the bandwidth widths were set to 1.5 and 0.5 nm respectively. To determine the proportion of entrapped calcein, its fluorescence was measured before and after the addition of 10  $\mu$ L of Triton X-100 solution (10% (v/v) in the MES/TRIS buffer). The fluorescence intensity, measured after addition of the detergent, corresponded to the complete calcein release, and was used to normalize the leakage.

To study the passive leakage, the calcein fluorescence intensity was measured from an aliquot of the stock LUVs suspension, freshly isolated by gel permeation chromatography, prior to ( $I_i$ ) and after ( $I_{i+T}$ ) the addition of Triton X-100. These intensity values corresponded to  $t = 0$  for the kinetic studies, and it was assumed that the calcein was completely encapsulated. After a given incubation time, the calcein fluorescence intensity was measured on another aliquot of the same stock LUVs suspension before ( $I_f$ ) and after ( $I_{f+T}$ ) the addition of Triton X-100. The percentage of encapsulated calcein remaining at that time in the LUVs was calculated as follows:

$$\% \text{ of encapsulated calcein} = \left( \frac{(I_{f+T} - I_f) / I_{f+T}}{(I_{i+T} - I_i) / I_{i+T}} \right) \times 100. \quad (2.1)$$

The % of release corresponded to (100 – % of encapsulated calcein).

The pH-triggered leakage of calcein was also examined. The pH was modified by adding aliquots of a diluted NaOH or HCl solution, and the calcein fluorescence intensities were measured immediately after the stabilization of pH, typically after ~2 minutes. The percentage of released calcein was calculated with the relation presented above, except  $I_i$  and  $I_{i+T}$  corresponded to the measurements at the initial pH, before and after the addition of Triton X-100 respectively.  $I_f$  and  $I_{f+T}$  were obtained on an aliquot at a modified pH, before and after the addition of Triton X-100 respectively. The pH effect was examined for either an increase or a decrease in pH. The calcein fluorescence intensity was relatively constant over the investigated pH range.<sup>25</sup>

The hydrodynamic diameters of the LUVs were measured at 25 °C using a Coulter N4 Plus quasi-elastic light scattering apparatus coupled with a Malvern autocorrelator. The scattering light intensity was adjusted by diluting the dispersions with the MES/TRIS buffer.

## 2.4 Results

### 2.4.1. IR spectroscopy experiments

The thermotropism of various PA-d<sub>31</sub>/sterol mixtures was examined at pH 7.4 and 8.4, using the shift of the symmetric C–D stretching mode of the methylene groups ( $\nu_{C-D}$ ) in the IR

spectra (Figure 2.2). As the samples were also used for  $^2\text{H}$  NMR spectroscopy, the deuterated form of the fatty acid was used; this also presents the advantage of avoiding spectral interferences associated with sterols in the C–H stretching region. The  $\nu_{\text{C-D}}$  mode is mainly sensitive to trans–gauche isomerisation along the acyl chains and to interchain coupling,<sup>27,28</sup> providing a sensitive probe for transitions involving the introduction of chain conformational disorder. At pH 7.4, the spectra of PA-d<sub>31</sub>/stigmasterol and PA-d<sub>31</sub>/ergosterol mixtures displayed, at low temperature, a  $\nu_{\text{C-D}}$  band at  $\sim 2088.5\text{ cm}^{-1}$ , a position indicative of deuterated lipids in the solid state.<sup>1, 29</sup> At  $\sim 55\text{ }^\circ\text{C}$ , an abrupt shift of the  $\nu_{\text{C-D}}$  band position was observed, leading to  $\nu_{\text{C-D}}$  band at  $2094.5\text{ cm}^{-1}$ , a value typical for disordered chains. This variation is therefore characteristic of a solid-to-disordered phase transition. In contrast, the  $\nu_{\text{C-D}}$  band position remained relatively constant at  $2091.5\text{ cm}^{-1}$  over the whole investigated temperature range for the PA-d<sub>31</sub>/dihydrocholesterol and PA-d<sub>31</sub>/7-dehydrocholesterol mixtures. This value is typical of those measured for systems in the lo phase. PA-d<sub>31</sub>/stigmastanol shows an intermediate behavior: there was a small shift of the  $\nu_{\text{C-D}}$  band between  $45$  and  $50\text{ }^\circ\text{C}$ , going from  $2089.5$  to  $2091.5\text{ cm}^{-1}$ . An analogous thermal behavior was observed at pH 8.4 except that the amplitude of the transition of the PA-d<sub>31</sub>/stigmasterol and PA-d<sub>31</sub>/ergosterol mixtures was considerably reduced. The  $\nu_{\text{C-D}}$  band was located at about  $2092\text{ cm}^{-1}$ , corresponding to the values observed for the lo phase.

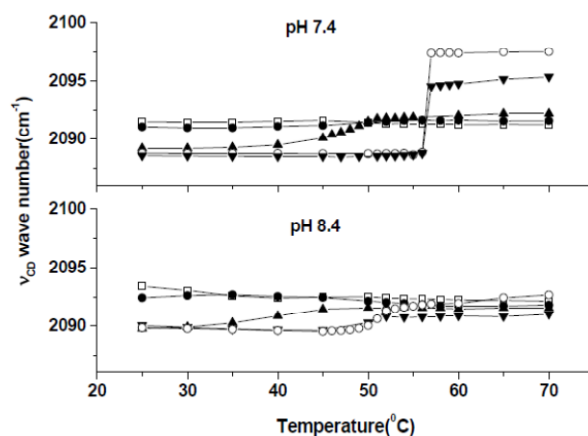


Figure 2.2. Thermotropism of PA- $d_{31}$  in PA- $d_{31}$ /sterol (3/7 molar ratio) mixtures at pH 7.4 and 8.4, probed using the  $\nu_{C-D}$  band position. The sterol in the mixture was dihydrocholesterol ( $\square$ ), 7-dehydrocholesterol ( $\bullet$ ), stigmasterol ( $\blacktriangle$ ), stigmasterol ( $\circ$ ), or ergosterol ( $\blacktriangledown$ ).

The protonation state of PA- $d_{31}$  has been examined using IR spectroscopy. This technique is highly suitable for addressing this question as the protonated and unprotonated forms lead to two well resolved bands.<sup>2, 4, 30</sup> The C=O stretching associated to the COOH group is located at around  $1700\text{ cm}^{-1}$  whereas the C–O stretching group of the COO<sup>-</sup> is found at  $1550\text{ cm}^{-1}$ , because of the weakening of the covalent bond. The changes associated with the pH variations are shown for the relevant region of the IR spectrum of PA/dihydrocholesterol mixture (Figure 2.3). At low pH, the region is dominated by a band at  $1700\text{ cm}^{-1}$ , showing that the fatty acid molecules were all protonated. Upon a pH increase, there was a decrease of the intensity of this component and, in parallel, the intensity of component associated to unprotonated acid, at  $1550\text{ cm}^{-1}$ , increased. These changes demonstrated the deprotonation of PA- $d_{31}$  inserted in these sterol-rich bilayers. The apparent  $pK_a$  could be estimated to  $\sim 7$ , a value consistent with the apparent  $pK_a$  reported for PA/Chol mixtures<sup>9</sup> as well as for PA incorporated in other fluid lipid matrices.<sup>30, 31</sup> Analogous changes were observed for the other sterol mixtures investigated in this work (data not shown).

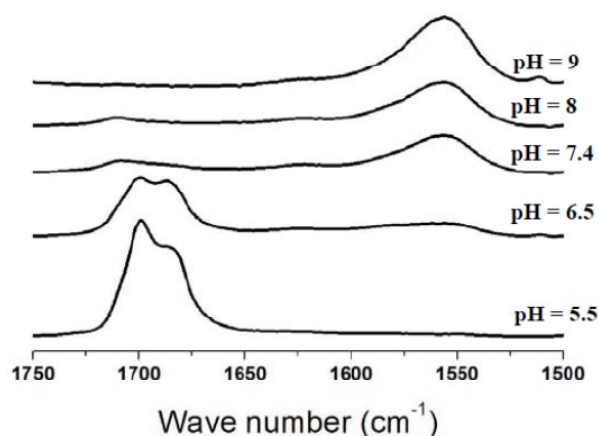


Figure 2.3. pH dependence of the  $\nu_{\text{CO}}$  mode of the PA carboxylic/carboxylate group in PA/dihydrocholesterol mixture (3/7 molar ratio) at room temperature. The spectra were normalized to provide a constant area of the  $\nu_{\text{CO}}$  bands.

The  $\text{CD}_2$  deformation mode  $\delta(\text{CD}_2)$ , between  $1080$ , and  $1100 \text{ cm}^{-1}$ , was examined to characterize the chain packing of the fatty acid (Figure 2.4). At  $30 \text{ }^\circ\text{C}$ , the  $\delta(\text{CD}_2)$  mode of PA- $d_{31}$ /stigmasterol and PA- $d_{31}$ /ergosterol mixtures gave rise, for both pH 7.4 and 8.4, to two components located at  $1091$  and  $1086 \text{ cm}^{-1}$ . This splitting is typical of crystalline fatty acid chains packed in an orthorhombic symmetry.<sup>32</sup> This splitting resulted from an interchain coupling that is only possible when the vibrations of adjacent molecules have similar frequencies. Therefore it implies that the sterol was practically excluded from the PA crystalline domains, as the splitting corresponded to that observed for pure PA- $d_{31}$ .<sup>32-34</sup> Only a single component at  $1088 \text{ cm}^{-1}$  was observed for the mixtures prepared from PA- $d_{31}$ /dihydrocholesterol and PA- $d_{31}$ /7-dehydrocholesterol mixtures at both pH. Therefore it is inferred that the fatty acid molecules in these mixtures do not form solid phase with orthorhombic chain packing. This single band is compatible with the formation of a lo lamellar phase as suggested from the  $\nu_{\text{C-D}}$  band position. In the case of PA- $d_{31}$ /stigmasterol mixture, it seems that there was the coexistence of the doublet at

1091 and 1086  $\text{cm}^{-1}$  and the single component at 1088  $\text{cm}^{-1}$ , giving rise to a broad signal in this region. The proportion of the doublet appears to be decreased at pH 8.4 compared to pH 7.4; this is consistent with the conclusion that higher pH favors the fluid phase, the solid phase being more stable at low pH.

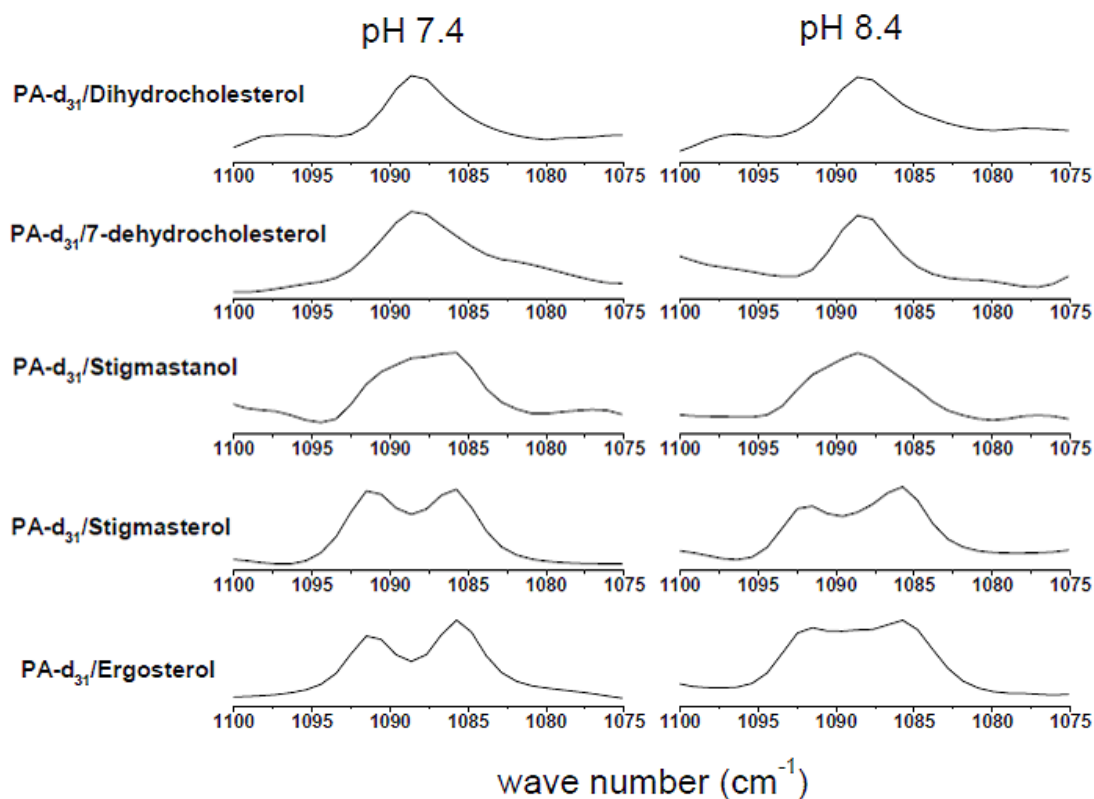


Figure 2.4. The CD<sub>2</sub> deformation band shape for various PA-d<sub>31</sub>/sterol mixtures (3/7 molar ratio, 30 °C).

## 2.4.2. NMR experiments

Figure 2.5 presents the  $^2\text{H}$  NMR spectra of PA- $\text{d}_{31}$ /dihydrocholesterol, and PA- $\text{d}_{31}$ /stigmasterol mixtures, with a molar ratio of 3/7, at various pH and temperatures; these are representative of the spectra recorded for the various PA- $\text{d}_{31}$ /sterol mixtures. The spectra of PA- $\text{d}_{31}$ /dihydrocholesterol system, pH 7.4 (Figure 2.5 B), are essentially characteristic of a fluid lamellar phase component; they correspond to several overlapping and unresolved powder patterns with different quadrupolar splittings, associated with the gradient of orientational order existing along the acyl chains.<sup>1, 5, 35, 36</sup> The quadrupolar splitting of the outermost doublet of the spectrum recorded at 25 °C is 54 kHz. This large value is typical of lipids in the  $\text{l}_\alpha$  phase.<sup>1, 5, 13</sup> The spectra of PA- $\text{d}_{31}$ /stigmasterol system recorded, at pH 7.4, include 3 components characteristic of different phases (Figure 2.5 C). First, a solid phase component corresponds to two superimposed powder patterns with quadrupolar splittings measured between their maxima of 35 and 120 kHz. This signal is consistent with solid fatty acid for which the acyl chain is in an all-trans conformation and immobile (on the NMR time scale).<sup>1, 35, 37</sup> The broader pattern is associated with the equivalent  $\text{CD}_2$  groups along the chain while the narrower powder pattern corresponds to the terminal  $\text{CD}_3$ . Second, a fluid lamellar phase is observed. Third, a narrow peak centered at 0 kHz is associated with isotropic phase. At 25 °C, the spectrum is essentially composed of the solid and  $\text{l}_\alpha$  components. Upon heating, there is a significant decrease in the proportion of the solid component. At 65 °C, the solid signal has completely disappeared and the apparition of the narrow line indicates the formation of a new phase, where fatty acid molecules experience isotropic motion. It should be noted that neither liquid-disordered phase nor gel phase was observed.

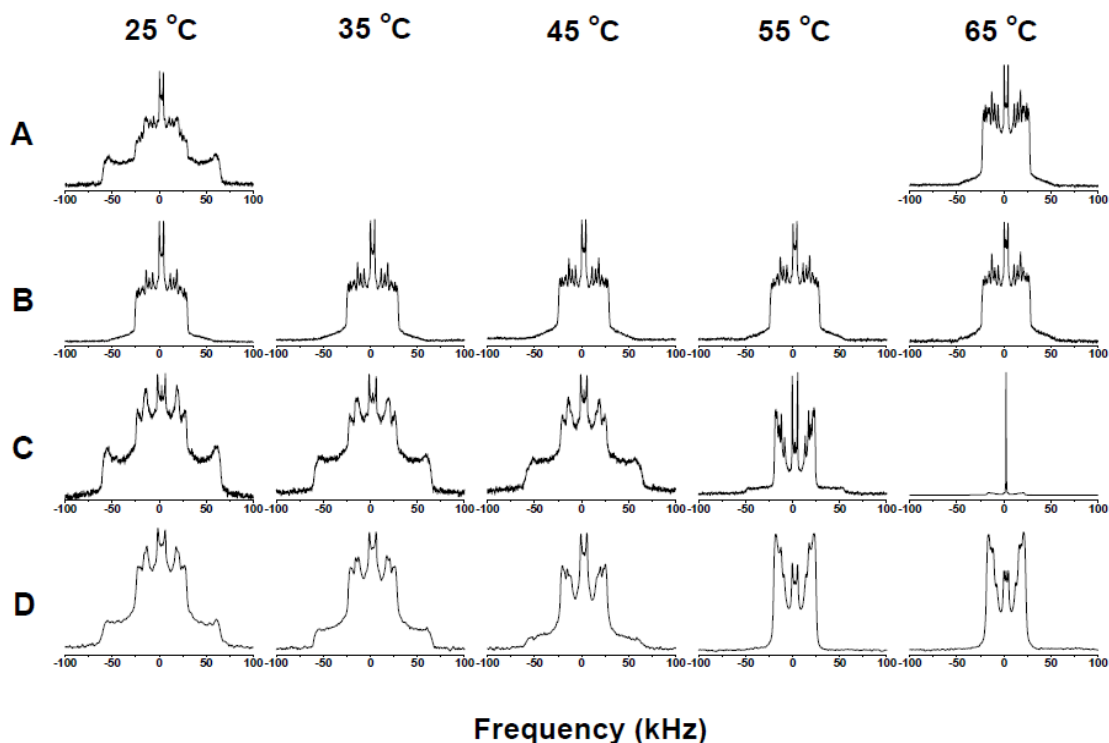


Figure 2.5.  $^2\text{H}$ -NMR spectra of (A) PA- $\text{d}_{31}$ /dihydrocholesterol mixture, pH 5.5; (B) PA- $\text{d}_{31}$ /dihydrocholesterol mixture, pH 7.4; (C) PA- $\text{d}_{31}$ /stigmasterol, pH 7.4; (D) PA- $\text{d}_{31}$ /stigmasterol, pH 8.4 (PA- $\text{d}_{31}$ /Sterol 3/7 molar ratio). Temperatures were indicated on the top of each column.

A decrease of pH favors the formation of the solid component. At 25 °C, the  $^2\text{H}$  NMR spectra of PA- $\text{d}_{31}$ /dihydrocholesterol mixture at pH 7.4 are typical of a lo phase. At pH 5.5, however, the spectrum includes a solid and a fluid lamellar components (Figure 2.5 A). The proportion of solid was estimated to 56%. At 65 °C, only the fluid component is observed and its width is found practically independent of the pH. The spectra of PA- $\text{d}_{31}$ /stigmasterol mixture show the same trend. For example, at 25 °C, the spectrum includes a larger proportion of the solid component at pH 7.4 than at pH 8.4. This feature is consistent with previous studies on PA/cholesterol systems.<sup>2</sup>

Figure 2.5 D shows the evolution of the  $^2\text{H}$  NMR spectrum of PA- $d_{31}$ /stigmasterol, pH 8.4, as a function of temperature. At low temperatures, the spectra show a coexistence of solid and lo phases. There is a melting of the solid phase between 45, and 55 °C, a temperature at which only the fluid component is observed. It is interesting to point out that in this case, as well as in the case of PA- $d_{31}$ /ergosterol, the spectra are typical of oriented bilayers. The intensity of the shoulders, corresponding to lipids with their rotation axis parallel with the magnetic field, is considerably reduced compared to the typical powder pattern associated to a random orientation distribution. By comparing the quadrupolar splittings of these spectra with those obtained with other sterols, the bilayers formed by these systems partially orient with their normal perpendicular with the external magnetic field. It was inferred from the spectra analysis assuming an ellipsoidal orientation distribution of the lipids that, at 65 °C, the ratio of long/short ellipsoidal axis was 2.3 and 2.1 for the PA- $d_{31}$ /stigmasterol and PA- $d_{31}$ /ergosterol mixtures, respectively.

In order to summarize the thermal evolution of the different phases, as calculated from the  $^2\text{H}$  NMR spectra, is presented in Figure 2.6. For PA- $d_{31}$ /dihydrocholesterol and PA- $d_{31}$ /7-dehydrocholesterol mixtures, the spectra indicated that the mixture formed exclusively a lo lamellar phase over the investigated temperature range. The mixtures with stigmastanol, stigmasterol, and ergosterol included, at 25 °C, the coexistence of a solid and a lo lamellar components. An increase in temperature led to the decrease of the proportion of solid PA- $d_{31}$  and eventually to the disappearance of this component; these transitions are consistent with the IR spectroscopy results. The mixtures including stigmasterol and ergosterol had the largest fraction of solid phase at low temperature. Above ~60 °C, no solid component could be observed. For these mixtures that included a solid fraction at low temperatures, it was also observed that heating

above 60 °C led to the formation of an isotropic phase (expressed on the figure as a decrease of the % of lo phase). The proportion of the isotropic phase increased upon heating to reach between 49 and 20% at 65 °C.

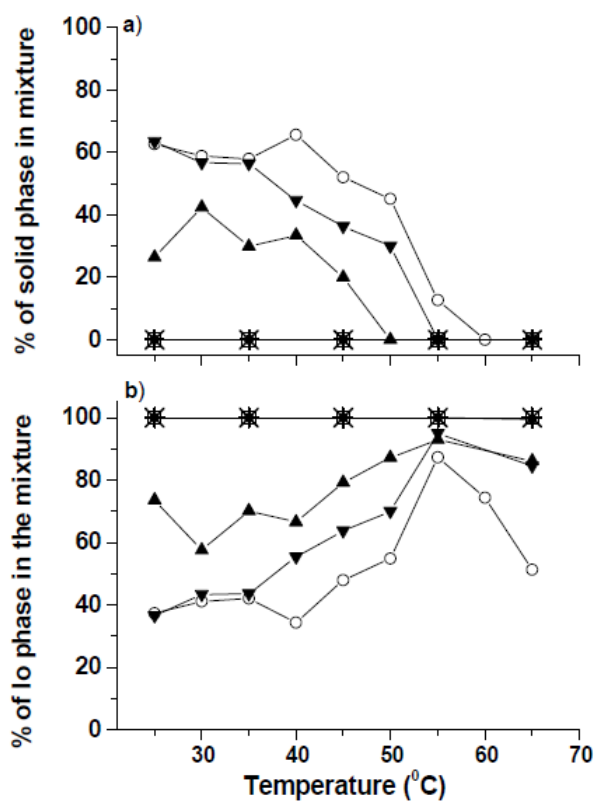


Figure 2.6. Thermal evolution of the phase composition of the various PA-d<sub>31</sub>/sterol mixtures (molar ratio of 3/7). a) Solid and b) lo phase proportions versus temperature for PA-d<sub>31</sub>/Chol (\*), PA-d<sub>31</sub>/dihydrocholesterol (□), PA-d<sub>31</sub>/7-dehydrocholesterol (●), PA-d<sub>31</sub>/stigmastanol (▲), PA-d<sub>31</sub>/stigmasterol (○), and PA-d<sub>31</sub>/ergosterol (▼) mixtures, pH 7.4.

The smoothed order profiles associated with the fluid lamellar component in the spectra of PA- $d_{31}$ /sterol mixtures, pH 8.4, are presented in Figure 2.7. This pH was selected because all the systems displayed lo phases except PA- $d_{31}$ /stigmasterol mixture at low temperature. The order profiles were all typical of the lo phase.<sup>1, 2, 5</sup> The region near the interface displayed a relatively constant and high orientational order, followed by an abrupt decrease of order along the chain toward the middle of the bilayer. The order parameter in the plateau region were very high, varying, at 25 °C, between 0.45 and 0.47, indicative of PA acyl chains that are nearly in an all-trans configuration. All the investigated sterols gave rise to high PA- $d_{31}$  acyl chain order. An increase of temperature led to a decrease of orientational order. Typically, between 25 and 65 °C, the averaged  $S_{C-D}$  decreased by about 10%. It should be noted that the fatty acid chain in the PA- $d_{31}$ /stigmastanol and PA- $d_{31}$ /stigmasterol mixtures was slightly less ordered near the end of the chain (carbon positions 14 to 16) than that observed for the mixtures with other sterols, suggesting a local effect of the bulky alkyl tail group.

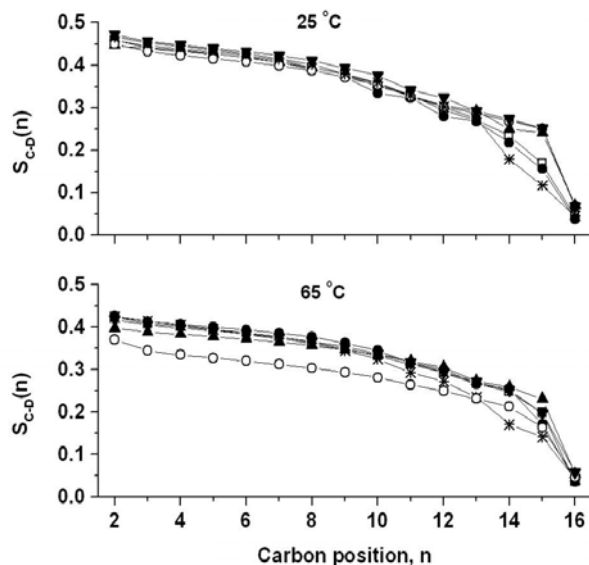


Figure 2.7. Orientational order profile of PA-d<sub>31</sub> alkyl chain, obtained from the lamellar fraction of PA-d<sub>31</sub>/Chol (\*), PA-d<sub>31</sub>/dihydrocholesterol (□), PA-d<sub>31</sub>/7-dehydrocholesterol (●), PA-d<sub>31</sub>/stigmastanol (▲), PA-d<sub>31</sub>/stigmasterol (○), and PA-d<sub>31</sub>/ergosterol (▼) mixtures. For all the mixtures, the PA-d<sub>31</sub>/sterol molar ratio was 3/7 and pH was 8.4.

### 2.4.3. PA/sterol LUVs

It has been shown that, despite the very high cholesterol content, it is possible to extrude the PA/Chol or PA/Schol mixtures, at neutral pH.<sup>4,9</sup> We have therefore examined the possibility to prepare LUVs from the PA/sterol mixtures. The extrusions were carried out at pH 7.4 and room temperature. Table 2.1 summarizes the results, including PA/Chol system as a control. Only the PA/ergosterol mixture could not be extruded in these conditions; the presence of solid particles blocking the pores of the filters was likely the origin of this phenomenon. For PA/Chol, PA/stigmastanol and PA/dihydrocholesterol mixtures, LUVs with a unimodal size distribution

were obtained and their average size, as determined by dynamic light scattering, was consistent with the diameter of the pores in the polycarbonate filters (100 nm). For PA/stigmasterol and PA/7-dehydrocholesterol mixtures, a bimodal distribution was observed after extrusion. The mean hydrodynamic diameter of one population was close to 100 nm, likely associated to isolated LUVs produced by the extrusion through the filters while the mean diameter of the other population was much larger than 100 nm. The trapping capacity of these LUVs was assessed by fluorescence. The initial self-quenching of calcein entrapped in the LUVs was between 0.80 and 0.93. These values were close to that expected for the encapsulation of a 80 mM calcein solution<sup>25,38</sup> demonstrating the efficient trapping during the extrusion process and the isolation of the calcein-loaded LUVs.

Table 2.1. Characteristics of extruded LUVs for various PA/sterol 3/7 (molar ratio) mixtures.

|                         | $d_{LUVs}$ (nm) (proportion) | Initial self-quenching |
|-------------------------|------------------------------|------------------------|
| PA/Chol                 | $117 \pm 22$ (100%)          | $0.871 \pm 0.013$      |
| PA/dihydrocholesterol   | $103 \pm 23$ (100%)          | $0.930 \pm 0.019$      |
| PA/7-dehydrocholesterol | $114 \pm 33$ (72%)           | $0.908 \pm 0.007$      |
|                         | $255 \pm 68$ (28%)           |                        |
| PA/ergosterol           | Impossible to extrude        |                        |
| PA/stigmastanol         | $121 \pm 21$ (100%)          | $0.80 \pm 0.10$        |
| PA/stigmasterol         | $80 \pm 10$ (52%)            | 0.844                  |
|                         | $192 \pm 37$ (48%)           |                        |

The passive release from these vesicles was determined as a function of time (Figure 2.8). The passive leakage was found to be dependent on the nature of the sterol. It could be characterized by the time for which half the calcein was released ( $t_{1/2}$ ). This parameter corresponded to 20, 30, and 70 days for PA/stigmasterol, PA/stigmastanol, and PA/7-dehydrocholesterol LUVs respectively. The leakage was even more limited for PA/Chol, as previously shown,<sup>4</sup> and for PA/dihydrocholesterol LUVs that showed a release of about 30% of the content after 80 days of incubation.

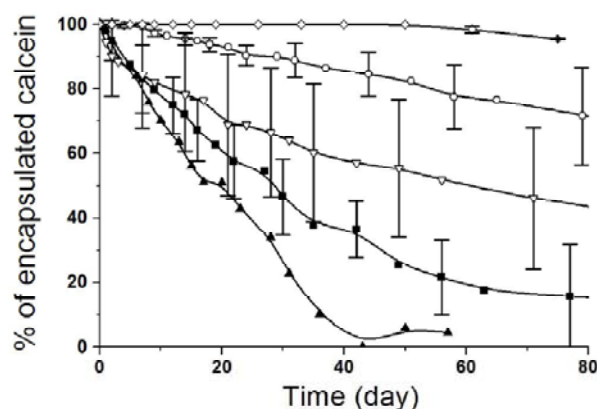


Figure 2.8. Passive leakage at room temperature from PA/Chol (◇), PA/dihydrocholesterol (○), PA/7-dehydrocholesterol (▽), PA/stigmastanol (■), and PA/stigmasterol (▲) LUVs. For all the mixtures, the PA/sterol molar ratio was 3/7 and pH was 7.4.

#### 2.4.4. Effect of pH on PA/sterol LUVs

Because of the presence of the carboxylic group, LUVs formed with Chol and Schol were shown to be pH sensitive.<sup>9</sup> In order to detail the impact of the sterol structure on the pH sensitivity, the leakage of PA/stigmastanol and PA/dihydrocholesterol LUVs (the 2 systems that provided LUVs with a unimodal size distribution) was characterized as a function of the external

pH; PA/Chol LUVs were also included in the study as a control. Figure 2.9 displays the potential of these LUVs for pH-triggered leakage as the content release is shown to be strongly dependent on the external pH. The pH profile of this release was similar for the 3 investigated systems. For  $\text{pH} \geq 6$ , the LUVs remained stable, even when the external pH was increased to 9.5. When the external pH was decreased to lower values, a release was then triggered. At pH 4, most of the content was rapidly liberated. The different structural details of the investigated sterols did not seem to have a significant impact on this behavior. The protonated/unprotonated state of the carboxylic group is a key parameter in this behavior<sup>4</sup> and most likely dictates the release properties.

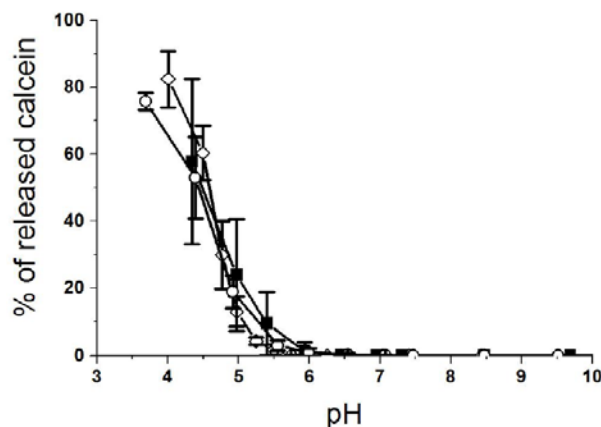


Figure 2.9. pH-triggered release of calcein from PA/Chol ( $\diamond$ ), PA/Dihydrocholesterol ( $\circ$ ), and PA/Stigmastanol ( $\blacksquare$ ) LUVs. The LUVs were prepared at pH 7.4 and the % release was measured after the change of the external pH.

## 2.5 Discussion

The present study reveals the impact of the nature of the sterol on the general behavior of PA/sterol systems. We show that, similar to previous observations with cholesterol and Schol,<sup>1,9</sup> mixtures of several neutral sterols with PA give rise to the formation of stable lamellar phases with a high sterol content. All the investigated membrane-active sterols were shown to induce the ordering of the PA alkyl chain, and to lead to the formation of fluid bilayers that could be extruded using standard extrusion techniques to provide LUVs. The alkyl chain ordering effect of the sterols is analogous to the previous observations on their effect on phospholipid bilayers.<sup>7, 10, 13, 36, 39-42</sup> The impact is associated with the presence of the 3-OH group that orients the sterol in the bilayers, the rigid and relatively flat steroid cycle network, and the flexible alkyl chain at position C17.

It should be pointed out that the sterol content in the bilayers investigated in the present paper is considerably higher than that typically used in phospholipid bilayers.<sup>8</sup> It has been shown that gel-phase bilayers could not be extruded by standard procedure.<sup>43</sup> Their resistance is associated with their high deformation modulus. The sterols of the non-phospholipidic bilayers prepared here appears to decrease the modulus in such a way that extrusion becomes possible if one excludes ergosterol; this sterol seems to have a limited solubility when combined with PA as discussed below.

The pH-sensitivity of the PA/sterol mixtures also displays similar features. The stability of the lamellar phase and the resulting liposomes is directly dictated by the protonation state of

the fatty acid. All the investigated mixtures were shown to form more stable lamellar phase at high pH, when most of the PA is unprotonated. At lower pH, when a significant fraction of the PA molecules are protonated, the bilayers become less stable. This behavior has been described in detail for the PA/Chol mixture.<sup>2,9</sup> In the investigated mixtures, we observed that a lower pH favored the formation of solid PA. In parallel, the decrease of the external pH triggered the release of the encapsulated material in the high sterol content LUVs. These results establish that the protonation state of the acid is a main feature dictating the bilayer stability. It has been proposed that the repulsion between the negatively charged unprotonated PA favors their mixing with the sterol molecules in order to limit this unfavorable contribution to the free energy.<sup>2</sup>

Even though a general behavior is induced by the various investigated neutral sterol, the nature of the sterol modulates its details in the mixtures with PA. On the basis of their behavior with PA, the investigated sterols can be divided into 2 groups: cholesterol, dihydrocholesterol and 7-dehydrocholesterol formed exclusively lamellar bilayers with 30 (mol) % PA at room temperature, at pH 7.4 whereas the mixtures with ergosterol, stigmasterol, and stigmasterol included a significant proportion of solid PA, as inferred from the <sup>2</sup>H NMR spectra and the  $\delta(\text{CD}_2)$  of the IR spectra. Moreover, the latter give rise to an isotropic phase upon heating above 60 °C. In parallel, the liposomes formed with sterol in the first group showed systematically a reduced passive permeability compared to those formed with a sterol from the second group. Ergosterol appears to be an extreme case in the second group because it was even impossible to obtain extruded liposomes, likely because it has a limited solubility with PA and the solid sterol particles would clog the filter pores. From a structural point of view, the sterols of the first group bear the same alkyl side chain at C17 whereas the sterol of the second group include a trans

double bond at C22–C23 and a methyl or ethyl group at C24. This difference is the likely origin of the different behavior. An alkyl substituent at C24 and a double bond between C22 and C23 have been previously identified as structural features limiting the interactions between the sterols and phospholipids.<sup>44</sup> These functional groups are proposed to lead to a bulkier and stiffer alkyl side chain at position 17. For example, the cross-sectional area of ergosterol was found to be significantly larger (+21%) than that of cholesterol.<sup>45</sup> Interestingly there is no consensus relative to the impact of this molecular change on the properties of phospholipid bilayers. Some studies report that the bulkier and stiffer alkyl chain limits the chain motions of the surrounding phospholipid and/or account for stronger van der Waals interactions and therefore causes a large ordering effect.<sup>10, 12</sup> An analogous rationale has been proposed to explain the reduced out-of-plane motion of ergosterol compared to cholesterol in DPPC fluid bilayers.<sup>11</sup> Conversely, other studies conclude that a large alkyl moiety at position 17 prevents the tight packing of the lipids and sterols bearing this bulky side chain lead to a reduced ordering effect compared to cholesterol. For example, it was observed that cholesterol leads to a larger stabilization of the lo phase in sphingomyelin bilayers compared to stigmasterol and ergosterol.<sup>46</sup> Similarly the condensing power of cholesterol on DPPC, sphingomyelin and POPC bilayers was found to be larger than that of ergosterol,<sup>12, 19, 47, 48</sup> a conclusion also supported by a monolayer study.<sup>49</sup> Cholesterol leads also to a larger increase of the bilayer bending rigidity than ergosterol.<sup>14</sup> These different effects may be related to the different parameters such as the unsaturation level of the alkyl chain of the interacting molecule, the proportion of sterol, and the temperature.<sup>10, 50</sup> In the present system, it is clear that the bulky alkyl group at position 17 unfavors the formation of fluid bilayers with PA. In parallel, a temperature increase promotes the formation of lo phase bilayers in the presence of the sterols with bulky alkyl groups, suggesting an entropy-driven phenomenon. It is proposed that the

bulky alkyl group reduces the van der Waals intermolecular interactions once incorporated in bilayer geometry. This decrease and the resulting reduction of the enthalpic term would lead to a phase separation and to the formation of solid PA- $d_{31}$  and, very likely, solid sterol. This conclusion is in good agreement with the limited solubility of stigmasterol recently reported in phospholipid bilayers that was attributed to "chain packing incompatibility".<sup>50</sup> A reduced solubility in phosphatidylcholine bilayers was also reported for stigmasterol and ergosterol compared to cholesterol.<sup>40</sup>

In addition to displaying a reduced propensity to form lo phase bilayers, stigmasterol, and stigmasterol mixed with PA- $d_{31}$  form LUVs with a reduced passive impermeability compared to cholesterol, dihydrocholesterol and 7-dehydrocholesterol. This observation could also be associated with the presence of the bulky alkyl side chain. The increased efflux could be due to an overall lipid packing which is not as tight as those obtained in the presence of sterol with a side chain at C17 identical to cholesterol. It could also be associated with a propensity of the mixture to phase separate. This hypothesis would be consistent with the reported effect of stigmasterol and cholesterol on the water permeability of phosphatidylcholine bilayers.<sup>39</sup> It was found that both sterols reduce the bilayer permeability to water but the effect of stigmasterol was less pronounced, an effect mainly attributed to the reduced alkyl chain ordering of the phosphatidylcholine.

In conclusion, under certain conditions, the mixtures of PA and various sterols can form fluid ordered bilayers, which are analogous to those previously reported for the PA/Chol and PA/Schol systems.<sup>1,2</sup> Conventional method can be used to extrude the PA/sterol mixtures to form stable LUVs, except PA/ergosterol system. The external pH can trigger the release of the

liposomes and the pH-sensitivity of these PA/sterol LUVs is particularly helpful for their use as nanocarriers for in vivo applications. All the sterols have the ability to order the acyl chain. However, different architectures of sterols have different propensities to form lo lamellar phase. Particularly, the structure of the alkyl tail chain has more pronounced effects than the ring network on the stability of the LUVs. The effect of the bulky group at the sterol C17 position on the neighboring alkyl chains is likely also present in phospholipid bilayers, as previously proposed.<sup>12, 19, 46-49</sup>

## **2.6 Acknowledgements**

Z.-K.C. is grateful to the China Scholarship Council and Université de Montréal for his scholarship. The authors would like to thank the Natural Sciences and Engineering Research Council of Canada for the financial support. This work was also funded by Fonds Québécois de la Recherche sur la Nature et les Technologies through its financial support to the Center for Self-Assembled Chemical Systems (CSACS).

## 2.7 References

1. Paré, C.; Lafleur, M., Formation of liquid ordered lamellar phases in the palmitic acid/cholesterol system. *Langmuir* **2001**, *17*, 5587-5594.
2. Ouimet, J.; Croft, S.; Paré, C.; Katsaras, J.; Lafleur, M., Modulation of the polymorphism of the palmitic acid/cholesterol system by the pH. *Langmuir* **2003**, *19*, 1089-1097.
3. Ouimet, J.; Lafleur, M., Hydrophobic match between cholesterol and saturated fatty acid is required for the formation of lamellar liquid ordered phases. *Langmuir* **2004**, *20*, 7474-7481.
4. Bastiat, G.; Oligier, P.; Karlsson, G.; Edwards, K.; Lafleur, M., Development of non-phospholipid liposomes containing a high cholesterol concentration. *Langmuir* **2007**, *23*, 7695-7699.
5. Vist, M. R.; Davis, J. H., Phase equilibria of cholesterol/dipalmitoylphosphatidylcholine mixtures:  $^2\text{H}$  nuclear magnetic resonance and differential scanning calorimetry. *Biochemistry* **1990**, *29*, 451-464.
6. Thewalt, J. L.; Bloom, M., Phosphatidylcholine: cholesterol phase diagrams. *Biophys. J.* **1992**, *63*, 1176-1181.
7. Paré, C.; Lafleur, M., Polymorphism of POPE/cholesterol system: a  $^2\text{H}$  nuclear magnetic resonance and infrared spectroscopic investigation. *Biophys. J.* **1998**, *74*, 899-909.
8. Bach, D.; Wachtel, E., Phospholipid/cholesterol model membranes: formation of cholesterol crystallites. *Biochim. Biophys. Acta* **2003**, *1610*, 187-197.
9. Bastiat, G.; Lafleur, M., Phase behavior of palmitic acid/cholesterol/cholesterol sulfate mixtures and properties of the derived liposomes. *J. Phys. Chem. B* **2007**, *111*, 10929-10937.
10. Endress, E.; Bayerl, S.; Prechtel, K.; Maier, C.; Merkel, R.; Bayerl, T. M., The effect of cholesterol, lanosterol, and ergosterol on lecithin bilayer mechanical properties at molecular and microscopic dimensions: a solid-state NMR and micropipet study. *Langmuir* **2002**, *18*, 3293-3299.
11. Endress, E.; Heller, H.; Casalta, H.; F., B. M.; Bayerl, T. M., Anisotropic motion and molecular dynamics of cholesterol, lanosterol, and ergosterol in lecithin bilayers studied by quasi-elastic neutron scattering. *Biochemistry* **2002**, *41*, 13078-13086.

12. Urbina, J. A.; Pekerar, S.; Le, H. B.; Patterson, J.; Montez, B.; Oldfield, E., Molecular order and dynamics of phosphatidylcholine bilayer membranes in the presence of cholesterol, ergosterol and lanosterol: a comparative study using  $^2\text{H}$ -,  $^{13}\text{C}$ - and  $^{31}\text{P}$ -NMR spectroscopy. *Biochim. Biophys. Acta* **1995**, *1238*, 163-176.
13. Henriksen, J.; Rowat, A. C.; Brief, E.; Hsueh, Y. W.; Thewalt, J. L.; Zuckermann, M. J.; Ipsen, J. H., Universal behavior of membranes with sterols. *Biophys. J.* **2006**, *90*, 1639-1649.
14. Henriksen, J.; Rowat, A. C.; Ipsen, J. H., Vesicle fluctuation analysis of the effects of sterols on membrane bending rigidity. *Euro. Biophys. J.* **2004**, *33*, 732-741.
15. E.Berring, E.; Borrenpohl, K.; J.Fliesler, S.; Serfis, A. B., A comparison of the behavior of cholesterol and selected derivatives in mixed sterol-phospholipid Langmuir monolayers: a fluorescence microscopy study. *Chem. Phys. Lipids* **2005**, *136*, 1-12.
16. Hsueh, Y.-W.; Gilbert, K.; Trandum, C.; Zuckermann, M.; Thewalt, J., The effect of ergosterol on dipalmitoylphosphatidylcholine bilayers: a deuterium NMR and calorimetric study. *Biophys. J.* **2005**, *88*, 1799-1808.
17. Kodama, M.; Shibata, O.; Nakamura, S.; Lee, S.; Sugihara, G., A monolayer study on three binary mixed systems of dipalmitoyl phosphatidyl choline with cholesterol, cholestanol and stigmaterol. *Colloids Surf., B* **2004**, *33*, 211-226.
18. Ollila, O. H. S.; Rog, T.; Karttunen, M.; Vattulainen, I., Role of sterol type on lateral pressure profiles of lipid membranes affecting membrane protein functionality: comparison between cholesterol, desmosterol, 7-dehydrocholesterol and ketosterol. *J. Struct. Biol.* **2007**, *159*, 311-323.
19. Paquet, M.-J.; Fournier, I.; Barwicz, J.; Tancredi, P.; Auger, M., The effects of amphotericin B on pure and ergosterol- or cholesterol-containing dipalmitoylphosphatidylcholine bilayers as viewed by  $^2\text{H}$  NMR. *Chem. Phys. Lipids* **2002**, *119*, 1-11.
20. Stottrup, B. L.; Keller, S. L., Phase behavior of lipid monolayers containing DPPC and cholesterol analogs. *Biophys. J.* **2006**, *90*, 3176-3183.
21. Barenholz, Y., Cholesterol and other membrane active sterols: from membrane evolution to "rafts". *Prog. Lipid Res.* **2002**, *41*, 1-5.
22. Sternin, E.; Bloom, M.; L., M. A., De-Pake-ing of NMR spectra. *J. Magn. Reson.* **1983**, *55*, 274-282.

23. Schäfer, H.; Mädler, B.; Sternin, E., Determination of orientational order parameters from  $^2\text{H}$  NMR spectra of magnetically partially oriented lipid bilayers. *Biophys. J.* **1998**, *74*, 1007-1014.
24. Lafleur, M.; Fine, B.; Sternin, E.; Cullis, P. R.; Bloom, M., Smoothed orientational order profile of lipid bilayers by  $^2\text{H}$ -nuclear magnetic resonance. *Biophys. J.* **1989**, *56*, 1037-1041.
25. Allen, T. M., Calcein as a tool in liposome methodology. In *Liposome technology*, Gregoriadis, G., Ed. CRC Press: Boca Raton, FC, 1984; pp 177-182.
26. Benachir, T.; Lafleur, M., Study of vesicle leakage induced by melittin. *Biochim. Biophys. Acta* **1995**, *1235*, 452-460.
27. Mantsch, H. H.; McElhaney, R. N., Phospholipid phase transitions in model and biological membranes as studied by infrared spectroscopy. *Chem. Phys. Lipids* **1991**, *57*, 213-226.
28. Kodati, V. R.; El-Jastimi, R.; Lafleur, M., Contribution of the intermolecular coupling and librational mobility in the methylene stretching modes in the infrared spectra of acyl chains. *J. Phys. Chem.* **1994**, *98*, 12191-12197.
29. Lafleur, M., Phase behaviour of model stratum corneum lipid mixtures: an infrared spectroscopy investigation. *Can. J. Chem.* **1998**, *76*, 1501-1511.
30. Gómez-Fernández, J. C.; Villalain, J., The use of FT-IR for quantitative studies of the apparent  $\text{pK}_a$  of lipid carboxyl groups and the dehydration degree of the phosphate group of phospholipids. *Chem. Phys. Lipids* **1998**, *96*, 41-52.
31. Lieckfeldt, R.; Villalain, J.; Gómez-Fernández, J.-C.; Lee, G., Apparent  $\text{pK}_a$  of the fatty acids within ordered mixtures of model human stratum corneum lipids. *Pharm. Res.* **1995**, *12*, 1614-1617.
32. Snyder, R. G.; Strauss, H. L.; Cates, D. A., Detection and measurement of microaggregation in binary mixtures of esters and of phospholipid dispersions. *J. Phys. Chem.* **1995**, *99*, 8432-8439.
33. Snyder, R. G.; Goh, M. C.; Srivatsavoy, V. J. P.; Strauss, H. L.; Dorset, D. L., Measurement of the growth kinetics of microdomains in binary n-alkane solid solutions by infrared spectroscopy. *J. Phys. Chem.* **1992**, *96*, 10008-10019.
34. Mendelsohn, R.; Moore, D. J., Vibrational spectroscopic studies of lipid domains in biomembranes and model systems. *Chem. Phys. Lipids* **1998**, *96*, 141-157.

35. Davis, J. H., Deuterium magnetic resonance study of the gel and liquid crystalline phases of dipalmitoyl phosphatidylcholine. *Biophys. J.* **1979**, *27*, 339-358.
36. Lafleur, M.; Cullis, P. R.; Bloom, M., Modulation of the orientational order profile of the lipid acyl chain in the L $\alpha$  phase. *Eur. Biophys. J.* **1990**, *19*, 55-62.
37. Kitson, N.; Thewalt, J.; Lafleur, M.; Bloom, M., A model membrane approach to the epidermal permeability barrier. *Biochemistry* **1994**, *33*, 6707-6715.
38. El Jastimi, R.; Lafleur, M., A dual-probe fluorescence method to examine selective perturbation of membrane permeability by melittin. *Biospectroscopy* **1999**, *5*, 133-140.
39. Schuler, I.; Milon, A.; Nakatani, Y.; Ourisson, G.; Albrecht, A.-M.; Benveniste, P.; Hartmann, M.-A., Differential effects of plant sterols on water permeability and on acyl chain ordering of soybean phosphatidylcholine bilayers. *Biophysics* **1991**, *88*, 6926-6930.
40. Schuler, I.; Duportail, G.; Glasser, N.; Benveniste, P.; Hartmann, M.-A., Soybean phosphatidylcholine vesicles containing plant sterols – a fluorescence anisotropy study. *Biochim. Biophys. Acta* **1990**, *1028*, 82-88.
41. Bernsdorff, C.; Winter, R., Differential properties of the sterols cholesterol, ergosterol, beta-sitosterol, trans-7-dehydrocholesterol, stigmasterol and lanosterol on DPPC bilayer order. *J. Phys. Chem. B* **2003**, *107*, 10658-10664.
42. Xu, X.; London, E., The effect of sterol structure on membrane lipid domains reveals how cholesterol can induce lipid domain formation. *Biochemistry* **2000**, *39*, 843-849.
43. Nayar, R.; Hope, M. J.; Cullis, P. R., Generation of large unilamellar vesicles from long-chain saturated phosphatidylcholines by extrusion technique. *Biochim. Biophys. Acta* **1989**, *986*, 200-206.
44. Halling, K. K.; Slotte, J. P., Membrane properties of plant sterols in phospholipid bilayers as determined by differential scanning calorimetry, resonance energy transfer and detergent-induced solubilization. *Biochim. Biophys. Acta* **2004**, *1664*, 161-171.
45. Hac-Wydro, K.; Dynarowicz-Latka, P.; Grzybowska, J.; Borowski, E., Interactions of amphotericin B derivative of low toxicity with biological membrane components - the Langmuir monolayer approach. *Biophys. Chem.* **2005**, *116*, 77-88.
46. Gao, W.-Y.; Quinn, P. J.; Yu, Z.-W., The role of sterol rings and side chain on the structure and phase behaviour of sphingomyelin bilayers. *Mol. Membr. Biol.* **2008**, *25*, 458-497.

47. Hac-Wydro, K.; Dynarowica-Latka, P., The impact of sterol structure on the interactions with sphingomyelin in mixed Langmuir monolayers. *J. Phys. Chem. B* **2008**, *112*, 11324-11332.
48. Arora, A.; Raghuraman, H.; Chattopadhyay, A., Influence of cholesterol and ergosterol on membrane dynamics: a fluorescence approach. *Biochem. Biophys. Res. Commun.* **2004**, *318*, 920-926.
49. Dynarowicz-Latka, P.; Seoane, R.; Minones, J.; Velo, M.; Minones, J., Study of penetration of amphotericin B into cholesterol or ergosterol containing dipalmitoyl phosphatidylcholine Langmuir monolayers. *Colloids Surf., B* **2002**, *27*, 249-263.
50. Hodzic, A.; Rappolt, M.; Amenitsch, H.; Laggner, P.; Pabst, G., Differential modulation of membrane structure and fluctuations by plant sterols and cholesterol. *Biophys. J.* **2008**, *94*, 3935-3944.

## **Chapter 3**

# **Formation of Fluid Lamellar Phase and Large Unilamellar Vesicles with Octadecyl Methyl Sulfoxide/Cholesterol Mixtures**

Zhong-Kai Cui, Guillaume Bastiat, and Michel Lafleur

Reprinted with permission from

*Langmuir*, 2010, **26**, 12733–12739

Copyright © 2010 American Chemical Society

### **3.1 Abstract**

Systems composed of a monoalkylated amphiphile and a sterol have been shown to form stable liquid-ordered (lo) lamellar phases; these include negatively charged mixtures of unprotonated palmitic acid/cholesterol (Chol) or cholesterol sulfate (Schol), and mixtures of positively charged cetylpyridinium chloride/Schol. Large unilamellar vesicles (LUVs) could be formed by these systems, using conventional extrusion methods. The passive permeability of these LUVs was drastically limited, a phenomenon associated with the high sterol content. In the present paper, we showed that octadecyl methyl sulfoxide (OMSO), a neutral monoalkylated amphiphile, can form, in the presence of cholesterol, LUVs that are stable at room temperature. Differential scanning calorimetry, infrared spectroscopy, and nuclear magnetic resonance spectroscopy of deuterium were used to characterize the phase behavior of OMSO/Chol mixtures. A temperature–composition diagram summarizing the behavior of the OMSO/Chol system is proposed; it includes a eutectic with an OMSO/Chol molar ratio of 5/5. It is found that the fluid phase observed at temperature higher than 43 °C is metastable at room temperature, and this situation allows extruding these mixtures to form stable LUVs at room temperature. This distinct behavior is associated with the strong H-bond capability of the sulfoxide group. The properties associated with this neutral formulation expand the potential of these non-phospholipid liposomes for applications in several areas such as drug delivery.

## 3.2 Introduction

It is now established that mixtures of monoalkylated amphiphiles with high sterol contents can form fluid bilayers. For example, mixtures of palmitic acid (PA) with various sterols, including cholesterol (Chol), and cholesterol sulfate (Schol), are found to self-assemble to provide stable lamellar structure in the liquid-ordered (lo) phase; in this phase, the lipids experience fast lateral and rotational diffusion but the PA alkyl chain displays high conformational order.<sup>1-5</sup> Similar structures are reported with cetylpyridinium chloride (CPC)/Schol,<sup>6</sup> and lyso-palmitoylphosphatidylcholine (lyso-PPC)/Chol,<sup>7</sup> whereas an analogous behavior is proposed for N-acylethanolamine (NAE)/Chol<sup>8</sup> mixtures. Typically, the monoalkylated amphiphile/sterol molar ratio of these bilayer-forming mixtures is between 5/5 and 3/7. Even though these monoalkylated amphiphiles or sterols do not form fluid lamellar phases once hydrated individually, their mixtures lead to stable lo-phase bilayers. These have a sterol/alkyl chain content considerably higher than typical phospholipid bilayers, considering that a phospholipid bears typically two alkyl chains.<sup>9-11</sup>

The main driving force associated with the formation of these fluid non-phospholipid bilayers is indeed the hydrophobic interactions, but the molecular prerequisites leading these molecules to self-assemble to form a fluid bilayer with alkyl chains highly ordered are not clearly established. The hydrophobic match between the apolar parts of the molecular constituents was shown to be critical for the formation of lo lamellar phases.<sup>2</sup> These bilayers are destabilized when the alkyl end chain of the sterol is bulky,<sup>5</sup> a feature that limits the ordering of the monoalkylated amphiphile, and consequently, the van der Waals interactions between the molecular species.

Electrostatic interactions appear also to play an essential role in the stability of these bilayers and of the resulting LUVs. So far, all the reported monoalkylated amphiphile/sterol mixtures forming stable fluid bilayers at room temperature include at least one molecular species bearing a charge. For example, it is striking that, at room temperature, stable fluid lamellar phases are obtained with unprotonated PA and cholesterol, with protonated PA and Chol, but not with protonated PA and cholesterol.<sup>12</sup> In fact, it has been shown that the stability of these bilayers as a function of pH is intimately related to the  $pK_a$  of the fatty acid used to form the bilayers.<sup>13</sup> Similar fluid lamellar phases are obtained with cholesterol mixed with CPC, a cationic monoalkylated amphiphile.<sup>6</sup> It was also reported that mixtures of lyso-PPC and cholesterol can form fluid bilayers;<sup>7</sup> in this case, even though the overall charge is nil, the zwitterionic nature of lyso-PPC provides a local negative charge, on the phosphate group, and a positive one, on the quaternary ammonium group. Unprotonated PA/Chol, protonated PA/Schol, and CPC/Schol systems, which form these fluid bilayers at room temperature, can be extruded using standard extrusion procedures to form large unilamellar vesicles (LUVs).<sup>4, 6, 12</sup> Interestingly, the permeability of these LUVs is drastically reduced compared with the conventional liposomes made by phospholipids, likely due to their high sterol content. The protonated PA/Chol system, which is completely neutral, can form fluid bilayers only above 50 °C while the components remain solid at room temperature.<sup>1</sup> In this case, it is impossible to extrude the mixture to form LUVs. Therefore, it appears that interfacial electrostatics plays a significant role in the stability of the lo-phase bilayers made of a monoalkylated amphiphile and a sterol.

In the present paper, we examine the possibility of using a neutral monoalkylated amphiphile and cholesterol to form completely neutral fluid bilayers. From an application point of view, neutral liposomes have been shown to display some distinct advantages. For example, it

has been shown that liposomes used as biocompatible drug carriers can present improved behavior for the immune-mediated clearance and the inflammatory response.<sup>14-16</sup> Moreover, neutral liposomes were shown to display a distinctly uniform brain distribution, insensitive to the entrapped chemical, making them attractive nanovectors for predictable drug delivery and for imaging agents of brain.<sup>17</sup> We used octadecyl methyl sulfoxide (OMSO) (Figure 3.1), a dimethyl sulfoxide analogue bearing an 18 carbon atoms alkyl chain; its alkyl chain length matches the hydrophobic section of cholesterol.<sup>2</sup> OMSO is a neutral molecule, but the sulfoxide group is a very good H-bond acceptor leading to strong H-bonds.<sup>18-21</sup> For example, it is proposed that the H-bond interactions involving dimethyl sulfoxide (DMSO) are strong enough to induce the formation of a eutectic complex with water,<sup>18, 22</sup> as well as with acetic acid.<sup>19</sup> In this work, we show that the particular H-bonding properties of the sulfoxide group lead to the possibility of forming fluid bilayers with OMSO and cholesterol mixtures, and these can be extruded to form, at room temperature, neutral LUVs. The phase behavior of OMSO/Chol mixtures was investigated by differential scanning calorimetry (DSC), infrared (IR) spectroscopy, and nuclear magnetic resonance spectroscopy of deuterium (<sup>2</sup>H NMR). A temperature–composition diagram summarizes the behavior of the OMSO/Chol mixtures. This diagram indicated the suitable conditions to prepare non-phospholipid liposomes, and we examined the possibility to extrude the OMSO/Chol mixtures to form LUVs and characterized the stability and the permeability of these resulting liposomes.

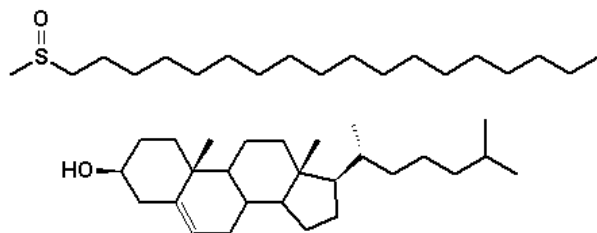


Figure 3.1. Chemical formula of OMSO and cholesterol.

### 3.3 Materials and methods

Octadecyl methyl sulfoxide (OMSO) was obtained from Narchem Corporation (Chicago, IL, USA). Cholesterol (Chol) (>99%), cholesterol-2,2,4,4,6- $d_5$  (Chol- $d_5$ ) (97 atom % D), tris(hydroxymethyl)aminomethane (TRIS) (99%), 2-[N-morpholino]ethanesulfonic acid (MES) (>99%), ethylenediaminetetraacetic acid (EDTA) (99%), NaCl (>99%), Triton X-100 (99%) and deuterium-depleted water (>99.99%) were purchased from Sigma Chemical Co. (St. Louis, MO, USA). Calcein (high purity) was obtained from Invitrogene (Burlington, ON, Canada), and Sephadex G-50 Medium from Pharmacia (Uppsala, Sweden). Methanol (spectrograde) was purchased from American Chemicals Ltd. (Montreal, QC, Canada), whereas benzene (high purity), was from BDH Inc. (Toronto, ON, Canada). All the chemicals were used without further purification.

Mixtures of OMSO and cholesterol were prepared by dissolving weighed amounts of the solids in a mixture of benzene/methanol 95/5 (v/v). The solutions were then frozen in liquid nitrogen and lyophilized for at least 16 h to allow complete sublimation of the organic solvent. Cholesterol was substituted with Cholesterol- $d_5$  for the  $^2\text{H}$  NMR experiments.

### 3.3.1 DSC, $^2\text{H}$ NMR, and IR spectroscopy

The freeze-dried lipid mixtures were hydrated with a MES/TRIS buffer (MES 50 mM, TRIS 50 mM, NaCl 10 mM, EDTA 5 mM) at pH 7.4. The buffer was prepared with Milli-Q water for DSC and IR spectroscopy and deuterium-depleted water for  $^2\text{H}$  NMR experiments. The final lipid concentration was 20 mg/mL for DSC, and 30 mg/mL for IR spectroscopy and  $^2\text{H}$  NMR experiments. The suspensions were subjected to five cycles of freezing-and-thawing (from liquid nitrogen temperature to  $\sim 70$  °C) and vortexed between successive cycles to ensure good hydration of the samples. The pH was measured and readjusted by the addition of HCl or NaOH diluted solution, if necessary. The samples were then incubated for at least one week at room temperature.

The DSC was performed with a VP-DSC microcalorimeter (MicroCal, Northampton, MA). The reference cell was filled with the buffer. The data acquisition was performed from 20 to 90 °C, at a heating rate of 20 °C/h. Data acquisition and treatment were performed with the *Origin* software (MicroCal software, Northampton, MA).

The  $^2\text{H}$  NMR spectra were recorded on a Bruker AV-600 spectrometer, using a Bruker static probe equipped with a 5 mm coil. A quadrupolar echo sequence was used with a  $90^\circ$  pulse of 3.0  $\mu\text{s}$  and an interpulse delay of 24  $\mu\text{s}$ . The recycling time was 30 s. In absence of a slow-relaxation component, namely, a solid phase, the recycling delay was reduced to 0.3 s. Typically, 5000 FIDs were coadded. The temperature was regulated using a Bruker VT-3000 controller, varying from low to high and then back to the initial temperature. In order to characterize the

kinetics of the solid phase formation, FIDs with the long (30 s) and short (0.3 s) delay were acquired in an alternating manner from a sample heated to 55 °C and then rapidly cooled down to 30 °C.

The IR spectra were recorded on a Thermo Nicolet 4700 spectrometer, equipped with a KBr beam splitter and a DTGS-L-alanine detector. Briefly, an aliquot of the sample was placed between two CaF<sub>2</sub> windows separated by a 5- $\mu$ m-thick Teflon ring. This assembly was inserted in a brass sample holder, whose temperature was controlled using Peltier thermopumps. Each spectrum was the result of 60 coadded scans acquired with a nominal 2 cm<sup>-1</sup> resolution and Fourier transformed using a triangular apodization function. The temperature was varied from low to high, with 2 °C steps and a 5 min incubation period prior to the data acquisition. The reported band positions correspond to the centers of gravity calculated from the top 5% of the band.

### 3.3.2 Permeability measurements

The permeability of LUVs was measured using a standard procedure based on the self-quenching property of calcein at high concentration.<sup>23, 24</sup> OMSO/Chol mixtures were hydrated, at a lipid concentration of 85 mM, with the MES/TRIS buffer, pH 7.4, and containing calcein (80 mM). The LUVs were prepared by extrusion using a hand-held Liposofast extruder (Avestin, Ottawa, Canada). The dispersions were passed 15 times through two stacked polycarbonate filters (100 nm pore size) at ~65 °C. Calcein-containing LUVs were separated at room temperature from free calcein by exclusion chromatography, using a column (diameter 1.5 cm, length 25 cm) filled

with Sephadex G-50 medium gel and an isoosmotic MES/TRIS buffer (MES 50 mM, TRIS 50 mM, NaCl 130 mM, EDTA 5 mM, pH 7.4) as eluent. The collected LUV fraction was diluted 100 times with this isoosmotic buffer to perform the measurements.

Immediately after the isolation and dilution of the calcein-loaded vesicles, the fluorescence intensity was measured from an aliquot of this stock LUVs suspension prior to ( $I_i$ ) and after ( $I_{i+T}$ ) the addition of 10  $\mu$ L of Triton X-100 solution (10% (v/v) in the external MES/TRIS buffer); these intensities were referred to as initial values, i.e., obtained at  $t = 0$ . After a given time, the calcein fluorescence intensity was measured on another aliquot of the LUV stock suspension before ( $I_f$ ) and after ( $I_{f+T}$ ) the addition of Triton X-100. The fluorescence intensity, measured after addition of the detergent, corresponded to the complete release of calcein and was used to normalize the leakage. The percentage of encapsulated calcein remaining at that time in the LUVs was calculated as follows:

$$\% \text{ of encapsulated calcein} = \left( \frac{(I_{f+T} - I_f) / I_{f+T}}{(I_{i+T} - I_i) / I_{i+T}} \right) \times 100 \quad (3.1)$$

The % of release corresponded to (100 – % of encapsulated calcein).

The potential pH-triggered leakage of calcein was also examined. The pH was modified by adding an aliquot of diluted NaOH or HCl solution directly to an aliquot of the LUV suspension. The calcein fluorescence intensities were measured after the stabilization of pH (typically after ~2 min). The percentage of released calcein was calculated with the eq 3.1, except  $I_i$  and  $I_{i+T}$  corresponded to the measurements at initial time and also initial pH (pH 7.4), whereas  $I_f$  and  $I_{f+T}$  were obtained from an aliquot at a modified pH, before and after the addition of Triton

X-100, respectively. The pH effect was examined for both increasing and decreasing pH values. The calcein fluorescence intensity was relatively constant over the investigated pH range.<sup>23</sup>

The calcein fluorescence intensity was measured using excitation and emission wavelengths of 490 and 513 nm, respectively by a SPEX Fluorolog spectrofluorimeter. All the leakage experiments were carried out at room temperature.

The hydrodynamic diameters of the LUVs were measured at 25 °C using a Coulter N4 Plus quasi-elastic light scattering apparatus coupled with a Malvern autocorrelator. The scattering intensity was adjusted by the dilution of the dispersion with the MES/TRIS buffer. The fluorescence and quasi-elastic light scattering measurements were carried out as closely as possible.

## **3.4 Results and discussion**

### **3.4.1 DSC experiments**

Figure 3.2 presents thermograms of OMSO/Chol mixtures with various compositions, hydrated at pH 7.4. For pure OMSO, a phase transition is observed at about 60 °C, corresponding to its melting. For an OMSO/Chol mixture with a molar ratio of 7/3, two maxima are observed, at about 44 and 58 °C (Figure 3.2b). The shape of the endotherm is associated with the shape of the phase coexistence region in the phase diagram, as discussed below. The first maximum corresponds to the beginning of the formation of a fluid phase, crossing a three-phase line from

solid phases to a region where there is coexistence of lo phase and solid OMSO. The rest of the endotherm corresponds to crossing the co-existence phase. The OMSO/Chol 5/5 mixture shows only one endothermic sharp peak at 43 °C, indicative of the formation of a eutectic mixture. For OMSO/Chol molar ratios of 3/7 and 1/9, the maximum at 43 °C is still present but another broader endothermic peak is observed at 70 °C for the 3/7 molar ratio and at 85 °C for the 1/9 molar ratio. A dehydration transition is observed for the solid cholesterol in excess water at ~72 °C<sup>25, 26</sup> and the observed endotherm is believed to be associated with excess solid cholesterol experiencing such a transition. This behavior is reminiscent of that previously observed by Ouimet et al.<sup>3</sup> for PA/Chol mixtures. That system showed, at pH 5.5, a eutectic behavior at similar proportions as a sharp transition from solid to fluid lamellar phase was observed at 53.5 °C, about 8 °C lower than the melting point of hydrated PA.<sup>3</sup> On the basis of these similarities, and the spectroscopic features reported below, a similar behavior is proposed for the OMSO/Chol mixtures. In this system, the eutectic composition corresponds to a 5/5 molar ratio and the solid to lo phase transition is observed at 43 °C.

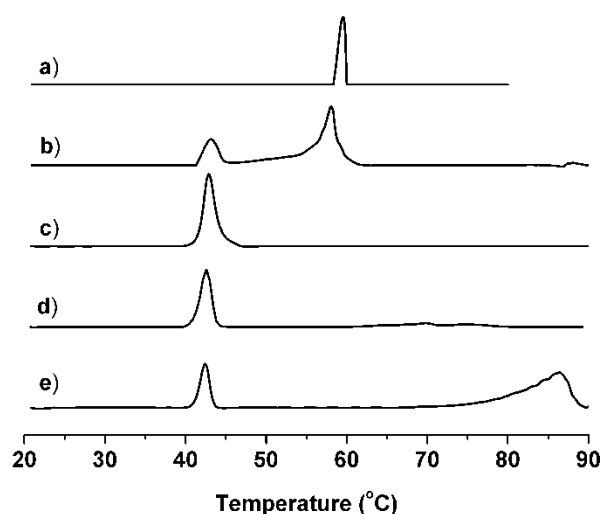


Figure 3.2. Thermograms of a) pure OMSO and of OMSO/Chol mixtures with molar ratio of b) 7/3, c) 5/5, d) 3/7, and e) 1/9; pH 7.4.

No peak is observed upon cooling the eutectic mixture from 90 to 20 °C. In addition, no endotherm is observed during a second heating. The endotherm associated with the solid to liquid phase transition reappears after ~3 days of incubation at room temperature. These results are indicative of the metastability of the phase formed at high temperature, and this aspect is discussed in the next section.

### 3.4.2 $^2\text{H}$ NMR experiments

Figure 3.3 – column A presents the evolution of the  $^2\text{H}$  NMR spectrum of an equimolar OMSO/Chol- $d_5$  mixture, at pH 7.4, as a function of increasing temperature. At 25 and 35 °C, a single broad powder pattern is observed and its quadrupolar splitting measured between the two maxima corresponds to 124 kHz. This profile is typical of solid cholesterol.<sup>1, 27</sup> The five deuterated positions give rise to similar splittings when the cholesterol molecules are immobile, the chemical shifts and the static quadrupolar constants of the various deuterated groups being very similar.<sup>28, 29</sup> At 45 °C and above, the  $^2\text{H}$  NMR spectrum is drastically modified: three reasonably well resolved powder patterns with reduced quadrupolar splittings are observed. No contribution of a solid phase can be observed. This transition between solid cholesterol and cholesterol solubilized in fluid bilayers is consistent with the results obtained from the DSC experiments. For cholesterol- $d_5$  in the OMSO/Chol mixture at 55 °C, the quadrupolar splittings measured between the maxima (the 90° orientation) are reported in Table 3.1. These values are very similar to those previously obtained for cholesterol- $d_5$  in various fluid bilayers including PA/Chol system,<sup>1</sup> phosphatidylcholine bilayers,<sup>30, 31</sup> model mixtures of stratum corneum lipids,<sup>27</sup> and biological membranes such as human red blood cell membranes,<sup>32</sup> and membranes of mycoplasma *Acholeplasma laidlawii* (strain B).<sup>33</sup> This correspondence strongly suggests a

similar orientation and dynamics of cholesterol in the OMSO/Chol fluid lamellar phase. The molecular design of cholesterol appears to strongly dictate its orientation in lipid bilayers with no considerable dependence on the composition of the matrix.

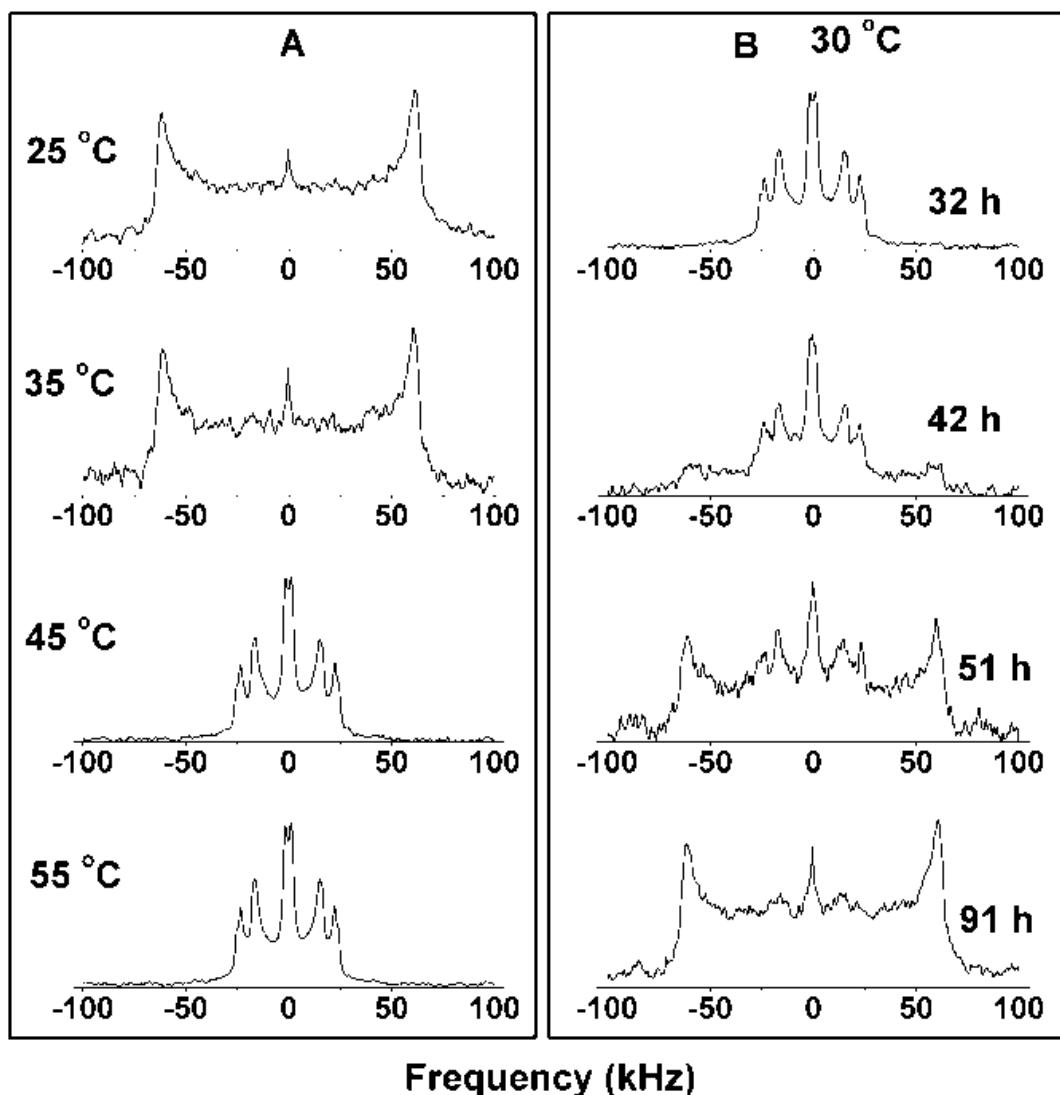


Figure 3.3.  $^2\text{H}$  NMR spectra of an equimolar OMSO/Chol- $d_5$  mixture, pH 7.4. Column A, from top to bottom, represents the thermal evolution of the spectrum as a function of increasing temperature. Column B presents the progressive solidification of cholesterol in OMSO/Chol metastable bilayers that were obtained from a rapid cooling of the sample from 55 to 30 °C.

Using an approach previously described,<sup>1, 31</sup> the residual quadrupolar splittings,  $\Delta\nu_Q$ , of the  $^2\text{H}$  NMR powder pattern could be described by the fast rotation of cholesterol along its long axis. In this case,  $\Delta\nu_Q$  is related to<sup>28, 34</sup>

$$\Delta\nu_Q = \frac{3}{2} A_Q \left( \frac{3 \cos^2 \theta - 1}{2} \right) S_{mol} S_{C-D} \quad (3.2)$$

where  $A_Q$  is the static quadrupolar constant (170 kHz for the C–D bonds<sup>29</sup>) and  $\theta$  is the angle between the bilayer normal and the magnetic field.  $S_{mol}$  denotes the fluctuations of the whole cholesterol molecule with respect to the bilayer normal, whereas  $S_{C-D}$  represents the averaged orientational intramolecular order parameter. For labeled cholesterol, the C–D bonds are linked to the steroid rigid rings, and consequently,  $S_{C-D}$  should be essentially representative of the fixed angle ( $\beta$ ) between the C–D bond and the cholesterol long axis, defined as the rotation axis. The specific assignment of the powder patterns to the various deuterated positions and the resulting specific orientation of the C–D bonds were reported for DMPC/Chol- $d_5$  systems<sup>29</sup> (Table 3.1). Using these  $\beta$  values, we could reproduce, within 3 kHz, the three measured quadrupolar splittings for OMSO/Chol system, using  $S_{mol}$  as the only adjustable parameter. The resulting  $S_{mol}$  is 0.92, a value similar to those previously obtained for cholesterol in lo phase bilayers formed with CPC/Chol,<sup>6</sup> PA/Chol,<sup>1</sup> and DMPC/Chol.<sup>31</sup> As  $S_{mol}$  is close to 1, it is concluded that the sterol long axis is essentially aligned parallel with the bilayer normal and it experiences very limited wobbling.

Table 3.1.  $^2\text{H}$  NMR parameters associated with cholesterol in equimolar OMSO/Chol- $d_5$  mixtures.

| position               | expt $\Delta\nu_Q$<br>(kHz) | $\beta$ obtained<br>from ref <sup>31</sup> | calcd                     |                        |
|------------------------|-----------------------------|--|---------------------------|------------------------|
|                        |                             |  | Calcd<br>$S_{\text{mol}}$ | $\Delta\nu_Q$<br>(kHz) |
| 2,4- $^2\text{H}^2$ ax | 45.4                        | 74.1                                       |                           | 46                     |
| 2,4- $^2\text{H}_2$ eq | 33.4                        | 66.2                                       | 0.92                      | 30                     |
| 6- $^2\text{H}$        | 4.0                         | 55.8                                       |                           | 3                      |

$^2\text{H}$  NMR spectroscopy allowed us to discover that the high-temperature structure was metastable at room temperature. The irreversibility of the transition can be assessed, for example, by cooling rapidly the OMSO/Chol- $d_5$  sample from 55 to 30 °C and by recording the  $^2\text{H}$  NMR spectrum as a function of time (Figure 3.3 column B). After rapid cooling to 30 °C, no solid phase is observed. The spectrum is practically identical to that measured at 55 °C, including essentially identical quadrupolar splittings. Progressively, the contribution of the solid phase appears and the spectrum becomes a combination of the spectra representative of solid cholesterol and cholesterol solubilized in fluid bilayers. After 91 h at 30 °C, cholesterol exists exclusively under the solid phase. We can describe the kinetics of this solidification of cholesterol in an OMSO/Chol- $d_5$  mixture using  $^2\text{H}$  NMR (Figure 3.4). Spectra, obtained from 100 scans, were recorded as a function of time using alternatively a long (30 s) and short (0.3 s) relaxation delay. The relaxation time of solid cholesterol- $d_5$  is about 4 s,<sup>33</sup> whereas it is less than 14 ms for cholesterol solubilized in a fluid bilayer.<sup>35</sup> As a consequence, essentially only the cholesterol molecules solubilized in the lo bilayers contribute to the spectra acquired with the short relaxation delay, while the spectra obtained with the long relaxation delay are representative of all the sterol molecules. The proportion of the lo phase is calculated from the ratio of the area

of the short-delay spectrum and that of the following long-delay spectrum. The suspension exists under a lo phase for the first 30 h following its cooling; consequently, the spectra acquired with long and short relaxation delays have the same area, leading to a lo phase proportion of 1. Afterward a transition toward the solid phase occurs, and finally, cholesterol exists essentially under the solid form after ~55 h. A residual proportion of lo phase is reported (~0.08), but it corresponds in fact to cholesterol in an isotropic phase, which shows up as a narrow peak right in the middle of the  $^2\text{H}$  NMR spectrum (Figure 3.3 column B). This phase is observed after the heating–cooling cycle but remains a minor proportion of cholesterol in the sample.

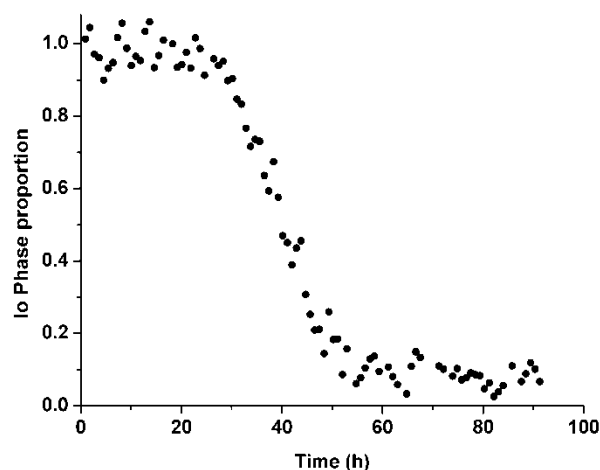


Figure 3.4. Kinetics of the crystallization of cholesterol in the metastable liquid ordered phase of an equimolar OMSO/Chol- $d_5$  mixture at 30 °C.

### 3.4.3 IR spectroscopy experiments

The thermal behavior of OMSO/Chol mixtures was examined by IR spectroscopy. The position of the symmetric C–H stretching ( $\nu_{\text{C-H}}$ ) mode, associated to OMSO alkyl chain, is mainly sensitive to the trans–gauche chain isomerization, and to the interchain coupling,

providing a sensitive probe for transitions involving the introduction of chain conformational disorder.<sup>36-38</sup> The melting of pure hydrated OMSO is easily detected by the abrupt shift of the  $\nu_{C-H}$  band from 2848 to about 2853.5  $\text{cm}^{-1}$ , at about 60 °C (Figure 3.5). This temperature corresponds to the transition identified by DSC. The two extreme  $\nu_{C-H}$  positions are representative of highly ordered and disordered chains, respectively.<sup>36, 39</sup> A transition between 42 and 47 °C was observed for equimolar OMSO/Chol system, in agreement with the thermogram presented in Figure 3.2c. At low temperatures, the position of the  $\nu_{C-H}$  band is about 2848  $\text{cm}^{-1}$ ; values below 2850  $\text{cm}^{-1}$  are generally associated with all-trans alkyl chains for molecules under a solid form.<sup>36, 39</sup> Therefore, those results are indicative of highly ordered alkyl chains of solid OMSO. At temperatures higher than the transition temperature, the position of the  $\nu_{C-H}$  band was shifted to  $\sim 2851 \text{ cm}^{-1}$ , a value lower than that observed for OMSO in the fluid state. This intermediate position corresponds to that observed for cholesterol-rich bilayers.<sup>12, 36, 40, 41</sup> The thermal behavior, as probed by IR spectroscopy, was also determined for other OMSO/Chol mixtures (3/7, 7/3, and 1/9 (mol/mol)). At low temperature, the position of the  $\nu_{C-H}$  band is  $\sim 2848 \text{ cm}^{-1}$  which indicates that OMSO alkyl chains are highly ordered, likely under a solid form.<sup>36, 39</sup> Upon heating above 43 °C, the position of the  $\nu_{C-H}$  band was abruptly shifted to  $\sim 2853 \text{ cm}^{-1}$  for the OMSO/Chol mixture (1/9); this value is similar to that observed for OMSO in the fluid state and is indicative of highly disordered alkyl chains. For thermal evolution of the position of the  $\nu_{C-H}$  band for the OMSO/Chol (3/7) mixture is similar to that of the eutectic composition. In the case of the OMSO/Chol (7/3) mixture, a shift of the  $\nu_{C-H}$  band by about 1  $\text{cm}^{-1}$  is observed at about 43 °C, followed by a more progressive shift of the band position between 43 and 60 °C, indicating the progressive disordering of OMSO alkyl chain.

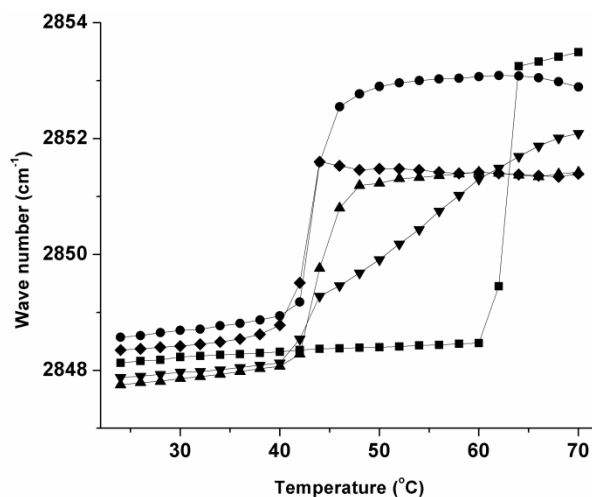


Figure 3.5. Lipid thermotropism, reported by the  $\nu_{\text{C-H}}$  band position from IR spectra, of hydrated OMSO (■), and of OMSO/Chol mixtures with various composition: 1/9 (●), 3/7 (◆), 5/5 (▲), and 7/3 (▼) (molar ratio), pH 7.4.

The metastability of the fluid phase was also investigated by IR spectroscopy. Figure 3.6 includes the variation of the  $\nu_{\text{C-H}}$  band position upon the cooling of an equimolar OMSO/Chol mixture, right after heating up to 70 °C. The  $\nu_{\text{C-H}}$  band position remains at  $\sim 2851 \text{ cm}^{-1}$  even at 25 °C, i.e., nearly 20 °C below the solid–lo phase transition observed upon heating. This observation is consistent with the bilayers remaining in a metastable lo phase. The  $\text{CH}_2$  deformation mode  $\delta(\text{CH}_2)$ , between  $1450$  and  $1480 \text{ cm}^{-1}$ , was also examined to confirm the lo phase metastability, because this mode is sensitive to the chain packing of the OMSO (Figure S3.1). At the beginning of the experiment, when the sample has been incubated for at least one week at room temperature, the  $\delta(\text{CH}_2)$  mode gives rise to two components located at  $1464$  and  $1472 \text{ cm}^{-1}$ . This splitting is typical of a solid phase for which the alkyl chain pack with an orthorhombic symmetry.<sup>42</sup> When the sample is cooled down to 30 °C after being heated at 70 °C, a single component at  $1468 \text{ cm}^{-1}$

is observed, confirming the existence of a metastable phase. The band splitting reappears as a function of time when the mixture is incubated at 30 °C.

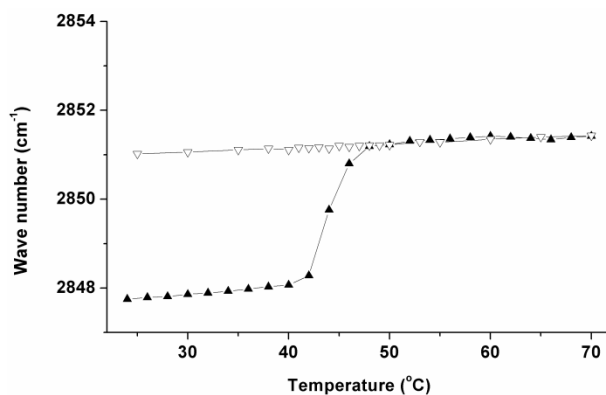


Figure 3.6. Lipid thermotropism, reported by the  $\nu_{C-H}$  band position from IR spectra, of an equimolar OMSO/Chol mixture: heating (▲) and cooling (▼), pH 7.4.

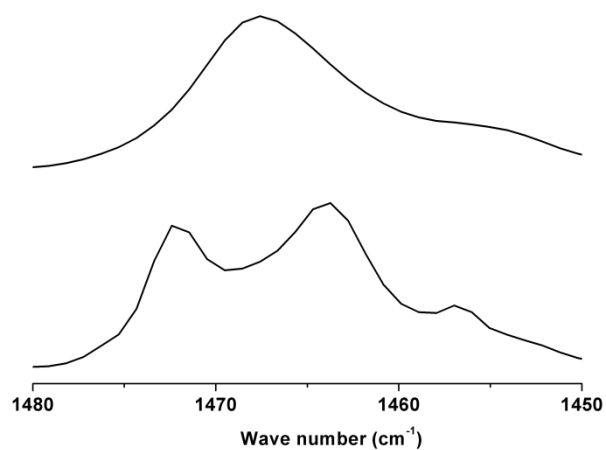


Figure S3.1. The  $\delta(\text{CH}_2)$  region of the IR spectrum recorded at 30 °C of an equimolar OMSO/Chol mixture after a one-week incubation at room temperature (bottom) and immediately after being cooled down from 65 °C (top).

## 3.4.4 OMSO/Chol temperature–composition diagram

In order to summarize the phase behavior revealed by the calorimetric and spectroscopic studies, an OMSO/Chol temperature–composition diagram is proposed (Figure 3.7). Below 43 °C, OMSO (as inferred from the low  $\nu_{C-H}$  band position) (Figure 3.5) and cholesterol (as inferred from the  $^2H$  NMR spectra) form solid phases. Upon heating, there is the formation of a lo lamellar phase, observed from the thermograms, the shift of the  $\nu_{C-H}$  position in IR spectroscopy, and the modification of the  $^2H$  NMR spectrum of cholesterol- $d_5$  that is associated with the introduction of molecular rotational freedom. The OMSO/Chol 5/5 molar ratio corresponds roughly to a eutectic composition, as the DSC endotherm is fairly narrow. Only the lo phase is present for  $T > 43$  °C on the basis of the fluid cholesterol  $^2H$  NMR spectra and the  $\nu_{C-H}$  band position consistent with alkyl chain in a lo phase. For  $T > 43$  °C, higher cholesterol proportion appears to lead to the coexistence of the lo phase and solid cholesterol. For these samples, the variation of the  $\nu_{C-H}$  band position (Figure 3.5) is consistent with the fluidification of the OMSO alkyl chain at 43 °C, crossing the three-phase line. The presence of solid cholesterol is suggested by the small endotherms at about 80 °C that could be attributed to the solid–solid dehydration of the sterol in excess. In addition, the impossibility to extrude the OMSO/Chol 3/7 mixture is compatible with solid cholesterol obstructing the filters. For OMSO proportions greater than the eutectic composition, the variation of the  $\nu_{C-H}$  band position (Figure 3.5) and the DSC curves are indicative of a two-phase region where there is the coexistence of OMSO solid phase with the lo phase. It can be observed that the OMSO chain disordering undergoes a fluidification over ~20 °C, between 43 °C (the fluidification temperature of the eutectic mixture) and 60 °C (the fluidification temperature of pure OMSO). Beyond 60 °C, pure OMSO becomes fluid according

to the results from IR spectroscopy and DSC. The exact structure of these self-assemblies is not known. Because it is a monoalkylated amphiphile, OMSO likely forms micelles. In this case, there should be a region where two fluid phases (the  $l_o$  phase and an OMSO-rich nonlamellar phase) coexist. Such region has been tentatively introduced in the temperature–composition diagram. However, it cannot be excluded that pure OMSO could form hydrated lamellar phases above 62 °C. In that case, a region where a single lamellar phase would continuously evolve from pure OMSO disordered lamellar phase to  $l_o$  phase cholesterol-containing bilayers would be present in the temperature–composition diagram. Additional experiments are required to identify the details of this fluid phase region.

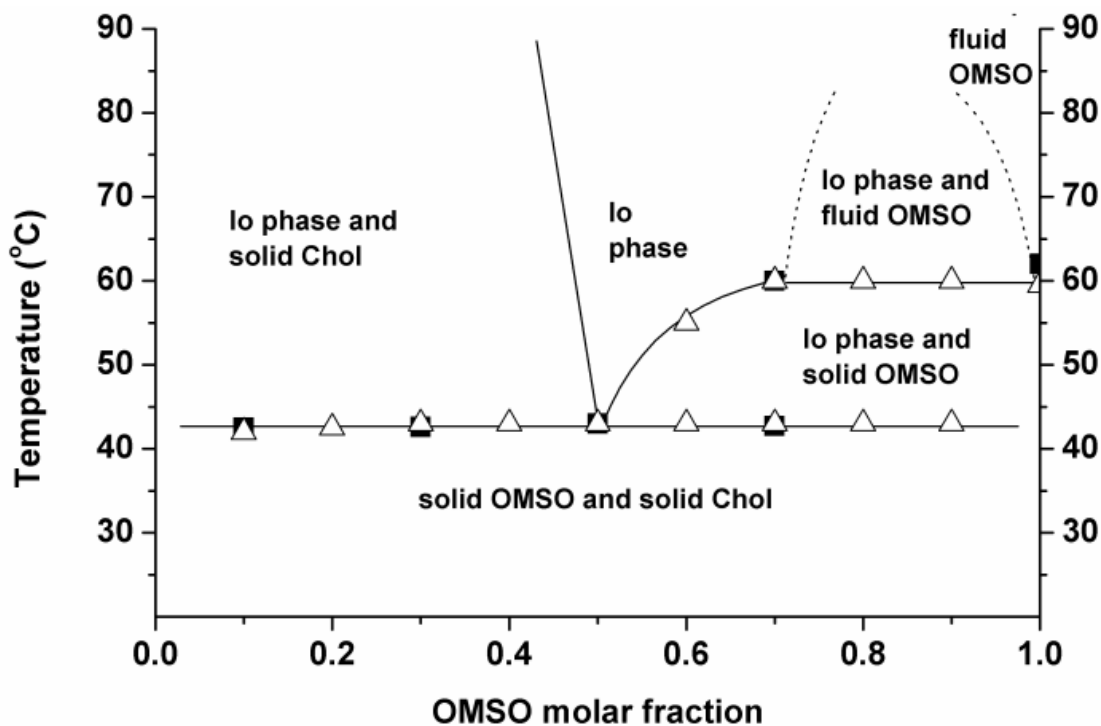


Figure 3.7. Proposed OMSO/Chol temperature–composition diagram. The phase boundaries identified by ■ were obtained from the shift of the  $\nu_{C-H}$  band position (see Figure 3.5). Those identified with  $\Delta$  were determined from the DSC thermograms (Figure 3.2). The borders of the lo–solid OMSO coexistence region are defined from both DSC and IR spectroscopy. The lo–fluid OMSO coexistence region (dotted lines) has been tentatively introduced to reconcile the formation of the lo phase by the eutectic mixture and the melting of OMSO.

### 3.4.5 OMSO/Chol LUVs

It has been shown that, despite their very high cholesterol content, it is possible to extrude several mixtures of sterols and monoalkylated amphiphiles when they form a lo phase.<sup>4, 6, 12</sup> Despite the fact that OMSO/Chol systems exist under a solid phase at room temperature, we have examined the possibility to prepare LUVs from the OMSO/Chol mixtures as the lo phase existing above 43 °C was found to be metastable at room temperature. Mixtures with various OMSO/Chol

molar ratios (3/7, 5/5 (the eutectic composition), and 7/3) were tentatively extruded, the LUVs being collected at room temperature. Table 3.2 reports the results of these attempts. It is impossible to extrude the 3/7 molar ratio OMSO/Chol mixture. It seems that the excess of the solid cholesterol plugs the pores of the polycarbonate filters. Conversely, extruded LUVs can be obtained from the OMSO/Chol mixtures with a 5/5 or 7/3 molar ratio. The quasi-elastic light scattering measurements indicate that the LUVs have, as expected, a hydrodynamic diameter consistent with the pore size of the filters (Table 3.2). The initial self-quenching of calcein entrapped in the LUVs was greater than 0.85, a typical value for entrapped calcein at a 80 mM concentration<sup>43</sup>. These results demonstrate the formation of LUVs with OMSO/Chol mixtures and their ability to encapsulate hydrophilic molecules. The passive release from calcein-loaded vesicles was determined (Figure 3.8). The leakage from OMSO/Chol LUVs (equimolar mixture) is very limited: even after 90 days, no significant release could be detected. Such limited passive permeability has been observed for LUVs prepared from sterol and palmitic acid.<sup>4, 12</sup>

Table 3.2. Hydrodynamic diameter of LUVs  $d_{LUVs}$  and initial self-quenching of calcein for various OMSO/Chol LUVs at pH 7.4.

| OMSO/Chol<br>molar ratio | $d_{LUVs}$ (nm)       | Initial self-<br>quenching |
|--------------------------|-----------------------|----------------------------|
| 3/7                      | Impossible to extrude |                            |
| 5/5                      | $112 \pm 8$           | $0.93 \pm 0.04$            |
| 7/3                      | $106 \pm 11$          | $0.91 \pm 0.02$            |

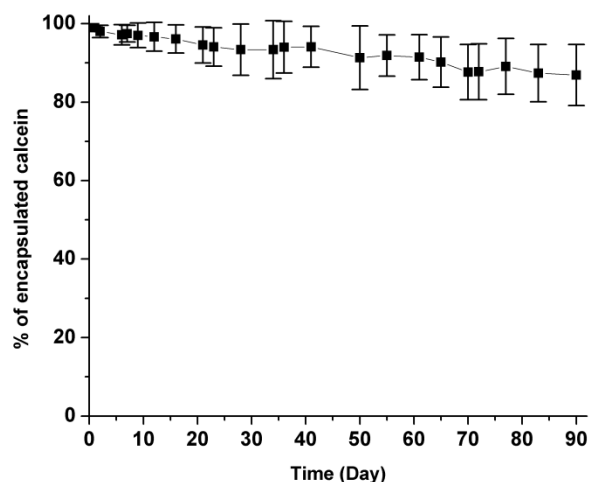


Figure 3.8. Passive calcein leakage from LUVs prepared from an equimolar OMSO/Chol mixture, at pH 7.4 and room temperature.

Considering the lifetime of the metastable  $l_0$  phase, it is inferred that these LUVs would exist under a solid form. We have carried out the IR spectroscopic analysis of OMSO/Chol LUVs, calcein-free or loaded with calcein; their behavior (Figure S3.2) is similar to that observed for multilamellar dispersions (Figure 3.6). Freshly prepared LUVs, which have been extruded, show, at room temperature, a  $\nu_{C-H}$  band position at around  $2851\text{ cm}^{-1}$ ; this value remains relatively constant up to  $60\text{ }^\circ\text{C}$ . Upon incubation at room temperature, the  $\nu_{C-H}$  band frequency decreases to  $\sim 2848\text{ cm}^{-1}$ , implying the rigidification of OMSO alkyl chains. An increase of the frequency of the  $\nu_{C-H}$  mode is observed upon heating, in agreement with thermal disordering of the chain. This behavior is not influenced by the presence of entrapped calcein.

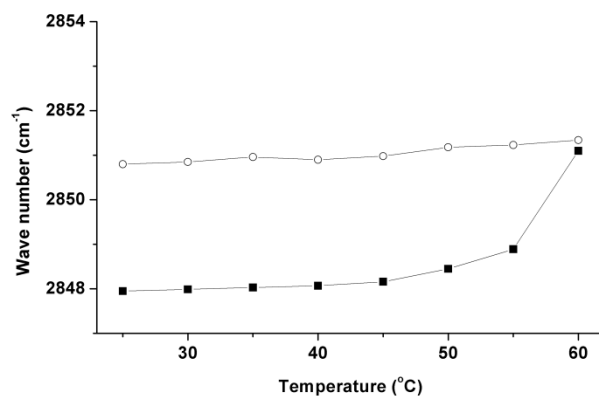


Figure S3.2a. LUVs thermotropism, reported by the  $\nu_{C-H}$  band position, of an equimolar OMSO/Chol mixture: right after extrusion (○), and ~60 h after extrusion (■), pH 7.4.

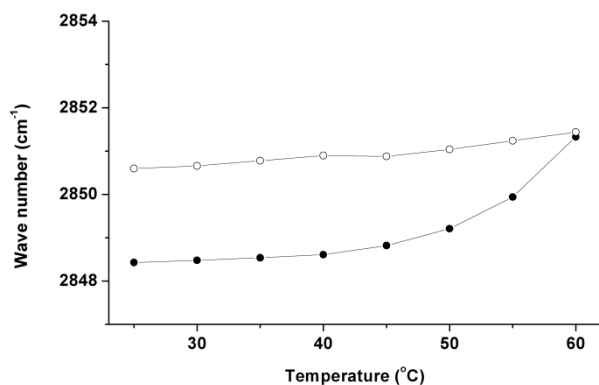


Figure S3.2b. LUVs with calcein inside thermotropism, reported by the  $\nu_{C-H}$  band position, of an equimolar OMSO/Chol mixture: right after extrusion (○), and ~60 h after extrusion (●), pH 7.4.

The stability of OMSO/Chol (5/5 molar ratio) LUVs was assessed as a function of pH (Figure 3.9), and the pH dependence of its calcein release is compared with that observed for PA/Chol (3/7 molar ratio) LUVs, a pH-sensitive system.<sup>4</sup> The pH was modified by adding an aliquot of diluted NaOH or HCl solution directly to an aliquot of an LUV suspension and the leakage measurements were carried out after the stabilization of pH (typically after ~2 min), at 25 °C. There is practically no impact of pH on calcein release from OMSO/Chol LUVs when

external pH is modified between 5.5 and 10. Because the OMSO/Chol system does not include any pH-sensitive group, it was expected that pH has little influence on their content release. This behavior contrasts with that of PA/Chol LUVs, for which no calcein release is observed between pH 6.5 to 10 but the calcein release is triggered at pH below 6.5; this pH-induced release was associated with the protonation of PA carboxylic group.<sup>4</sup> In addition, we have examined the influence of the pH on the LUV size, using quasi-elastic light scattering. The size of OMSO/Chol LUVs remains constant at about 100 nm between pH 2 and 12. This behavior also contrasts with the previous aggregation/fusion observed below pH 6 for PA/Chol LUVs,<sup>4</sup> an observation that was accompanied by the release of the entrapped calcein. In the case of OMSO/Chol LUVs, the absence of effect of pH on the LUV size and permeability illustrates the stability of these LUVs and is consistent with the hypothesis that the pH-triggered release is intimately associated with the change of surface charge density caused by the protonation/deprotonation of the carboxylic group of the fatty acid.<sup>13</sup>

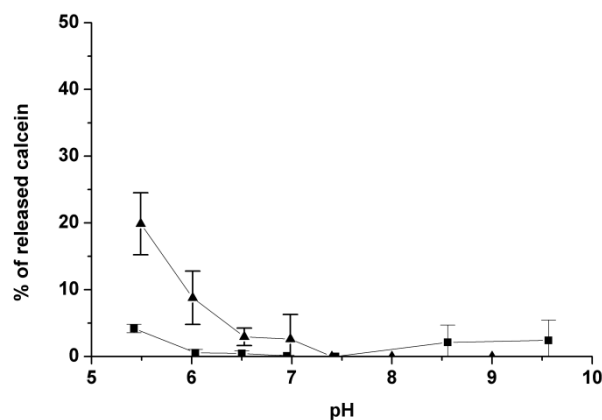


Figure 3.9. Effect of the external pH on the calcein release, for OMSO/Chol 5/5 (■) and PA/Chol 3/7 (▲) LUVs. The measurements were carried out at room temperature, ~2 min after the pH change.

### 3.5 Concluding remarks

This work extends the compositions of non-phospholipid liposomes formed with a monoalkylated amphiphile and a very high sterol content. It is possible to prepare fluid ordered bilayers when neutral OMSO and cholesterol are mixed. Because of the metastability of the lo phase at room temperature, the equimolar OMSO/Chol mixture can be extruded by conventional methods and form LUVs whose passive permeability is very limited. It is, to our knowledge, the first neutral system to form stable non-phospholipid liposomes with such high cholesterol content. This unique behavior is directly associated with OMSO properties. OMSO has an 18 carbon atom alkyl chain, providing a hydrophobic match with cholesterol. This equivalence is a contribution to the free energy favoring the mixing of the two species and was shown to be a prerequisite for the formation of stable lo-phase bilayers.<sup>2</sup> At the interfacial level, the sulfoxide group provides a strong H-bond acceptor, a feature that appears to be critical for the distinct behavior of its mixtures with cholesterol. Two aspects of the intermolecular interactions could contribute to this behavior. First, S=O forms H bonds with hydroxyl groups that are stronger than those formed with C=O;<sup>20, 21</sup> and those between OMSO and cholesterol could be sufficient to promote the mixing of the two species resulting in the formation of fluid bilayers. The strong H-bond network at the interface could be associated with the formation of the metastable phase if the solidification requires a significant rearrangement of this network. Actually, seminal work from Hargreaves and Deamer<sup>44</sup> suggested, for analogous mixtures of alkylated soaps and homologous fatty alcohols, that the stabilizing interaction required to form fluid bilayers was an interfacial H-bond network between the constituents. Second, the sulfoxide group interacts also strongly with water,<sup>18, 22</sup> and these interactions may provide the suitable hydration of the interface for forming

fluid bilayers. In the other monoalkylated amphiphile/sterol systems forming fluid lamellar self-assemblies at room temperature, the presence of a charged functional group may play the role of ensuring proper interfacial hydration. The solidification of the lipid species would require the dehydration of the head groups; the energy required to break the interacting S=O/H<sub>2</sub>O pair (or even complex) could be considerable, leading to a slow interface dehydration and, as a consequence, the existence of the metastable phase. These two phenomena can both contribute to the behavior of the OMSO/Chol system. The properties associated with this distinct behavior expand the potential of these liposomes for applications in several areas such as drug delivery.

## **3.6 Acknowledgements**

The authors thank the Natural Sciences and Engineering Research Council of Canada and the Fonds Québécois de la Recherche sur la Nature et les Technologies for the financial support. Z.-K. C is grateful to Université de Montréal and China Scholarship Council for his scholarship. We thank Cédric Malveau, Department of Chemistry, Université de Montréal, for his technical support during the NMR experiments, and Patrick Oliger for carrying out preliminary experiments.

### 3.7 References

1. Paré, C.; Lafleur, M., Formation of liquid ordered lamellar phases in the palmitic acid/cholesterol system. *Langmuir* 2001, *17*, 5587-5594.
2. Ouimet, J.; Lafleur, M., Hydrophobic match between cholesterol and saturated fatty acid is required for the formation of lamellar liquid ordered phases. *Langmuir* 2004, *20*, 7474-7481.
3. Ouimet, J.; Croft, S.; Paré, C.; Katsaras, J.; Lafleur, M., Modulation of the polymorphism of the palmitic acid/cholesterol system by the pH. *Langmuir* 2003, *19*, 1089-1097.
4. Bastiat, G.; Oliger, P.; Karlsson, G.; Edwards, K.; Lafleur, M., Development of non-phospholipid liposomes containing a high cholesterol concentration. *Langmuir* 2007, *23*, 7695-7699.
5. Cui, Z.-K.; Bastiat, G.; Jin, C.; Keyvanloo, A.; Lafleur, M., Influence of the nature of the sterol on the behavior of palmitic acid/sterol mixtures and their derived liposomes. *Biochim. Biophys. Acta* 2010, *1798*, 1144-1152.
6. Phoeung, T.; Morfin Huber, L.; Lafleur, M., Cationic detergent/sterol mixtures can form fluid lamellar phases and stable unilamellar vesicles. *Langmuir* 2009, *25*, 5778-5784.
7. Gater, D. L.; Seddon, J. M.; Law, R. V., Formation of the liquid-ordered phase in fully hydrated mixtures of cholesterol and lysopalmitoylphosphatidylcholine. *Soft Matter* 2008, *4*, 263-267.
8. Ramakrishnan, M.; Tarafdar, P. K.; Kamlekar, R. K.; Swamy, M. J., Differential scanning calorimetric studies on the interaction of N-acylethanolamines with cholesterol. *Curr. Sci.* 2007, *93*, 234-238.
9. Bach, D.; Wachtel, E., Phospholipid/cholesterol model membranes: formation of cholesterol crystallites. *Biochim. Biophys. Acta* 2003, *1610*, 187-197.
10. Huang, J.; Buboltz, J. T.; Feigenson, G. W., Maximum solubility of cholesterol in phosphatidylcholine and phosphatidylethanolamine bilayers. *Biochim. Biophys. Acta* 1999, *1417*, 89-100.
11. Huang, J.; Feigenson, G. W., A microscopic interaction model of maximum solubility of cholesterol in lipid bilayers. *Biophys. J.* 1999, *76*, 2142-2157.

12. Bastiat, G.; Lafleur, M., Phase behavior of palmitic acid/cholesterol/cholesterol sulfate mixtures and properties of the derived liposomes. *J. Phys. Chem. B* 2007, *111*, 10929-10937.
13. Phoeung, T.; Aubron, P.; Rydzek, G.; Lafleur, M., pH triggered release from non phospholipid liposomes modulated by the pKa of the included fatty acid. *Langmuir* 2010, *26*, 12769-12776.
14. Lian, T.; Ho, R. J. Y., Trends and developments in liposome drug delivery systems. *J. Pharm. Sci.* 2001, *90*, 667-680.
15. Immordino, M. L.; Dosio, F.; Cattel, L., Stealth liposomes: review of the basic science, rationale, and clinical applications, existing and potential. *Int. J. Nanomed.* 2006, *1*, 297-315.
16. Ngo, K. X.; Umakoshi, H.; Shimanouchi, T.; Kuboi, R., Characterization of heat-induced interaction of neutral liposome with lipid membrane of streptomyces griseus cell. *Colloids Surf., B* 2009, *73*, 399-407.
17. Saito, R.; Krauze, M. T.; Noble, C. O.; Tamas, M.; Drummond, D. C.; Kirpotin, D. B.; Berger, M. S.; Park, J. W.; Bankiewicz, K. S., Tissue affinity of the infusate affects the distribution volume during convection-enhanced delivery into rodent brains: implications for local drug delivery. *J. Neurosci. Methods* 2006, *154*, 225-232.
18. Cowie, J. M. G.; Toporowski, P. M., Association in the binary liquid system dimethyl sulphoxide-water. *Can. J. Chem.* 1961, *39*, 2240-2243.
19. Saleh, M. A.; Ahmed, O.; Ahmed, M. S., Excess molar volume, viscosity and thermodynamics of viscous flow of the system dimethylsulfoxide and acetic acid. *J. Mol. Liq.* 2004, *115*, 41-47.
20. Wang, N.-N.; Li, Q.-Z.; Yu, Z.-W., Hydrogen bonding interactions in three 2-mercaptoethanol system: an excess infrared spectroscopic study. *Appl. Spectrosc.* 2009, *63*, 1356-1362.
21. Abraham, M. H.; Platts, J. A., Hydrogen bond structural group constants. *J. Org. Chem.* 2001, *66*, 3484-3491.
22. Rasmussen, D. H.; Mackenzie, A. P., Phase diagram for the system water-dimethylsulphoxide. *Nature* 1968, *220*, 1315-1317.
23. Allen, T. M., Calcein as a tool in liposome methodology. In *Liposome technology*, Gregoriadis, G., Ed. CRC Press: Boca Raton, FC, 1984; pp 177-182.

24. Benachir, T.; Lafleur, M., Study of vesicle leakage induced by melittin. *Biochim. Biophys. Acta* 1995, 1235, 452-460.
25. Loomis, C. R.; Shipley, G. G.; Small, D. M., The phase behavior of hydrated cholesterol. *J Lipid Res* 1979, 20, 525-535.
26. Epand, R. M.; Bach, D.; Borochoy, N.; Wachtel, E., Cholesterol crystalline polymorphism and the solubility of cholesterol in phosphatidylserine. *Biophys. J.* 2000, 78, 866-873.
27. Fenske, D. B.; Thewalt, J. L.; Bloom, M.; Kitson, N., Model of stratum corneum intercellular membranes:  $^2\text{H}$  NMR of macroscopically oriented multilayers. *Biophys. J.* 1994, 67, 1562-1573.
28. Seelig, J., Deuterium magnetic resonance: theory and application to lipid membranes. *Q. Rev. Biophys.* 1977, 10, 353-418.
29. Dufourc, E. J.; Parish, E. J.; Chitrakorn, S.; Smith, I. C. P., Structural and dynamical details of cholesterol-lipid interaction as revealed by deuterium NMR. *Biochemistry* 1984, 23, 6062-6071.
30. Douliez, J.-P.; Leonard, A.; Dufourc, E. J., Conformational order of DMPC sn-1 versus sn-2 chains and membrane thickness: an approach to molecular protrusion by solid state  $^2\text{H}$  NMR and neutron diffraction. *J. Phys. Chem.* 1996, 100, 18450-18457.
31. Marsan, M. P.; Muller, I.; Ramos, C.; Rodriguez, F.; Dufourc, E. J.; Czaplicki, J.; Milon, A., Cholesterol orientation and dynamics in dimyristoylphosphatidylcholine bilayers: a solid state deuterium NMR analysis. *Biophys. J.* 1999, 76, 351-359.
32. Kelusky, E. C.; Dufourc, E. J.; Smith, I. C. P., Direct observation of molecular ordering of cholesterol in human erythrocyte membranes. *Biochim. Biophys. Acta* 1983, 735, 302-304.
33. Monck, M. A.; Bloom, M.; Lafleur, M.; Lewis, R. N. A. H.; McElhaney, R. N.; Cullis, P. R., Evidence for two pools of cholesterol in the *Acholeplasma laidlawii* strain B membrane: a deuterium NMR and DSC study. *Biochemistry* 1993, 32, 3081-3088.
34. Davis, J. H., The description of membrane lipid conformation, order and dynamics by  $^2\text{H}$ -NMR. *Biochim. Biophys. Acta* 1983, 737, 117-171.
35. Dufourc, E. J.; Smith, I. C. P., A detailed analysis of the motions of cholesterol in biological membranes by  $^2\text{H}$ -NMR relaxation. *Chem. Phys. Lipids* 1986, 41, 123-135.

36. Mantsch, H. H.; McElhaney, R. N., Phospholipid phase transitions in model and biological membranes as studied by infrared spectroscopy. *Chem. Phys. Lipids* 1991, *57*, 213-226.
37. Kodati, R. V.; Lafleur, M., Comparaison between orientational and conformational orders in fluid lipid bilayers. *Biophys. J.* 1993, *64*, 163-170.
38. Kodati, V. R.; El-Jastimi, R.; Lafleur, M., Contribution of the intermolecular coupling and librotorsional mobility in the methylene stretching modes in the infrared spectra of acyl chains. *J. Phys. Chem.* 1994, *98*, 12191-12197.
39. Moore, D. J.; Rerek, M. E.; Mendelsohn, R., FTIR spectroscopy studies of the conformational order and phase behavior of ceramides. *J. Phys. Chem. B* 1997, *101*, 8933-8940.
40. Paré, C.; Lafleur, M., Polymorphism of POPE/cholesterol system: a  $^2\text{H}$  nuclear magnetic resonance and infrared spectroscopic investigation. *Biophys. J.* 1998, *74*, 899-909.
41. Chen, H.-C.; Mendelsohn, R.; Rerek, M. E.; Moore, D. J., Effect of cholesterol on miscibility and phase behavior in binary mixtures with synthetic ceramide 2 and octadecanoic acid. Infrared studies. *Biochim. Biophys. Acta* 2001, *1512*, 345-356.
42. Snyder, R. G.; Strauss, H. L.; Cates, D. A., Detection and measurement of microaggregation in binary mixtures of esters and of phospholipid dispersions. *J. Phys. Chem.* 1995, *99*, 8432-8439.
43. El Jastimi, R.; Lafleur, M., A dual-probe fluorescence method to examine selective perturbation of membrane permeability by melittin. *Biospectroscopy* 1999, *5*, 133-140.
44. Hargreaves, W. R.; Deamer, D. W., Liposomes from ionic, single-chain amphiphiles. *Biochemistry* 1978, *17*, 3759-3768.

## **Chapter 4**

# **Formation of pH-Sensitive Cationic Liposomes From a Binary Mixture of Monoalkylated Primary Amine and Cholesterol**

Zhong-Kai Cui, Anne Bouisse, Nicolas Cottenye, and Michel Lafleur

Reprinted with permission from

*Langmuir*, 2012, **28**, 13668-13674

Copyright © 2012 American Chemical Society

## **4.1 Abstract**

It has been shown that mixtures of monoalkylated amphiphiles and sterols can form liquid-ordered (lo) lamellar phases. These bilayers can be extruded using conventional methods to obtain large unilamellar vesicles (LUVs) that have very low permeability and a specific response to a given stimulus. For example, pH variations can trigger the release from LUVs formed with palmitic acid and sterols. In the present work, the possibility to form non phospholipid liposomes with mixtures of stearylamine (SA) and cholesterol (Chol) was investigated. The phase behavior of these mixtures was characterized by differential scanning calorimetry, infrared, and  $^2\text{H}$  NMR spectroscopy. It is found that this particular mixture can form a lo lamellar phase that is pH-sensitive as the system undergoes a transition from a lo phase to a solid state when pH is increased from 5.5 to 12. LUVs have been successfully extruded from equimolar SA/Chol mixtures. Release experiments as a function of time revealed the relatively low permeability of these systems. The fact that the stability of these liposomes is pH dependent implies that these LUVs display an interesting potential as new cationic carriers for pH-triggered release. This is the first report of non phospholipid liposomes with high sterol content combining an overall positive charge and pH-sensitivity.

## 4.2 Introduction

Liposomes have been attracting considerable interest since British hematologist Dr. Alec Bangham et al. first reported their discovery in 1964.<sup>1</sup> Over the last 50 years, liposomal nanotechnology has significantly evolved, and now liposomes have found applications in many fields including nanopharmaceutics,<sup>2</sup> cosmetics,<sup>3</sup> food,<sup>4</sup> and textile<sup>5</sup> industries. Liposomes are essentially used as nanocontainers for protecting, transporting and targeting solutes. Molecular features can be introduced in liposomes in order to craft some beneficial properties. For example, pH-sensitive liposomes are of interest for the release of encapsulated solutes at a specific location in cells or organisms where a distinct local pH prevails.<sup>6</sup> Similarly, cationic liposomes display distinct advantages for some applications related to vectorization and delivery. For instance, in gene therapy, cationic liposomes are reported to interact and complex with DNA or oligonucleotides, markedly prevent nuclease degradation, enhance cellular uptake rate of oligonucleotide, and result in a better intracellular distribution.<sup>7-9</sup> Cationic liposomes were also shown to enhance the stability of some anticancer drugs, such as paclitaxel,<sup>10</sup> to improve cancer cell uptake and to target tumor microvasculature endothelial cells.<sup>11-13</sup> Cationic liposomes were shown to be useful for dermal and transdermal drug delivery,<sup>3, 14, 15</sup> and were found to have high affinity to bacteria biofilms.<sup>16</sup>

Over the past decade, it has been reported that cholesterol (Chol) and other sterols can induce the formation of fluid lamellar phases when mixed with monoalkylated amphiphiles, such as palmitic acid (PA),<sup>17-19</sup> *N*-acylethanolamine,<sup>20</sup> lyso-palmitoylphosphatidylcholine (lyso-PPC),<sup>21</sup> cetylpyridinium chloride (CPC)<sup>22</sup> octadecyl methyl sulfoxide (OMSO),<sup>23</sup> and

cetyltrimethylammonium bromide (CTAB).<sup>24</sup> Even though these monoalkylated amphiphiles or sterols do not form fluid lamellar phases once hydrated individually, their mixtures lead to stable liquid-ordered (lo) bilayers. Typically, these fluid bilayers include a high sterol content, varying between 50 and 75 mol %. At this point, some molecular prerequisites for fluid-bilayer formation have been identified. The hydrophobic match between the length of the alkyl chain (14–18 carbon atoms) of the monoalkylated amphiphiles and that of the hydrophobic segment of cholesterol is essential for the formation of lo bilayers.<sup>25</sup> The stability of those bilayers has been found to be intimately associated with the bilayer surface electrostatics. The presence of bilayer interfacial charges is suggested to be a key element in the intermolecular interactions between the bilayer components and is believed to contribute to the proper hydration of the interface. It has been established that large unilamellar vesicles (LUVs) can be obtained from these fluid bilayers using conventional extrusion methods. As the stability of PA/sterol bilayers is dictated by the protonation state of the fatty acid, the resulting liposomes are found to be pH-sensitive, the modulation of the bulk pH resulting in switching between the protonation/deprotonation states of PA molecules.<sup>18,26</sup> Moreover, it has been shown that one can control the pH at which the release is triggered by using PA derivatives with different  $pK_a$ .<sup>27</sup>

In this Article, we report the development of non phospholipid liposomes that are both cationic and pH sensitive, two features that have never been jointly crafted in a liposome. This investigation aims essentially at establishing that specific properties can be introduced in liposomes based on the current understanding of the rules dictating the formation of stable self-assemblies. We examined the possibility of forming liposomes using stearylamine (SA) as the monoalkylated amphiphile, and cholesterol. The primary amine is a functional group whose protonation/deprotonation state can be exploited to control the surface charge density. The  $pK_a$  of

monomeric stearylamine is 10.6,<sup>28</sup> while its apparent  $pK_a$  when inserted in phosphatidylcholine bilayers is approximately 9.5.<sup>29</sup> Stearylamine was also selected because the length of its 18 carbon alkyl chain matches the hydrophobic section of cholesterol.<sup>25</sup> This fatty amine has been previously used to provide a cationic charge to phospholipid liposomes.<sup>14</sup> First, the phase behavior of SA/Chol mixtures in different proportions was characterized by differential scanning calorimetry (DSC), infrared (IR) spectroscopy, and nuclear magnetic resonance spectroscopy of deuterium (<sup>2</sup>H NMR), to identify the conditions leading to the formation of lo phase bilayers. Second, we examined the possibility to extrude the SA/Chol mixtures forming fluid bilayers to obtain LUVs and characterized the stability and the permeability of these resulting liposomes. Finally, the pH-sensitivity of those cationic liposomes was assessed.

### 4.3 Materials and methods

Cholesterol (>99%), stearylamine (99%), tris(hydroxymethyl)aminomethane (TRIS) (99%), 2-[*N*-morpholino]ethanesulfonic acid (MES) (>99%), ethylenediaminetetraacetic acid (EDTA) (99%), NH<sub>4</sub>Cl (>99%), NaCl (>99%) and cholesterol-2,2,4,4,6-*d*<sub>5</sub> (Chol-*d*<sub>5</sub>) were supplied by Sigma Chemical Co. (St. Louis, MO). 1-palmitoyl-2-oleyl-*sn*-glycerophosphocholine (POPC) was purchased from Avanti Polar Lipids, Inc. (Alabaster, AL). <sup>3</sup>H-glucose was obtained from Perkin Elmer (Boston, MA). Sephadex G-50 Medium was purchased from Pharmacia (Uppsala, Sweden). Methanol (spectrograde) and benzene (high purity) were obtained from American Chemicals Ltd. (Montreal, QC, Canada) and BDH Inc. (Toronto, ON, Canada), respectively. All solvents and products were used without further purification.

Mixtures of stearylamine and cholesterol were prepared by dissolving weighed amounts of the solid chemicals in a mixture of benzene/methanol 90/10 (v/v). The solutions were then frozen in liquid nitrogen and lyophilized for at least 16 h to allow complete sublimation of the organic solvent. Cholesterol was substituted by cholesterol-*d*<sub>5</sub> for the <sup>2</sup>H NMR experiments. The freeze-dried lipid mixtures were hydrated with a MES/TRIS buffer (TRIS 50 mM, MES 50 mM, NaCl 130 mM, EDTA 0.5 mM) providing a buffered range between pH 5 and 9, or with a TRIS/NH<sub>4</sub>Cl buffer (TRIS 50 mM, NH<sub>4</sub>Cl 50 mM, NaCl 130 mM, EDTA 0.5 mM) providing a buffered range between pH 7 and 11. The buffers were prepared with Milli-Q water for DSC and IR spectroscopy. Deuterium-depleted water was used for <sup>2</sup>H NMR experiments. The final lipid concentration was 20 mg/mL for DSC and 30 mg/mL for IR and <sup>2</sup>H NMR spectroscopy experiments. To ensure a good hydration of the samples, the suspensions were subjected to five temperature cycles from liquid nitrogen temperature to ~70 °C, and were vortexed between successive cycles. After hydration, the pH was measured and readjusted, if necessary, by the addition of an aliquot of diluted HCl or NaOH solution.

DSC was performed with a VP-DSC microcalorimeter (MicroCal, Northampton, MA). The reference cell was filled with the corresponding buffer. Data acquisition was performed from 25 to 80 °C, at a heating rate of 40 °C/h. Data acquisition and treatment were performed with the Origin software (MicroCal software, Northampton, MA).

IR spectra were recorded on a Thermo Nicolet 4700 spectrometer, equipped with a KBr beam splitter and a DTGS-L-alanine detector. An aliquot of the sample was placed between two BaF<sub>2</sub> windows separated by a 5 µm-thick Teflon ring. This assembly was inserted into a brass

sample holder, whose temperature was controlled by Peltier thermopumps. Each spectrum was the result of 60 scans with a nominal  $2\text{ cm}^{-1}$  resolution, Fourier transformed using a triangular apodization function. The temperature was varied from low to high, and there was a 5 min incubation period prior to the data acquisition. The reported band positions correspond to the centers of gravity calculated from the top 5% of the band.

$^2\text{H}$  NMR spectra were recorded on a Bruker AV-400 spectrometer, using a Bruker static probe equipped with a 10 mm coil. The hydrated lipid suspension was transferred into a homemade Teflon holder that filled the coil. A quadrupolar echo sequence was used with a  $90^\circ$  pulse of  $5.5\ \mu\text{s}$  and an interpulse delay of  $30\ \mu\text{s}$ . The recycling time was 30 s. In the absence of a slow-relaxation solid phase, the recycling delay was reduced to 0.3 s. Typically 5000 FIDs were coadded. The temperature was regulated using a Bruker VT-3000 controller, and the data acquisition was carried out as a function of increasing temperature.

LUVs were prepared by extrusion using a hand-held Liposofast extruder (Avestin, Ottawa, Canada). The dispersions were passed 15 times through two stacked polycarbonate filters (100 nm pore size) at room temperature. The chemical composition of the extruded liposomes corresponded to the initial SA/Chol proportions, as assessed by mass spectrometry. The hydrodynamic diameter and the zeta potential of resulting LUVs were measured at  $25\ ^\circ\text{C}$ , using a Malvern Zetasizer.

The glucose passive permeability of the LUVs was evaluated. Glucose (240 mM and an aliquot of  $^3\text{H}$ -glucose) was added to the SA/Chol mixtures, hydrated with a TRIS/ $\text{NH}_4\text{Cl}$  buffer

(TRIS 50 mM, NH<sub>4</sub>Cl 50 mM, NaCl 10 mM, EDTA 0.5 mM), pH 7.5, before the freeze-and-thaw cycles. The lipid concentration was 30 mg/mL, while the radioactivity was ~43 μCi/mL. After extrusion, the glucose-containing vesicles were isolated at room temperature from the free glucose by gel permeation chromatography using Sephadex G-50 (column diameter, 1.5 cm; length, 25 cm), equilibrated with a TRIS/NH<sub>4</sub>Cl buffer (TRIS 50 mM, NH<sub>4</sub>Cl 50 mM, NaCl 130 mM, EDTA 0.5 mM), isoosmotic with the glucose-containing buffer. The lipid concentration was then ~3 mg/mL. The glucose passive release was determined as a function of time by isolating the entrapped glucose of a 100 μL aliquot of the vesicle suspension using a Sephadex G-50 spin column (0.4 cm in diameter, 7 cm in length). The radioactivity of an aliquot of the harvested fraction was measured. To take into account the sample dilution on the spin column, an aliquot of POPC liposomes, used as an internal standard, was added to the sample right before the spin column. POPC concentration in the harvested fraction was quantified using the Bartlett method.<sup>30</sup> The potential pH-triggered leakage of glucose was also examined. The external pH was modified by adding an aliquot of diluted HCl or NaOH solution to the LUVs suspension. Spin columns were used to isolate the released glucose, and % release was calculated as described above. The sample radioactivity was measured on a Beckman LS6500 counter.

## **4.4 Results and discussion**

### **4.4.1 Thermal phase behavior of SA/Chol mixtures**

We first explored the phase behavior of the SA/Chol mixtures in order to identify whether this mixture can lead to the formation of a fluid lamellar phase, a prerequisite to the formation of

liposomes. The thermal behavior of SA/Chol mixtures with various compositions was examined by DSC. Figure 4.1 presents the thermograms of these mixtures hydrated at pH 5.5, a low pH ensuring the protonation of the amine groups. For pure stearylamine, the thermogram showed a sharp peak at about 58 °C, corresponding to the melting of the amphiphile. The presence of cholesterol, up to 30% molar ratio, led to a small downshift of the peak, while its width increased. When stearylamine and cholesterol were in equal molar proportion, no peak could be observed, suggesting the absence of transition over the whole investigated temperature range. For SA/Chol mixtures with larger cholesterol contents, a broad endothermic peak was observed at ~35 °C. This endotherm is believed to be associated with excess solid cholesterol experiencing the transition from the anhydrous form I to the anhydrous form II.<sup>31</sup> During the cooling, a transition was observed at 24 °C (data not shown), corresponding to the conversion of cholesterol anhydrous form II into its form I with a hysteresis of ~10 °C, in agreement with a previous report.<sup>31</sup> Therefore, it is inferred that proportions of cholesterol larger than 50 mol % led to solid cholesterol, suggesting that the solubility limit of cholesterol in the SA/Chol system had been reached.

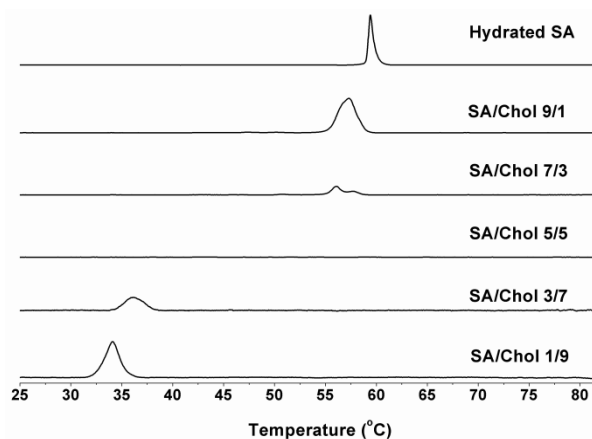


Figure 4.1. Thermograms of hydrated pure SA and of SA/Chol mixtures of various molar ratios, pH 5.5.

The thermal behavior of SA/Chol mixtures was also examined by IR spectroscopy. The position of the symmetric C–H stretching ( $\nu_{\text{C-H}}$ ) mode, associated with the stearylamine alkyl chain, is mainly influenced by the trans–gauche chain isomerization and by the interchain coupling. As a consequence, it constitutes a sensitive probe for transitions involving a change in chain conformational order.<sup>32-34</sup> The melting of pure hydrated stearylamine was easily detected at about 58 °C by the abrupt shift of the  $\nu_{\text{C-H}}$  band from  $\sim 2849.7$  to  $\sim 2852.7$   $\text{cm}^{-1}$  (Figure 4.2). These positions are representative of highly ordered and disordered chains, respectively. The presence of cholesterol induced an increase of the  $\nu_{\text{C-H}}$  band wavenumber below the transition temperature and a reduction above the transition temperature; these changes led to the disappearance of the phase transition. This impact of cholesterol is reminiscent of its well-established effect on phospholipid bilayers,<sup>35,36</sup> as cholesterol decreases and ultimately abolishes the gel to liquid crystalline phase transitions of phospholipids. An analogous effect is also observed for the mixtures of cholesterol with some monoalkylated amphiphiles, including palmitic acid and octadecyl methyl sulfoxide.<sup>23, 26</sup> In these cases, however, in contrast with phospholipid/cholesterol bilayers, the monoalkylated amphiphile and the sterol exist in solid form below the transition temperature. At low temperatures, cholesterol prevents the formation of a solid phase by the monoalkylated amphiphiles, introduces fluidity in the self-assembly, and promotes the formation of a lo lamellar phase. At temperatures higher than the transition temperature, it orders the amphiphile alkyl chain, favoring again the formation of lo lamellar phases. The overall effect is a reduction of the frequency shift associated with of the transition, consistent with the DSC results. For mixtures containing 50 mol % or more cholesterol, the  $\nu_{\text{C-H}}$  position was  $\sim 2851$   $\text{cm}^{-1}$  over the investigated temperature range, a value observed for lo lamellar phases.<sup>32,37</sup>

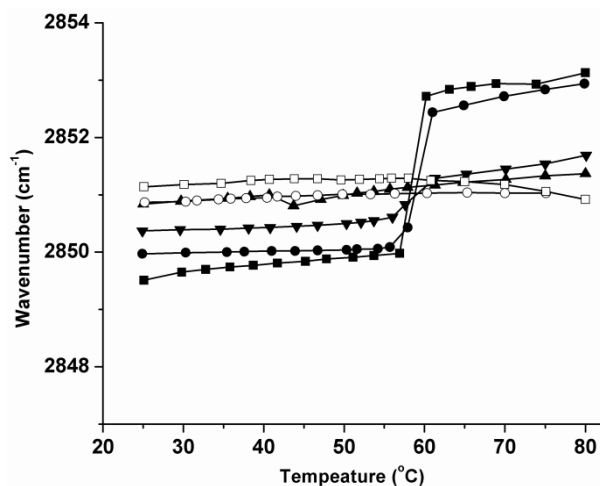
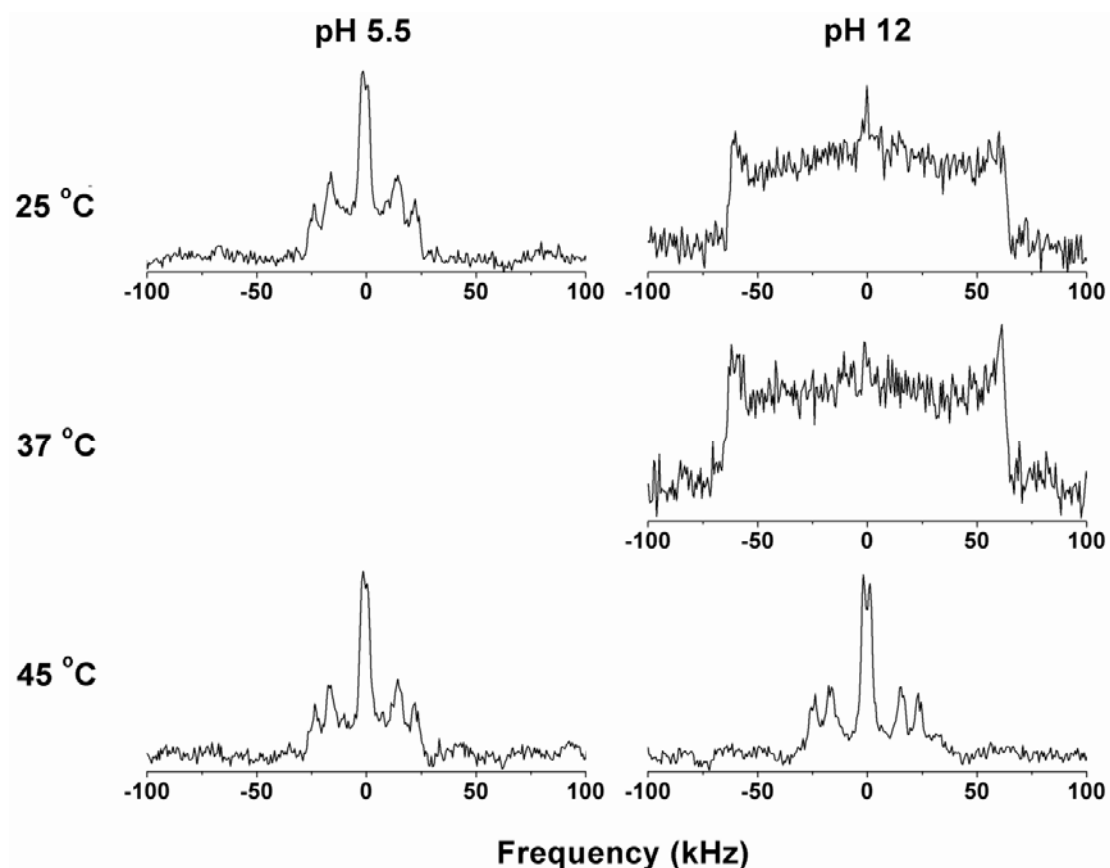


Figure 4.2. Thermotropism, reported by the  $\nu_{C-H}$  band position of the IR spectra, of hydrated SA (■), and of SA/Chol mixtures with various compositions: 1/9 (□), 3/7 (○), 5/5 (▲), 7/3 (▼), and 9/1 (●) (molar ratio), pH 5.5.

The  $\nu_{C-H}$  position of the IR spectra essentially reported the behavior of stearylamine alkyl chain in the mixtures. To investigate the phase behavior from the cholesterol point of view,  $^2\text{H}$  NMR spectroscopy of mixtures including deuterated cholesterol was carried out. Figure 4.3 presents  $^2\text{H}$  NMR spectra of equimolar SA/Chol- $d_5$  mixtures. At pH 5.5, the spectra displayed three fairly well-resolved powder patterns, typical of cholesterol solubilized in fluid bilayers. These spectra were very similar to those obtained for Chol- $d_5$  inserted in other fluid bilayers formed by monoalkylated amphiphiles and cholesterol, such as PA/Chol<sup>17</sup> and OMSO/Chol<sup>23</sup> systems, in phosphatidylcholine bilayers,<sup>38, 39</sup> and even in biological membranes such as human red blood cell membranes,<sup>40</sup> and membranes of mycoplasma *Acholeplasma laidlawii* (strain B).<sup>41</sup> The quadrupolar splittings measured between the maxima are reported in Table 4.1. Using a model previously described,<sup>17, 39</sup> it was possible to reproduce the experimental values of quadrupolar splittings, assuming that cholesterol had axially symmetric motions in the bilayers,

and that the orientation of this axis of rotation in cholesterol molecule was similar to that determined for phospholipid bilayers.  $\beta$  is the fixed angle between the C–D bond and the cholesterol long axis, defined as the rotation axis. The values that we used (Table 4.1) were those previously determined for cholesterol embedded in a phosphatidylcholine matrix.<sup>39</sup> Therefore, the only fitting parameter in this approach is the molecular order parameter,  $S_{\text{mol}}$ , describing the whole-body motion of cholesterol. The fitted value for  $S_{\text{mol}}$  in the SA/Chol- $d_5$  equimolar mixture was 0.95, indicating that the axis of rotation of cholesterol is practically parallel to the bilayer normal and that the molecules experience practically no wobbling. Such structure and dynamics were also proposed for the other cholesterol-containing systems mentioned above, and this behavior seems to be rather general. Combining DSC, IR, and  $^2\text{H}$  NMR results, we conclude that an equimolar SA/Chol mixture forms a fluid bilayer phase over the investigated temperature range.

Figure 4.3.  $^2\text{H}$  NMR spectra of an equimolar SA/Chol- $d_5$  mixture.Table 4.1.  $^2\text{H}$  NMR parameters associated with cholesterol in equimolar SA/Chol- $d_5$  mixtures, at 45 °C.

| pH  | position               | exp $\Delta\nu_Q$<br>(kHz) | $\beta$ obtained<br>from ref <sup>39</sup> | calcd $S_{\text{mol}}$ | calcd $\Delta\nu_Q$<br>(kHz) |
|-----|------------------------|----------------------------|--|------------------------|------------------------------|
| 5.5 | 2,4- $^2\text{H}_2$ ax | 46.8                       | 74.1                                       | 0.95                   | 46.9                         |
|     | 2,4- $^2\text{H}_2$ eq | 33.6                       | 66.2                                       |                        | 31.0                         |
|     | 6- $^2\text{H}$        | 3.0                        | 55.8                                       |                        | 3.2                          |
| 12  | 2,4- $^2\text{H}_2$ ax | 50.0                       | 74.1                                       | 1                      | 49.4                         |
|     | 2,4- $^2\text{H}_2$ eq | 34.2                       | 66.2                                       |                        | 32.6                         |
|     | 6- $^2\text{H}$        | 4.3                        | 55.8                                       |                        | 3.3                          |

## 4.4.2 Effect of pH on the phase behavior of SA/Chol mixtures

The selection of stearylamine as the monoalkylated amphiphile was based on the hypothesis that the primary amine group could introduce in the system a pH sensitivity that may be exploited to trigger the release from the derived liposomes. Therefore, we examined the impact of pH on the phase behavior of the equimolar SA/Chol mixture, using DSC, IR, and  $^2\text{H}$  NMR spectroscopy. No transition was observed by DSC for the equimolar SA/Chol mixture when the bulk pH was between 5.5 and 9 (Figure 4.4). This observation is consistent with the IR results as the  $\nu_{\text{C-H}}$  position of the mixture spectra was, for these pH values, around  $2851\text{ cm}^{-1}$  over the whole investigated temperature range (Figure 4.5). These findings indicate the formation of a stable lo lamellar phase in these conditions.

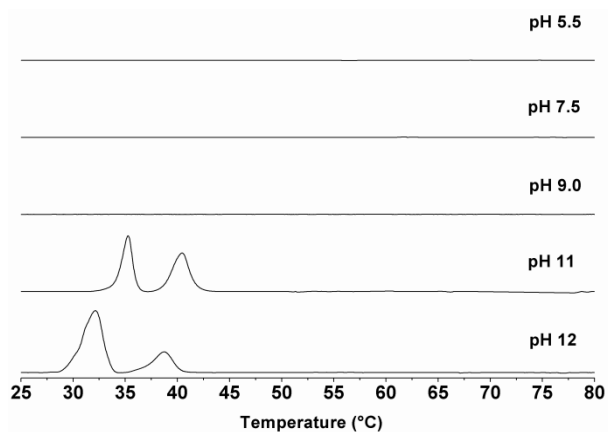


Figure 4.4. Thermograms of equimolar SA/Chol mixtures at various pH values.

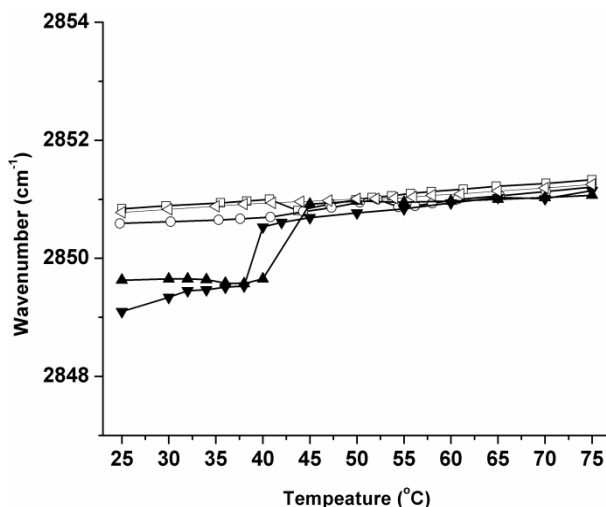


Figure 4.5. Thermotropism, reported by the  $\nu_{\text{C-H}}$  band position of the IR spectra, of equimolar SA/Chol mixtures at pH 5.5 ( $\square$ ), 7.5 ( $\triangleleft$ ), 9.0 ( $\circ$ ), 11 ( $\blacktriangledown$ ) and 12 ( $\blacktriangle$ ).

When the pH was increased to 11 and 12, the thermograms revealed two maxima, at around 34 and 40 °C. The transition at around 40 °C was also detected by IR spectroscopy from the shift of the  $\nu_{\text{C-H}}$  frequency, going from lower than 2850  $\text{cm}^{-1}$  at low temperatures to  $\sim 2851 \text{ cm}^{-1}$  above the transition temperature. These values suggest that stearylamine chains underwent a transition from a solid to a lo lamellar phase. At pH 12, 25 °C, a single broad powder pattern was observed in the  $^2\text{H}$  NMR spectrum of the SA/Chol- $d_5$  mixture (Figure 4.3). The quadrupolar splitting between the two maxima was 125 kHz. These spectra are identical to that obtained from solid cholesterol, all five deuterated positions giving rise to this single and maximum quadrupolar splitting, suggesting that the cholesterol molecules are immobile.<sup>17, 42</sup>  $^2\text{H}$  NMR spectra indicated that, at pH 12, cholesterol remained in a solid phase up to 37 °C. At 45 °C, the characteristic profile of cholesterol solubilized in fluid bilayers was obtained, and the solid-cholesterol contribution could no longer be observed. The quadrupolar splittings associated with this mobile cholesterol were very similar to those measured at pH 5.5 (Table 4.1). Therefore, the transition

observed at 40 °C was assigned to a transition from a solid to a lo lamellar phase in the equimolar SA/Chol mixture. The transition at about 35 °C observed in the thermograms recorded at high pH (Figure 4.4) is suggested to be associated with a crystalline reorganization of stearylamine. This transition was observed in the thermogram of pure hydrated stearylamine at pH 12, whereas the chain melting temperature of stearylamine was 66 °C in these conditions (data not shown). Furthermore, at pH 12, X-ray diffraction patterns obtained from pure hydrated stearylamine showed different crystalline features at 25 and 45 °C.

These results altogether established that, in the equimolar mixture at pH < 9, protonated stearylamine is well mixed with cholesterol molecules, leading to the formation of stable lo lamellar phases. However, pH values greater than 9 lead to a phase separation giving rise to solid cholesterol as well as solid stearylamine; this behavior is associated with the deprotonated state of the amine group. Cholesterol however reduces the chain melting transition of stearylamine to ~40 °C and, above this transition temperature, lo lamellar phases formed with stearylamine and cholesterol were observed. We can conclude that the bilayers formed by an equimolar SA/Chol mixture at pH ≤ 9 are positively charged and pH-sensitive. Therefore, we examined whether they represent an opportunity to create novel pH-sensitive non phospholipid liposomes.

#### 4.4.3 Liposome properties

The phase behavior of an equimolar SA/Chol mixture guided our selection of conditions that could lead to the formation of liposomes. It was shown previously that lo bilayers made of monoalkylated amphiphiles and sterols can be extruded despite their high sterol content.<sup>22, 23, 43</sup> The SA/Chol system displayed a similar behavior, and LUVs could be obtained by extrusion

from this mixture, at  $\text{pH} \leq 9.5$ . Table 4.2 reports the size and the zeta potential of the resulting liposomes. The measured liposome diameters were, as expected, slightly larger than the pore size of the extrusion filters, and these sizes remained constant over at least 1 month. However, at  $\text{pH}$  10.5 and 11.5, the extrusion process was impossible as solid lipids would simply obstruct the filter pores. The liposomal surface charge density can be conveniently investigated by microelectrophoresis and characterized by the zeta potential. The zeta potential of 100 nm liposomes made from equimolar SA/Chol mixtures (Table 4.2) was 43 and 33 mV at  $\text{pH}$  7.5 and 8.5, respectively, indicating that the suspension is stable.<sup>44</sup> The size increase and the small decrease of the LUV zeta potential observed with the  $\text{pH}$  increase are likely associated with the progressive deprotonation of the amine groups.

Table 4.2. Characteristics of extruded LUVs for equimolar SA/Chol mixtures at various  $\text{pH}$  values<sup>a</sup>

| $\text{pH}$ | $d_{\text{LUVs}}$ (nm) | Zeta potential (mV) |
|-------------|------------------------|---------------------|
| 7.5         | $101 \pm 5$            | $43 \pm 3$          |
| 8.5         | $113 \pm 10$           | $33 \pm 2$          |
| 9.5         | $170 \pm 7$            | $24 \pm 2$          |

<sup>a</sup> The samples were hydrated in TRIS/ $\text{NH}_4\text{Cl}$  buffers with  $\text{pH}$  varying from 7.5 to 9.5

We have determined the permeability of the liposomes formed with an equimolar SA/Chol mixture, at pH 7.5. The passive leakage of glucose from these vesicles is presented in Figure 4.6. A progressive release was observed, and it took approximately 30 days to have about 90% of the entrapped glucose released. As a comparison, more than 90% of encapsulated glucose leaked out from phosphatidylcholine liposomes containing between 40 and 50 mol % cholesterol within 10 days.<sup>43, 45</sup> Therefore, we can conclude that the passive permeability of the SA/Chol liposomes is considerably more limited than that of cholesterol-containing phospholipid liposomes. It is proposed that the high cholesterol content makes the bilayers more rigid and thicker, resulting in a lower permeability. This cationic formulation seems however to be somewhat more permeable than PA/Chol liposomes. Only 10% of entrapped glucose was released after 30 days from the latter.<sup>43</sup> This increased impermeability may be associated with the higher cholesterol content as these LUVs were formed with PA/Chol mixtures in a molar ratio of 30/70.

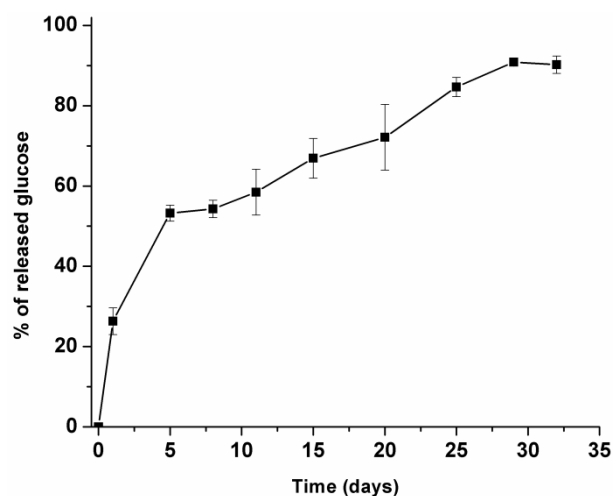


Figure 4.6. Passive release of equimolar SA/Chol LUVs, at room temperature, pH 7.5. (n=3)

Because of the impact of the amine protonation state on the phase behavior of the SA/Chol mixture reported above, the LUVs formed with this mixture were expected to be pH-sensitive. To demonstrate the pH-triggered release, we modified the external pH of a suspension of glucose-loaded liposomes initially prepared at pH 7.5 from an equimolar SA/Chol mixture, and the glucose release was measured. Figure 4.7 shows that the content release was strongly dependent on the external pH. For  $\text{pH} < 9.5$ , practically no leakage was observed. Conversely, for  $\text{pH} \geq 11$ , the entrapped glucose was completely released within 10 min. The release profile as a function of pH is reminiscent of a titration curve with an inflection point at pH 10, corresponding to the  $\text{p}K_a$  of the amine group.<sup>29</sup> The rapid pH-triggered release is associated with the fact that neutral stearylamine and cholesterol molecules phase separate at high pH and exist in solid forms in these conditions. As pH was increased above 9.5, macroscopic aggregates could be observed in the samples, and vesicles could no longer be detected by dynamic light scattering. The formation of solid phases by the components would indeed be accompanied by the release of glucose that was initially entrapped in the liposomes. The reported behavior is reminiscent of PA/sterol LUVs, which are also pH-sensitive. A sudden burst of release of the entrapped materials was observed when the pH was lowered and PA became neutral (i.e., protonated).<sup>18, 43</sup> The protonated/deprotonated state of the pH-sensitive group appears to be the crucial parameter leading to the triggered release.

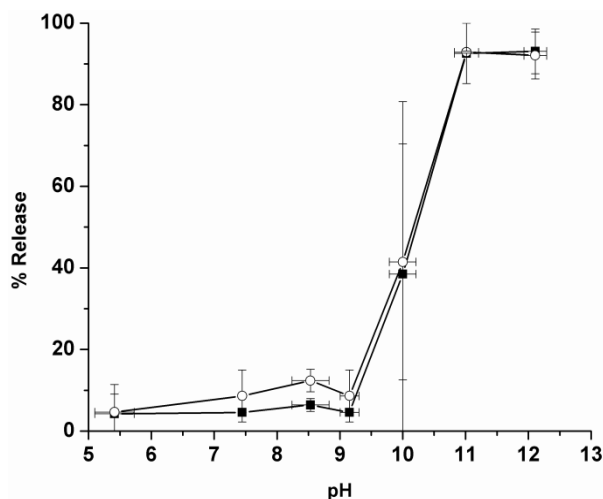


Figure 4.7. pH-triggered release of glucose from LUVs obtained from an equimolar SA/Chol mixture. The measurements were carried out at room temperature, ~10 min (■) and ~1 h (○) after the external pH change. (n=3)

These new findings reinforce the hypothesis that interfacial charges play a pivotal role in the stability of the fluid bilayers formed by binary mixtures of a monoalkylated amphiphile bearing a small polar head group (e.g., carboxylic, ammonium, etc) and a sterol. The binary mixtures that could form lo lamellar phases include unprotonated PA/Chol,<sup>26</sup> protonated PA/cholesterol sulfate (Schol),<sup>19</sup> CPC/Chol, CPC/Schol,<sup>22</sup> CTAB/Chol,<sup>24</sup> *N*-alkylethanolamine/Chol<sup>20</sup> and lyso-PPC/Chol<sup>21</sup> systems. All of these mixtures include at least one charge at the head group level; it could be a zwitterionic headgroup like in the case of lyso-PPC. The stability associated with the presence of an interfacial charge is exemplified by the mixtures that include an ionizable group such as a carboxylic group<sup>19, 26</sup> or an amine group (this work). In the presence of cholesterol, stable lo lamellar phases are obtained at room temperature when the monoalkylated amphiphile bears a charge: a negatively charged unprotonated carboxylic group in the case of fatty acids<sup>17, 19, 26</sup> and a positively charged protonated amine group in the case of

stearylamine (this work). When the pH is modified in such a way that the monoalkylated amphiphile becomes neutral (a pH decrease in the case of PA to provide the protonated form and a pH increase in the case of stearylamine to provide the unprotonated form), the mixtures with cholesterol lead to a phase separation and to the disruption of the fluid bilayers.<sup>19,26</sup> It was found that the charge can also be carried by the sterol molecule as negatively charged cholesterol sulfate forms stable lamellar phases in the presence of neutral protonated PA.<sup>19</sup> The importance of the interfacial charges in the stability of these fluid bilayers is proposed to arise from two phenomena. First, the lipid mixing is promoted by the presence of a charged species as the mixing would lead to a reduction of the unfavorable electrostatic repulsion. Such effect would exist for mixtures formed by a charged and a neutral species as well as in the cases where the two species bear charges of opposite sign such as CPC and Chol.<sup>22</sup> Indeed, electrostatic stabilization would not be observed if the two species both carry negative charges such as in the case of unprotonated PA and Chol, which do not mix and do not lead to the formation of a lo lamellar phase.<sup>19</sup> Second, the presence of interfacial charges is proposed to provide an appropriate hydration of the bilayer interface, a feature that is critical for the formation of a fluid bilayer.<sup>23</sup>

In conclusion, we discovered the possibility to form a lo lamellar phase with a binary mixture including stearylamine and cholesterol. These fluid bilayers were stable at room temperature only for pH lower than the  $pK_a$  of the amine group ( $pH < 9.5$ ). We also demonstrate that it is possible to extrude liposomes from the equimolar SA/Chol mixtures, leading to LUVs that display a positive zeta potential, are relatively impermeable, and are pH-sensitive. This new formulation not only extends the family of non phospholipid liposomes with high sterol contents, but it also establishes that the identified molecular requirements allow designing tailored liposomes from monoalkylated amphiphiles and sterol. In this Article, we targeted the formation

of cationic liposomes with a simple and cheap amphiphile. On the basis of the same rationale, we believe that it is possible to create novel cationic formulations using analogous molecules such as alkylated imidazole and glucosamine that would offer the opportunity to tune the pH-triggered release of the liposome content, based on their respective  $pK_a$ . Such advances present a new avenue for making potentially useful nanovectors.

## **4.5 Acknowledgements**

Z.-K. C. is grateful to the China Scholarship Council and Université de Montréal for his scholarship. We would like to thank the Natural Sciences and Engineering Research Council of Canada for financial support. This work was also funded by Fonds Québécois de la Recherche sur la Nature et les Technologies through its financial support to the Center for Self-Assembled Chemical Systems (CSACS). We thank Guillaume Bastiat for carrying out preliminary experiments.

## 4.6 References

1. Bangham, A. D.; Horne, R. W., Negative staining of phospholipids and their structural modification by surface-active agents as observed in the electron microscope. *J. Mol. Biol.* **1964**, *8*, 660-668.
2. Torchilin, V. P., Recent advances with liposomes as pharmaceutical carriers. *Nat. Rev. Drug Discovery* **2005**, *4*, 145-160.
3. Papakostas, D.; Rancan, F.; Sterry, W.; Blume-Peytavi, U.; Vogt, A., Nanoparticles in dermatology. *Arch. Dermatol. Res.* **2011**, *303*, 533-550.
4. Fathi, M.; Mozafari, M. R.; Mohebbi, M., Nanoencapsulation of food ingredients using lipid based delivery systems. *Trends Food Sci. Technol.* **2012**, *23*, 13-27.
5. Barani, H.; Montazer, M., A review on applications of liposomes in textile processing. *J. Liposome Res.* **2008**, *18*, 249-262.
6. Drummond, D. C.; Zignani, M.; Leroux, J.-C., Current status of pH-sensitive liposomes in drug delivery. *Prog. Lipid Res.* **2000**, *39*, 409-460.
7. Xu, Y.; Szoka, F. C., Mechanism of DNA release from cationic liposome/DNA complexes used in cell transfection. *Biochemistry* **1996**, *35*, 5616-5623.
8. Zelphati, O.; Szoka, F. C., Intracellular distribution and mechanism of delivery of oligonucleotides mediated by cationic lipids. *Pharm. Res.* **1996**, *13*, 1367-1372.
9. Hong, K.; Zheng, W.; Baker, A.; Papahadjopoulos, D., Stabilization of cationic liposome-plasmid DNA complexes by polyamines and poly(ethylene glycol)-phospholipid conjugates for efficient in vivo gene delivery. *FEBS Lett.* **1997**, *400*, 233-237.
10. Campbell, R. B.; Balasubramanian, S. V.; Straubinger, R. M., Influence of cationic lipids on the stability and membrane properties of paclitaxel-containing liposomes. *J. Pharm. Sci.* **2001**, *90*, 1091-1105.
11. Dabbas, S.; Kaushik, R. R.; Dandamudi, S.; Kuesters, G. M.; Campbell, R. B., Importance of the liposomal cationic lipid content and type in tumor vascular targeting: physicochemical characterization and in vitro studies using human primary and transformed endothelial cells. *Endothelium* **2008**, *15*, 189-201.

12. Loney, C.; Vandenbranden, M.; Ruyschaert, J. M., Cationic liposomal lipids: From gene carriers to cell signaling. *Prog. Lipid Res.* **2008**, *47*, 340-347.
13. Campbell, R. B.; Balasubramanian, S. V.; Straubinger, R. M., Phospholipid-cationic lipid interactions: influences on membrane and vesicle properties. *Biochim. Biophys. Acta* **2001**, *1512*, 27-39.
14. Gonzalez-Rodriguez, M. L.; Rabasco, A. M., Charged liposomes as carriers to enhance the permeation through the skin. *Expert Opin. Drug Deliv.* **2011**, *8*, 857-871.
15. Geusens, B.; Strobbe, T.; Bracke, S.; Dynoodt, P.; Sanders, N.; Van Gele, M.; Lambert, J., Lipid-mediated gene delivery to the skin. *Eur. J. Pharm. Sci.* **2011**, *43*, 199-211.
16. Kim, H. J.; Gias, E. L. M.; Jones, M. N., The adsorption of cationic liposomes to *Staphylococcus aureus* biofilms. *Colloids Surf., A* **1999**, *149*, 561-570.
17. Paré, C.; Lafleur, M., Formation of liquid ordered lamellar phases in the palmitic acid/cholesterol system. *Langmuir* **2001**, *17*, 5587-5594.
18. Cui, Z.-K.; Bastiat, G.; Jin, C.; Keyvanloo, A.; Lafleur, M., Influence of the nature of the sterol on the behavior of palmitic acid/sterol mixtures and their derived liposomes. *Biochim. Biophys. Acta* **2010**, *1798*, 1144-1152.
19. Bastiat, G.; Lafleur, M., Phase behavior of palmitic acid/cholesterol/cholesterol sulfate mixtures and properties of the derived liposomes. *J. Phys. Chem. B* **2007**, *111*, 10929-10937.
20. Ramakrishnan, M.; Tarafdar, P. K.; Kamlekar, R. K.; Swamy, M. J., Differential scanning calorimetric studies on the interaction of N-acylethanolamines with cholesterol. *Curr. Sci.* **2007**, *93*, 234-238.
21. Gater, D. L.; Seddon, J. M.; Law, R. V., Formation of the liquid-ordered phase in fully hydrated mixtures of cholesterol and lysopalmitoylphosphatidylcholine. *Soft Matter* **2008**, *4*, 263-267.
22. Phoeung, T.; Morfin Huber, L.; Lafleur, M., Cationic detergent/sterol mixtures can form fluid lamellar phases and stable unilamellar vesicles. *Langmuir* **2009**, *25*, 5778-5784.
23. Cui, Z.-K.; Bastiat, G.; Lafleur, M., Formation of fluid lamellar phase and large unilamellar vesicles with octadecyl methyl sulfoxide/cholesterol mixtures. *Langmuir* **2010**, *26*, 12733-12739.
24. Cano-Sarabia, M.; Angelova, A.; Ventosa, N.; Lesieur, S.; Veciana, J., Cholesterol induced CTAB micelle-to-vesicle phase transitions. *J. Colloid Interface Sci.* **2010**, *350*, 10-15.

25. Ouimet, J.; Lafleur, M., Hydrophobic match between cholesterol and saturated fatty acid is required for the formation of lamellar liquid ordered phases. *Langmuir* **2004**, *20*, 7474-7481.
26. Ouimet, J.; Croft, S.; Paré, C.; Katsaras, J.; Lafleur, M., Modulation of the polymorphism of the palmitic acid/cholesterol system by the pH. *Langmuir* **2003**, *19*, 1089-1097.
27. Phoeung, T.; Aubron, P.; Rydzek, G.; Lafleur, M., pH-triggered release from nonphospholipid LUVs modulated by the pKa of the included fatty acid. *Langmuir* **2010**, *26*, 12769-12776.
28. Jeong, M. W.; Oh, S. G.; Kim, Y. C., Effects of amine and amine oxide compounds on the zeta-potential of emulsion droplets stabilized by phosphatidylcholine. *Colloids Surf., A* **2001**, *181*, 247-253.
29. Ptak, M.; Egret-Charlier, M.; Sanson, A.; Bouloussa, O., A NMR study of the ionization of fatty acids, fatty amines and N-acylamino acids incorporated in phosphatidylcholine vesicles. *Biochim. Biophys. Acta* **1980**, *600*, 387-397.
30. Bartlett, G. R., Phosphorous assay in column chromatography. *J. Biol. Chem.* **1958**, *234*, 466-468.
31. Epand, R. M.; Bach, D.; Borochoy, N.; Wachtel, E., Cholesterol crystalline polymorphism and the solubility of cholesterol in phosphatidylserine. *Biophys. J.* **2000**, *78*, 866-873.
32. Mantsch, H. H.; McElhaney, R. N., Phospholipid phase transitions in model and biological membranes as studied by infrared spectroscopy. *Chem. Phys. Lipids* **1991**, *57*, 213-226.
33. Kodati, R. V.; Lafleur, M., Comparaison between orientational and conformational orders in fluid lipid bilayers. *Biophys. J.* **1993**, *64*, 163-170.
34. Kodati, V. R.; El-Jastimi, R.; Lafleur, M., Contribution of the intermolecular coupling and librational mobility in the methylene stretching modes in the infrared spectra of acyl chains. *J. Phys. Chem.* **1994**, *98*, 12191-12197.
35. Paré, C.; Lafleur, M., Polymorphism of POPE/cholesterol system: a <sup>2</sup>H nuclear magnetic resonance and infrared spectroscopic investigation. *Biophys. J.* **1998**, *74*, 899-909.
36. Mouritsen, O. G.; Zuckermann, M. J., What's so special about cholesterol? *Lipids* **2004**, *39*, 1101-1113.

37. Chen, H. C.; Mendelsohn, R.; Rerek, M. E.; Moore, D. J., Effect of cholesterol on miscibility and phase behavior in binary mixtures with synthetic ceramide 2 and octadecanoic acid. Infrared studies. *Biochim. Biophys. Acta* **2001**, *1512*, 345-356.
38. Dufourc, E. J.; Parish, E. J.; Chitrakorn, S.; Smith, I. C. P., Structural and dynamical details of cholesterol-lipid interaction as revealed by deuterium NMR. *Biochemistry* **1984**, *23*, 6062-6071.
39. Marsan, M. P.; Muller, I.; Ramos, C.; Rodriguez, F.; Dufourc, E. J.; Czaplicki, J.; Milon, A., Cholesterol orientation and dynamics in dimyristoylphosphatidylcholine bilayers: a solid state deuterium NMR analysis. *Biophys. J.* **1999**, *76*, 351-359.
40. Kelusky, E. C.; Dufourc, E. J.; Smith, I. C. P., Direct observation of molecular ordering of cholesterol in human erythrocyte membranes. *Biochim. Biophys. Acta* **1983**, *735*, 302-304.
41. Monck, M. A.; Bloom, M.; Lafleur, M.; Lewis, R. N. A. H.; McElhaney, R. N.; Cullis, P. R., Evidence for two pools of cholesterol in the *Acholeplasma laidlawii* strain B membrane: a deuterium NMR and DSC study. *Biochemistry* **1993**, *32*, 3081-3088.
42. Fenske, D. B.; Thewalt, J. L.; Bloom, M.; Kitson, N., Model of stratum corneum intercellular membranes: <sup>2</sup>H NMR of macroscopically oriented multilayers. *Biophys. J.* **1994**, *67*, 1562-1573.
43. Bastiat, G.; Oligier, P.; Karlsson, G.; Edwards, K.; Lafleur, M., Development of non-phospholipid liposomes containing a high cholesterol concentration. *Langmuir* **2007**, *23*, 7695-7699.
44. Muller, R. H.; Jacobs, C.; Kayser, O., Nanosuspensions as particulate drug formulations in therapy rationale for development and what we can expect for the future. *Adv. Drug Deliv. Rev.* **2001**, *47*, 3-19.
45. Demel, R. A.; Kinsky, S. C.; Kinsky, C. B.; Van Deenen, L. L. M., Effects of temperature and cholesterol on the glucose permeability of liposomes prepared with natural and synthetic lecithins. *Biochim. Biophys. Acta* **1968**, *150*, 655-665.

## **Chapter 5**

# **Introduction of Interfacial Cholesterol-Anchored Polyethylene Glycol in Sterol-Rich Non Phospholipid Liposomes**

Zhong-Kai Cui, Katarina Edwards, and Michel Lafleur

Ready to be submitted

Keywords: Palmitic acid, Cholesterol, PEG, Liposomes, Active loading, Permeability

## **5.1 Abstract**

Grafting hydrophilic flexible polymers on the liposomal surface has successfully limited the rapid clearance of liposomes from the blood stream and has promoted their use as nanocarriers in intravenous therapy. Recently, several formulations of liposomes made of sterols and monoalkylated amphiphiles have been reported. They have a high sterol content and display a very limited permeability. In the present paper, we report the possibility to prepare these non phospholipid liposomes with interfacial polyethylene glycol (PEG). Cholesterol (Chol), one of the liposome components, was chosen as the PEG anchor. Up to 20 mol % of PEGylated cholesterol (PEG-Chol) could be introduced in liposomes prepared with palmitic acid (PA) and cholesterol without significant perturbations. Higher proportion of PEG-Chol led to the formation of mixed micelles. In the presence of 10 mol % PEG-Chol, the PA/Chol/PEG-Chol liposomes showed a very limited permeability to calcein and doxorubicin. Moreover they were shown to be stable from pH 5.5 to 9.5. We also report that, even in the presence of interfacial PEG, doxorubicin could be actively loaded in PA/Chol/PEG-Chol liposomes and a high drug loading efficiency (84%) and a high drug to lipid ratio (0.06) were obtained. These distinct properties suggest that PA/Chol/PEG-Chol liposomes have an interesting potential as nanovectors for intravenous drug delivery.

## 5.2 Introduction

It has been recognized that phospholipid liposomes could be used as drug vehicle for more than 35 years.<sup>1</sup> Liposomes are biocompatible, biodegradable, biologically inert, weakly immunogenic, and they display a low intrinsic toxicity. All these features make them attractive drug carriers.<sup>2-4</sup> The vectorization of drugs by liposomes presents several advantages over the free drug form. This approach can provide a slow release that expands the period during which the drug level remains in the therapeutic window. It can target, passively or actively, specific sites. It can reduce the acute toxicity of drugs. One of the limitations of liposomes used as drug carriers for intravenous administration, however, is their rapid capture and removal from the blood circulation by the mononuclear phagocyte system (MPS),<sup>5</sup> leading to their accumulation in the liver and the spleen.<sup>6, 7</sup> Because it leads to a tighter chain packing, the incorporation of cholesterol in liposomes reduces the transfer of lipids to high density lipoproteins and also prevents protein binding, extending the liposome circulation lifetime in the blood stream.<sup>8-11</sup> A major breakthrough for improving circulation time and reducing MPS uptake was the introduction of gangliosides and sialic acid derivatives, such as monosialoganglioside (GM1)<sup>12, 13</sup> at the water/liposome interface. A similar effect was observed with interfacial polyethylene glycol (PEG).<sup>14, 15</sup> This protective effect has been associated with the steric stabilization of liposomes.<sup>12, 16-19</sup> The flexible chain of a glycolipid or a hydrophilic polymer occupies the space adjacent to the liposome surface, excluding other macromolecules, including lipoproteins, fibronectins, immunoglobulins, etc. Consequently, this shielding inhibits the interactions of MPS with liposomes and prolongs the liposome circulation lifetime. Such liposomes are referred to as stealth liposomes.<sup>4, 20, 21</sup>

PEG is an appealing macromolecule for obtaining stealth liposomes. It is a linear polymer with several suitable properties including biocompatibility, good solubility in aqueous and organic media, low toxicity, low immunogenicity and antigenicity, and good excretion kinetics.<sup>4</sup> Furthermore, its molecular weight can be easily modulated and it is relatively cheap to produce. It has been shown that PEG with a molecular weight between 1000 and 5000, anchored in bilayers with a phosphatidylethanolamine (PE) moiety displays a good miscibility with phospholipids; up to 11 mol % PEG could be grafted without observing phase separation or micelle formation.<sup>22, 23</sup> It was shown that the maximum circulation time of liposomes in the blood stream was obtained for liposomes with 5–10 mol % of interfacial PEG with a molecular weight of 1000 or 2000 (anchored with distearoylphosphatidylethanolamine (DSPE) in that study).<sup>18</sup> The protection of liposomes against phagocytosis was also improved with introducing PEG with a molecular weight of 2000 at its interface.<sup>15</sup> An increase of the PEG molecular weight to 5000 had no effect on half-life time of liposomes in the blood stream or, in some reports, slightly decreased it.<sup>15</sup>

PEG is water soluble and, in order to immobilize the macromolecule at the liposome interface, it must be anchored. The most current method utilized for achieving this goal is to covalently attach PEG to a phospholipid or a sterol. Because of the reactivity of the amine group, PEG-PE is commonly used.<sup>4</sup> PEG-coupled with ceramide has also been synthesized as a neutral alternative.<sup>24</sup> Ishiwata and coll.<sup>25</sup> used a sterol anchored PEG for modifying the liposome surface. PEGylated cholesteryl ether led to an increased liposome circulation time in the blood stream similar to that previously obtained with PEG-DSPE.<sup>25-27</sup> PEG cholesteryl ester was also synthesized and incorporated in phospholipid liposomes and niosomes to achieve long circulation lifetime.<sup>27-30</sup> As hydrophobic anchor for PEG, cholesterol is an alternative that presents distinct

advantages. First, the chain ordering effects of cholesterol leads to fluid and less permeable bilayers. Second, it is electrically neutral and this property provides a reduced binding of plasma proteins to liposomes.<sup>31</sup> Third, cholesterol is chemically stable, a useful feature regarding storage.<sup>32</sup>

It has been shown that it is possible to form non phospholipid liposomes with monoalkylated amphiphiles and sterols. The binary mixtures that could successfully form liposomes include negatively charged mixtures of unprotonated palmitic acid (PA) or its analogues with cholesterol (Chol) or some other sterols,<sup>33-35</sup> mixtures of negatively charged cholesterol sulphate (Schol) with neutral protonated PA or its analogues,<sup>34, 36</sup> mixtures of positively charged cetylpyridinium chloride and Schol,<sup>37</sup> stearylamine and Chol,<sup>38</sup> and completely neutral mixtures of octadecyl methyl sulfoxide/Chol.<sup>39</sup> A distinct feature of these non phospholipid liposomes is their high sterol content, which is between 50 and 70 mol %. This peculiar composition leads to a passive permeability that is drastically limited compared to traditional phospholipid liposomes. For example, it was found that about 70% of entrapped calcein, a negatively charged fluorophore, was still encapsulated after 1.5 years.<sup>34</sup> In addition, these liposomes are pH sensitive when they include a fatty acid or an alkylated primary amine as the monoalkylated amphiphile. The pH-triggered release could be fine-tuned by selecting a fatty acid with an appropriate  $pK_a$ .<sup>34</sup> Because of these properties, non phospholipid sterol-rich liposomes display an interesting potential as drug vectors, especially in the cases of challenging drugs that leak rapidly from conventional phospholipid liposomes such as 5-FU.<sup>40</sup> However, preliminary pharmacokinetics studies showed that, despite the very tight lipid chain packing that

could limit protein adsorption, these sterol-rich liposomes were cleared very rapidly (less than 5 minutes) from the blood stream in rats (unpublished results).

In the present study, we examined the possibility of introducing PEGylated cholesterol (PEG-Chol) in non phospholipid liposomes made of PA/Chol mixtures in order to combine the incomparably low permeability of those with improved blood circulation lifetime (Figure 5.1). We have determined the impact of the incorporation of PEG-Chol on the stability of these unusual bilayers using deuterium and pulsed-field-gradient  $^1\text{H}$  NMR, as well as cryo-electron microscopy. We investigated the amount of PEG-Chol that could be included in the non phospholipid bilayers without significant perturbation. We examined also the possibility to extrude the ternary mixtures to form large unilamellar vesicles (LUVs) and characterized the stability, the permeability and the pH sensitivity of the resulting liposomes. These findings provide us with a more detailed understanding of the influence of the hydration of the liposome interface on the stability of these self-assemblies. The present study also displays the feasibility of actively loading a drug in these non phospholipid vesicles. Active loading is an advantageous way to obtain high drug loading efficiency and high drug to lipid ratios, two parameters presenting considerable benefit for therapeutic purposes and the pharmaceutical industries. Because these liposomes with high sterol content are very impermeable, active loading may present a specific challenge. In addition, the presence of interfacial PEG likely reduces the internal vesicular volume, may induce some shielding of the pH at the interface, and as a consequence, may be unfavorable for high active-loading efficiency. For example, it was recently reported that the passive encapsulation efficiency of pentoxifylline in conventional liposomes was 10% whereas it dropped to 4.5% for PEG5000-Chol modified liposomes.<sup>29</sup> We have

therefore investigated whether LUVs prepared from PA/Chol/PEG-Chol mixtures could be actively loaded with doxorubicin (DOX). DOX is a commercially available anticancer drug efficacious against a broad spectrum of solid and hematopoietic malignant disease.<sup>41</sup> Its use is restricted by severe side effects such as vomiting, bone marrow suppression, alopecia, mucositis, cardiotoxicity and myelosuppression.<sup>42, 43</sup> Liposomal DOX has been shown to have improved therapeutic index and decreased toxicity.<sup>44, 45</sup> It is somehow a benchmark regarding drug active loading. DOX is an amphipathic weak base that can be actively loaded into the aqueous compartment of phospholipid liposomes through ammonium sulphate gradient with a high drug loading efficiency. The ammonium sulphate gradient approach does not require the preparation of liposomes in acidic pH, nor to alkalize the extraliposomal aqueous phase, by contrast with other chemical approaches used for active loading.<sup>46</sup>

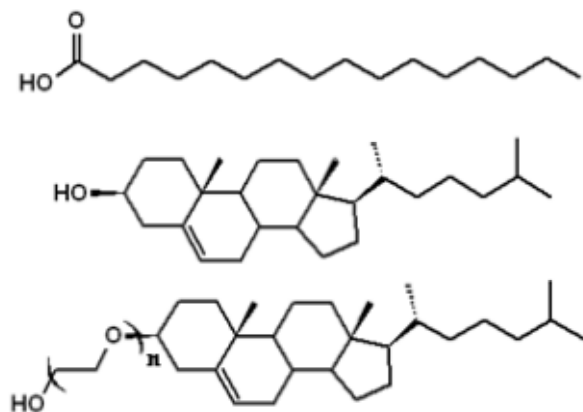


Figure 5.1. Chemical formula of PA, cholesterol and PEGylated cholesterol.

## 5.3 Materials and methods

### 5.3.1 Materials

Hydroxypolyethyleneglycol cholesteryl ether (PEG2000-Chol) was purchased from NOF Corporation (Tokyo, Japan). Cholesterol (> 99%), palmitic acid (99%), tris(hydroxymethyl)aminomethane (TRIS) (99%), 2-[N-morpholino]ethanesulfonic acid (MES) (> 99%), ethylenediaminetetraacetic acid (EDTA) (99%), NaCl (> 99%), Triton X-100 (99%), and deuterium-depleted water (> 99.99%) were supplied by Sigma Chemical Co. (St. Louis, MO, USA). Perdeuterated palmitic acid (PA-*d*<sub>31</sub>) (98.9%) and deuterium oxide (> 99%, D<sub>2</sub>O) were from CDN Isotopes (Pointe-Claire, QC, Canada). Calcein (high purity) has been obtained from Invitrogen (Burlington, ON, Canada). Sephadex G-50 Medium was purchased from Pharmacia (Uppsala, Sweden). Methanol (spectrograde) and benzene (high purity) were obtained from A&C American Chemicals Ltd. (Montreal, Qc, Canada), and BDH Inc. (Toronto, ON, Canada), respectively. Doxorubicin hydrochloride salt (DOX) (> 99%) was obtained from LC Laboratories (Woburn, MA, USA). Ammonium sulfate (> 99.0%) and Dowex<sup>®</sup> 50WX4 were supplied by Alfa Aesar (Ward Hill, USA). Dowex<sup>®</sup> 50WX4 was obtained as a strongly acidic cation exchange resin and converted to the sodium form. All solvents and products were used without further purification.

### 5.3.2 Mixture preparation

Mixtures of PA/Chol/PEG-Chol were prepared by dissolving weighed amounts of the solid chemicals in a mixture of benzene/methanol 90/10 (v/v). The solution were then frozen in liquid nitrogen and lyophilized for at least 16 h to allow complete sublimation of the organic solvent. For the NMR experiments, PA was replaced by PA- $d_{31}$ .

### 5.3.3 $^2\text{H}$ NMR spectroscopy

In order to form multilamellar vesicles (MLVs), the freeze-dried lipid mixtures were hydrated with a MES/TRIS buffer (TRIS 50 mM, MES 50 mM, NaCl 10 mM, EDTA 5 mM) providing a buffered range between pH 5 and 9. The MES/TRIS buffer was prepared with deuterium depleted water for the  $^2\text{H}$  NMR experiments. The final lipid concentration was 30 mg/mL. The suspensions were subjected to five cycles of freezing-and-thawing (from liquid nitrogen temperature to  $\sim 70$  °C) and vortexed between successive cycles, to ensure a good hydration of the samples. The samples were then transferred into homemade Teflon holders. The  $^2\text{H}$  NMR spectra were recorded on a Bruker AV-600 spectrometer, using a Bruker static probe equipped with a 5 mm coil. A quadrupolar echo sequence was used with a  $90^\circ$  pulse of 2.9  $\mu\text{s}$  and an interpulse delay of 35  $\mu\text{s}$ . The recycling time was 60 s. In absence of a slow-relaxation component, namely a solid phase, the recycling delay was reduced to 0.3 s. Typically 4 000 FIDs were coadded. The temperature was regulated using a Bruker VT-3000 controller. The proportion of the isotropic phase could be estimated from the signal integrations prior to and after the elimination of the narrow central peak in the  $^2\text{H}$  NMR spectra.

5.3.4  $^1\text{H}$  NMR diffusion experiments

In order to assess the inclusion of PEG-Chol in the liposomes, the diffusion coefficient of PEG was determined on extruded samples prepared from different composition, using  $^1\text{H}$  pulsed-field-gradient NMR. MLVs prepared in a  $\text{D}_2\text{O}$ -based MES/TRIS buffer were extruded using a handheld Liposofast extruder (Avestin, Ottawa, Canada). Typically the dispersions were passed 15 times through two stacked polycarbonate filters (200 nm pore size) at room temperature.  $^1\text{H}$  NMR diffusion experiments were performed on a Bruker AV-400 spectrometer operating at 400 MHz for  $^1\text{H}$ . The diffusion measurements were carried out at 25 °C using a Bruker diffusion probe (Diff60) equipped with a  $^1\text{H}/^2\text{H}$  5 mm coil. This probe includes one gradient coil, along the  $z$  axis, capable of delivering magnetic field gradients up to 2900 G/cm. The gradient strength was calibrated from the diffusion coefficient of 1%  $\text{H}_2\text{O}$  in a  $\text{D}_2\text{O}$  sample. The diffusion coefficient was measured using the stimulated echo (STE).<sup>47</sup> Trapezoidal gradient pulses ( $\delta$ ) of 1.50 ms and interpulse delays ( $\Delta$ ) of 100 ms were applied. The diffusion coefficients were obtained by fitting the variation of the echo intensity as a function of the gradient strength ( $G$ ) using the following equation:

$$\ln(S/S_0) = -(G\gamma\delta)^2 D(\Delta - \delta/3) \quad (5.1)$$

where  $S$  and  $S_0$  are the integrated echo intensities with and without a field gradient and  $\gamma$  the gyromagnetic ratio of the investigated nucleus. Typically, 32 scans were coadded for a given gradient strength and 32 gradient magnitudes were used for each attenuation curve. The temperature of the sample was controlled using the gradient coil cooling unit. The sample temperature was calibrated using ethylene glycol.

### 5.3.5 LUVs characterization

In order to examine the possibility to prepare LUVs from the PA/Chol/PEG-Chol ternary systems, samples of different compositions prepared in a MES/TRIS buffer were extruded using a standard protocol (see above). Two stacked 100 nm polycarbonate filters were used. The hydrodynamic diameters of the LUVs were measured at 25 °C using a Malvern nanosizer. The scattering light intensity was adjusted by diluting the dispersions with the MES/TRIS buffer.

The conditions for the cryogenic transmission electron microscopy (Cryo-TEM) technique are detailed elsewhere.<sup>48</sup> Briefly, an aliquot of the sample (~ 1 µL) was deposited on a copper grid covered with a carbon-reinforced holey polymer film, dabbed with a filter paper to form a thin film (10–500 nm) and incubated in a custom-built climate chamber at 25 °C and > 99% relative humidity. The grid was then plunged into liquid ethane. The vitrified sample was kept below –165 °C and protected from ambient conditions during the transfer from the preparation chamber to the microscope as well as during the data acquisition. The micrographs were obtained using a Zeiss EM 902A Transmission Electron Microscope (Carl Zeiss NTS, Oberkochen, Germany), in the zero loss bright-field mode, with an accelerating voltage of 80 kV. The digital images were recorded under a low dose conditions with a BioVision Pro-SM Slow scan CCD camera (Proscan GmbH, Scheuring, Germany) and their contrast was enhanced using an underfocus of 1–2 µm.

### 5.3.6 Permeability measurements

The permeability of the LUVs was measured using a standard procedure based on the self-quenching property of calcein at high concentration.<sup>49, 50</sup> Briefly, LUVs loaded with calcein (80 mM) were prepared from PA/Chol/PEG-Chol mixtures hydrated with a MES/TRIS buffer, pH 8.4. The calcein-containing LUVs (100 nm pore size) were separated from free calcein by gel permeation chromatography, using Sephadex G-50 Medium gel (column diameter 1.5 cm, length 25 cm), equilibrated with an iso-osmotic MES/TRIS buffer (MES 50 mM, TRIS 50 mM, NaCl 130 mM, EDTA 5 mM, pH 8.4). The collected vesicle fraction was diluted 100 times with buffers of different pH and this was set as time = 0. These stock LUV suspensions were then incubated at room temperature.

In order to study the passive leakage (external pH 8.4, corresponding to the internal pH), the calcein fluorescence intensity was measured from an aliquot of the stock LUV suspension freshly isolated by gel permeation chromatography, prior to ( $I_i$ ) and after ( $I_{i+T}$ ) the addition of Triton X-100 (10  $\mu$ L of a 10 (v/v)% solution prepared in the MES/TRIS buffer). It was assumed that calcein was initially completely encapsulated whereas the fluorescence intensity measured after addition of Triton X-100 corresponded to the complete release of entrapped calcein.

After a given incubation time, the calcein fluorescence intensity was measured on another aliquot of the same stock LUV suspension before ( $I_f$ ) and after ( $I_{f+T}$ ) the addition of Triton X-100. The percentage of encapsulated calcein at that time in the LUVs was calculated according to:

$$\% \text{ of encapsulated calcein} = \left( \frac{(I_{f+T} - I_f) / I_{f+T}}{(I_{i+T} - I_i) / I_{i+T}} \right) \times 100 \quad (5.2)$$

The % of release corresponded to (100 – % of encapsulated calcein).

The pH-triggered leakage of calcein was also examined. The percentage of released calcein was calculated using Equation 5.2, except  $I_i$  and  $I_{i+T}$  corresponded to the measurements at pH 8.4, the initial pH, before and after the addition of Triton X-100 respectively.  $I_f$  and  $I_{f+T}$  were obtained on an aliquot at a modified pH, before and after the addition of Triton X-100 respectively. The pH effect was examined for either an increase or a decrease in pH. The calcein fluorescence intensity was relatively constant over the investigated pH range.<sup>49</sup>

The fluorescence intensities were recorded using a Photon Technology International spectrofluorometer. The excitation and emission wavelengths were set to 490 and 513 nm respectively and the band path widths were set to 1.0 and 1.6 nm for the excitation and emission monochromators, respectively.

### 5.3.7 Active loading experiments

Active loading was carried out using an ammonium sulfate gradient.<sup>46</sup> PA/Chol/PEG-Chol solid mixtures were hydrated with an ammonium sulfate solution (120 mM). The PA/Chol/PEG-Chol LUVs (100 nm diameter) were prepared as described above. The ammonium sulfate gradient was created by gel permeation chromatography, using Sephadex G-50 Medium gel (column diameter 1.5 cm, length 25 cm), equilibrated with an iso-osmotic NaCl solution (150

mM). A DOX solution, prepared in water containing 150 mM NaCl, was added to the collected vesicles in order to have a DOX/lipid molar ratio of 1/15. The LUVs suspensions were incubated at  $\sim 70$  °C for 24 hours. In order to determine the drug loading efficiency, the LUV suspensions incubated with DOX were diluted 100-folds with the NaCl solution. Converted Dowex<sup>®</sup> 50WX4 resin was added to an aliquot to remove the free DOX by complexation. The sample was centrifuged at 4000 rpm for 3 min and the DOX absorbance at 480 nm was measured. The absorbance was also measured for an aliquot without resin to obtain the total amount of DOX. The release of liposome-entrapped DOX was also characterized by UV-vis spectroscopy using the resin treatment to eliminate the released drug. HPLC-MS analysis was carried out on LUV aliquots treated with the resin in order to quantify the drug to lipid ratio.

## 5.4 Results

### 5.4.1 Characterization of phase behaviors

Figure 5.2 presents the  $^2\text{H}$  NMR spectra of PA- $d_{31}$ /Chol/PEG-Chol mixtures of various compositions. In these mixtures, the PA- $d_{31}$ /sterol molar ratio was always 30/70 and cholesterol was progressively substituted by PEG-Chol. This set of data provides us with the proportion of PEG-Chol that can be incorporated in the mixture while keeping a fluid lamellar arrangement. The spectra of PA- $d_{31}$ /Chol (30/70) mixture, pH 8.4 (Figure 5.2A, top row), are essentially characteristic of a fluid lamellar phase. They correspond to several overlapping powder patterns with different quadrupolar splittings, associated with the gradient of orientational order existing along the acyl chains.<sup>51-54</sup> The quadrupolar splitting of the outermost doublet of the spectrum

recorded at 25 °C was 55 kHz; this large value is typical of lipids in the lo phase.<sup>51, 52, 55</sup> These spectra indicate that the lo phase formed by this mixture is stable over the whole investigated temperature range, in agreement with previous results.<sup>51</sup> Actually, temperature variations between 25 and 60 °C had limited effect on these systems, the value of the quadrupolar splitting of the outermost doublet decreasing by only ~5 kHz. Once 20% or more of PEG-Chol was introduced in the liposomes, a narrow peak centered at 0 kHz appeared, indicating the formation of an isotropic phase. The evolution of the proportion of isotropic phase in the ternary systems, as a function of PEG-Chol content is summarized in Figure 5.3. For PEG-Chol content lower than or equal to 20%, all the fatty acid appeared to exist in the fluid lamellar phase. Larger proportion of PEG-Chol led to a steady increase of the proportion of the isotropic phase. More than 85% of PA-*d*<sub>31</sub> exists in the isotropic phase for the PA-*d*<sub>31</sub>/Chol/PEG-Chol 30/20/50 mixture. Higher temperatures favored the formation of the isotropic phase in the mixtures including 30% or more of PEG-Chol (Figure 5.2A).

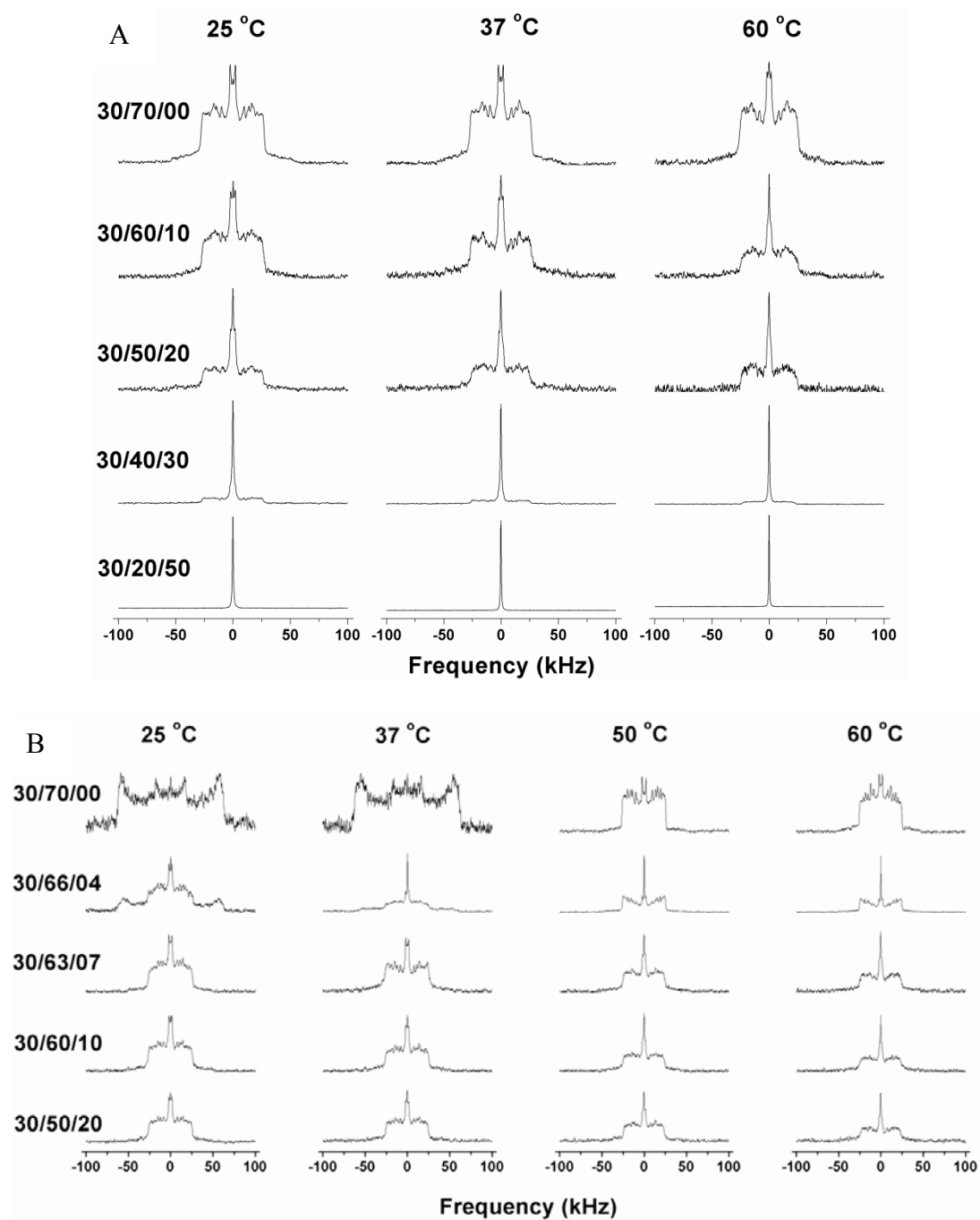


Figure 5.2.  $^2\text{H}$  NMR spectra of PA- $d_{31}$ /Chol/PEG-Chol mixtures, pH 8.4 (A) and 5.0 (B). Temperatures and molar ratios are indicated on the top of each column and on the left of each row, respectively.

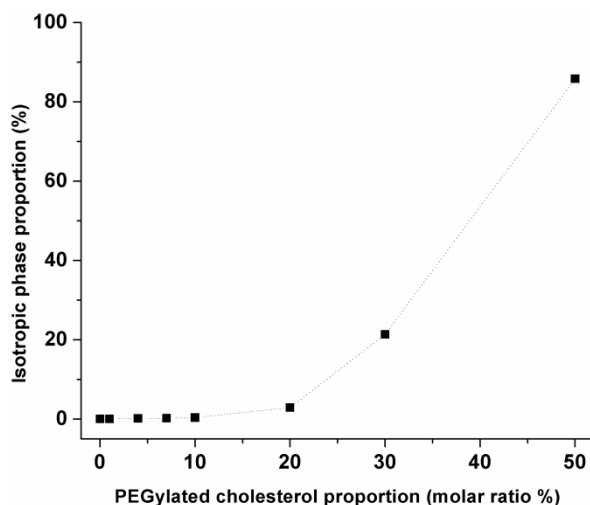


Figure 5.3. Dependence of the proportion of isotropic phase on the PEG-Chol content in the PA- $d_{31}$ /Chol/PEG-Chol mixtures, at 25 °C and pH 8.4. The PA/sterol ratio remained 3/7.

It has been shown that a decrease of pH favors the formation of solid components in the PA/Chol system,<sup>33, 56</sup> a property giving rise to pH-sensitive formulations. In order to investigate the pH sensitivity of the PEG-containing mixtures, their spectra were recorded at pH 5.0 (Figure 5.2B). At temperatures below 50 °C, the spectra of a PA- $d_{31}$ /Chol 30/70 mixture displayed only a signal typical of solid and immobile PA- $d_{31}$ . At 50 °C and above, the solid signal completely disappeared and only a fluid lamellar component was observed, in agreement with previously reports.<sup>33, 56</sup> Its width was found to be very similar to that observed at pH 8.4 (Figure 5.2A), suggesting a comparable orientational order of the alkyl chain. The presence of PEG-Chol in the mixtures led to the formation of fluid bilayers at low temperatures (below 50 °C). For example, at 25 °C, the spectrum of PA- $d_{31}$ /Chol (30/70) mixture indicated that the fatty acid was completely solid whereas it was completely in a fluid lamellar phase in the PA- $d_{31}$ /Chol/PEG-Chol 30/63/07 mixture. The coexistence of solid and fluid bilayers was observed for the mixtures containing 4% of PEG-Chol. The presence of PEG-Chol in the mixture downshifted the solid-to-fluid lamellar

phase transition as the system containing 4% PEG-Chol was completely fluid at 37 °C and that with 7% PEG-Chol existed in the fluid lamellar phase over the whole investigated temperature range. At high temperatures and pH 8.4, the presence of PEG-Chol has a very limited effect on the PA- $d_{31}$ /Chol/PEG-Chol mixtures. The  $^2\text{H}$  NMR spectra indicated the formation of fluid bilayers and the measured quadrupolar splittings were similar to those obtained for the mixture without PEG-Chol in the same conditions. By promoting the formation of fluid bilayers at low temperatures, PEG-Chol inhibits the pH sensitivity of the PA/Chol mixture; stable fluid bilayers were observed between pH 5.0 and 8.4 when the system included between 7 and 20% of PEG-Chol.

The  $^2\text{H}$  NMR spectra provided a detailed characterization of the phase behavior from the fatty acid (PA- $d_{31}$ ) point of view. In order to examine the behavior of PEG-Chol in these systems, we have measured the diffusion of PEG using pulsed-field-gradient  $^1\text{H}$  NMR. This analysis is based on the assumption that it is possible to distinguish between PEG-Chol inserted in 200 nm liposomes and PEG-Chol that would exist under a micellar form on the basis of the PEG diffusion coefficient. Typically, there is one order of magnitude difference in the diffusion coefficient of micelles ( $\sim 10^{-11}$  m<sup>2</sup>/s) and of liposomes ( $\sim 10^{-12}$  m<sup>2</sup>/s).<sup>57</sup> The diffusion coefficient was obtained from the PEG-Chol band at  $\sim 3.66$  ppm. For all the investigated PA- $d_{31}$ /Chol/PEG-Chol mixtures (PEG-Chol proportions varying from 0 to 100), a single exponential could reproduce the decay of the relative signal as a function of the gradient strength (see Eq. 5.1), and consequently, a single diffusion coefficient was inferred (Figure 5.4). Pure PEG-Chol in D<sub>2</sub>O forms micelles.<sup>25</sup> The measured diffusion coefficient was  $2.0 \times 10^{-11}$  m<sup>2</sup>/s, a value corresponding to that reported for PEG2000-PE micelles.<sup>58</sup> When PEG-Chol was mixed with PA and cholesterol

and its proportion was between 1 and 20%, the PEG diffusion coefficients were relatively constant and corresponded to about  $2.4 \times 10^{-12}$  m<sup>2</sup>/s. This value is consistent with the diffusion coefficients reported for PEG2000-PE inserted in 100 nm phospholipid liposomes ( $\sim 5 \times 10^{-12}$  m<sup>2</sup>/s).<sup>58</sup> When the proportion of PEG-Chol was increased, the PEG diffusion coefficient also increased to reach, in the case of PA-*d*<sub>31</sub>/Chol/PEG-Chol 30/20/50 LUVs, a value similar to that of pure PEG-Chol in D<sub>2</sub>O. These results showed that PEG-Chol was successfully introduced in the fluid bilayers made of PA and cholesterol up to 20%. When its proportion was higher, the formation of smaller self-assemblies that diffused faster than liposomes was reported. This conclusion is in good agreement with the <sup>2</sup>H NMR results indicating the fast isotropic motions of PA-*d*<sub>31</sub> in the mixtures where the proportion of PEG-Chol was higher than 20%.

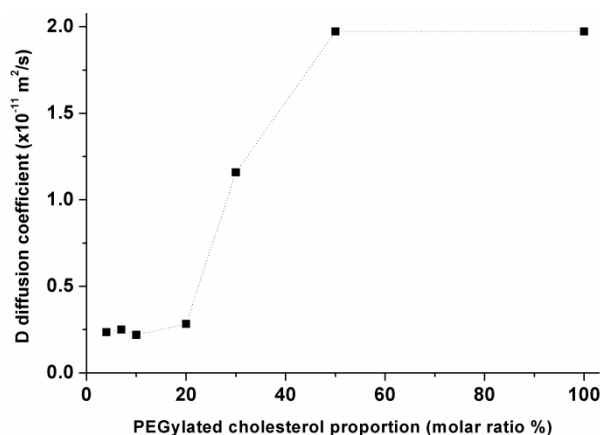


Figure 5.4. Variation of the diffusion coefficient of PEG as a function of the PEG-Chol content in the PA-*d*<sub>31</sub>/Chol/PEG-Chol LUVs, at 25 °C and pH 8.4. The PA/sterol ratio remained 3/7.

#### 5.4.2 Dynamic light scattering and cryo-TEM

It has been shown that, despite their very high cholesterol content, it is possible to extrude several mixtures of sterols and monoalkylated amphiphiles when they form a lo phase.<sup>33, 35-37</sup> We

examined the influence of PEG-Chol on the extrusion process of the PA/Chol/PEG-Chol ternary systems. Table 5.1 summarizes the characterization of the extruded LUVs by dynamic light scattering. LUVs with a unimodal size distribution were obtained from the extrusion of PA/Chol/PEG-Chol fluid bilayers with 30/66/04 and 30/60/10 molar ratios. Their average diameter was about 100 nm between pH 5.5 and 9.5, consistent with the pore diameter of the polycarbonate filters (100 nm). This observation is consistent with the existence of stable bilayers inferred from  $^2\text{H}$  NMR. PA/Chol/PEG-Chol LUVs were also examined by cryo-TEM (Figure 5.5). The impact of pH was studied by varying the external and internal pH to 8.4 or 5.0. The mixture containing 4% PEG-Chol, with internal/external pH 8.4/8.4 led predominantly to spherical vesicles of fairly uniform size. When both inside and outside pH of LUVs were 5.0, LUVs (Figure 5.5b) were also obtained but it seemed that they were less spherical than those formed at pH 8.4. The morphology of the vesicles prepared in the presence of 10% PEG-Chol were affected; although spherical and unilamellar vesicles dominated the samples, elongated, peanut-like, and convex (red blood cell like) shaped vesicles were observed for both pH 8.4/8.4 and 5.0/5.0.

Table 5.1. Hydrodynamic diameter of PA/Chol/PEG-Chol LUVs  $d_{\text{LUVs}}$  at various pH values.

| Molar ratio | 30/66/04               | 30/60/10               |
|-------------|------------------------|------------------------|
| pH          | $d_{\text{LUVs}}$ (nm) | $d_{\text{LUVs}}$ (nm) |
| 5.5         | $92 \pm 9$             | $92 \pm 5$             |
| 6.5         | $88 \pm 3$             | $89 \pm 6$             |
| 7.4         | $93 \pm 2$             | $92 \pm 5$             |
| 8.4         | $102 \pm 10$           | $92 \pm 7$             |
| 9.5         | $88 \pm 4$             | $90 \pm 6$             |

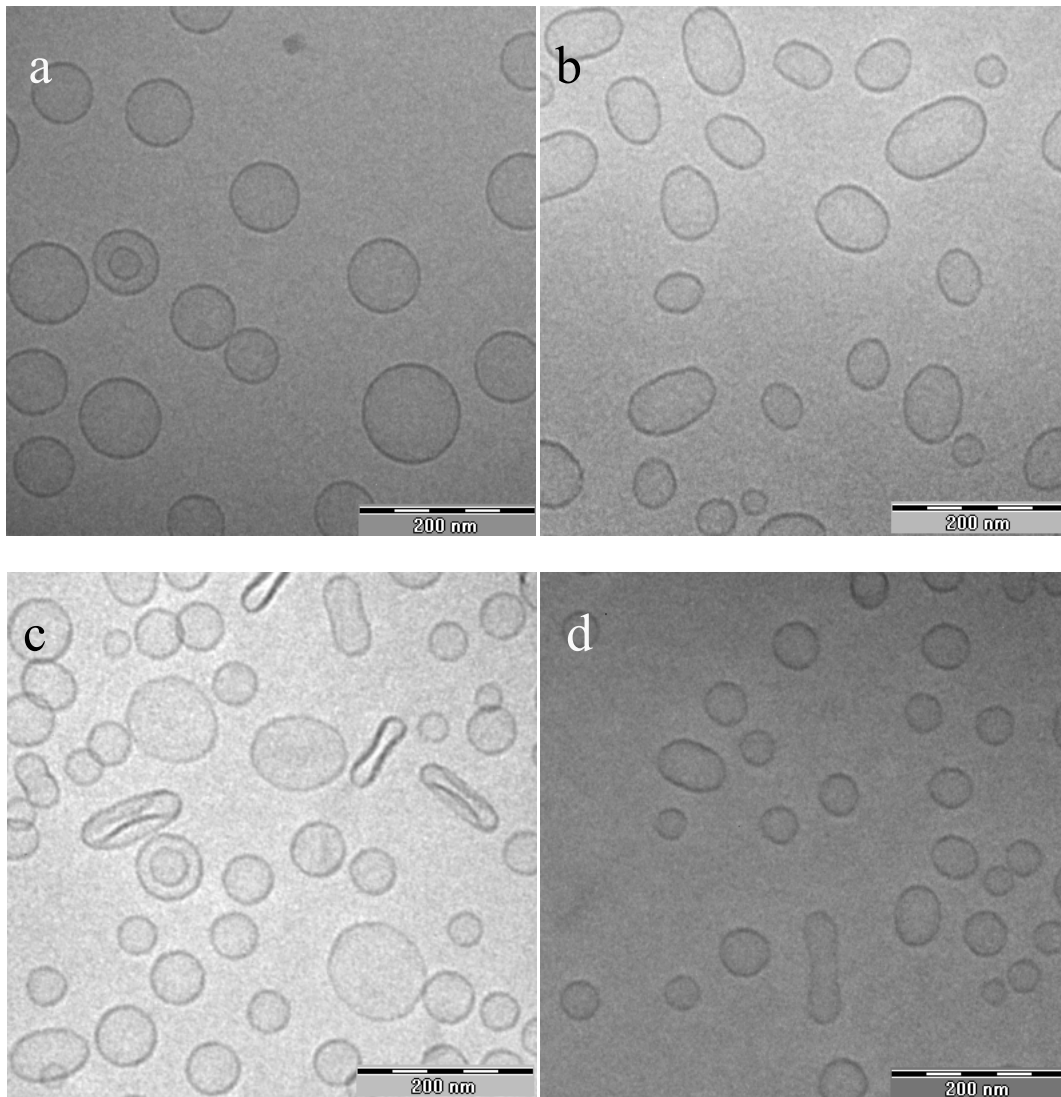


Figure 5.5. Cryo-micrographs of extruded PA/Chol/PEG-Chol LUVs in molar ratio of 30/66/04 (a) pH 8.4/8.4 inside/outside, (b) pH 5.0/5.0, and in a molar ratio of 30/60/10 (c) pH 8.4/8.4, (d) pH 5.0/5.0. Bar, 200 nm.

## 5.4.3 PA/Chol/PEG-Chol LUV permeability

The PA/Chol/PEG-Chol LUVs loaded with calcein were prepared by extrusion at pH 8.4 as described above. The entrapped calcein showed an initial self-quenching of more than 0.90, a value close to that expected for an 80 mM calcein solution.<sup>49, 59</sup> The passive release of calcein from these vesicles at pH 8.4 was determined as a function of time (Figure 5.6). The leakage from PA/Chol/PEG-Chol LUVs (with a molar composition of 30/66/04 and 30/60/10) was very limited: even after three months, no significant release could be detected. This notable ability to retain the encapsulated calcein is one of the most efficient reported for PEGylated liposomes. For example, it compares advantageously to DPPC/Chol/PEG-DSPE liposomes, for which more than 30% of calcein leaked out within 3 hours.<sup>60</sup>

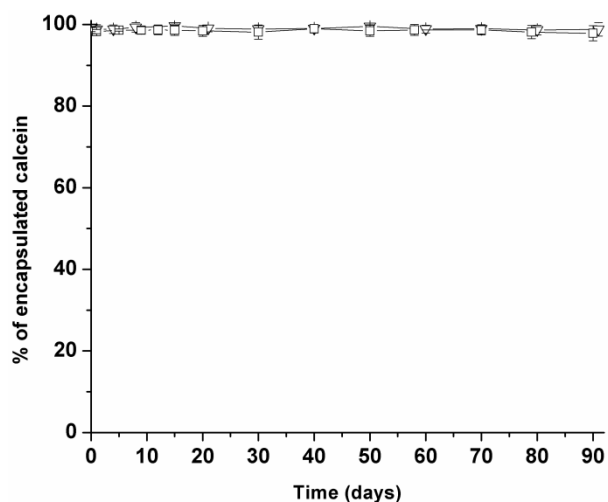


Figure 5.6. Passive leakage of entrapped calcein from PA/Chol/PEG-Chol 30/66/04 ( $\Delta$ ) and 30/60/10 ( $\nabla$ ) (molar ratio) LUVs, measured at room temperature, pH 8.4.

The permeability of the PA/Chol/PEG-Chol LUVs was also assessed as a function of pH (Figure 5.7). As shown previously,<sup>35</sup> PA/Chol LUVs (30/70 molar ratio) are pH-sensitive: they were stable between pH 7 and 9.5 whereas a significant calcein release was observed for pH 6.0 or below. Contrasting with this behavior, no significant calcein release was observed from the LUVs containing PEGylated cholesterol when the external pH was modified between 5.5 and 9.5. These results indicate that the presence of PEG-Chol in the LUVs impedes their pH sensitivity.

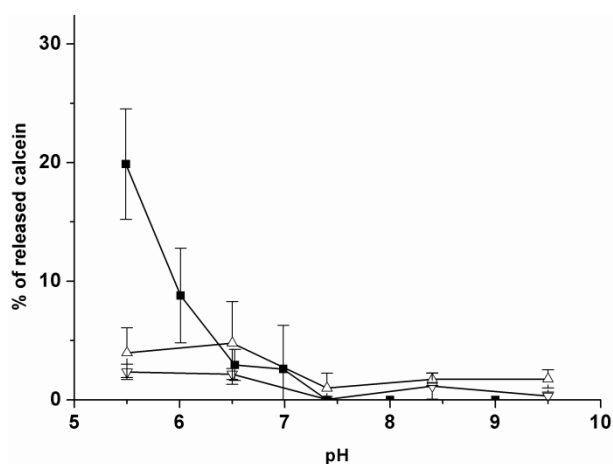


Figure 5.7. Effect of the external pH on the calcein release from PA/Chol/PEG-Chol 30/70/00 (■), 30/66/04 (Δ) and 30/60/10 (▽) LUVs. The measurements were carried out at room temperature, ~24 h after the pH change.

#### 5.4.4 DOX active loading and release

A transmembrane ammonium gradient across a liposome membrane induces a transmembrane pH gradient that can drive DOX across the bilayer.<sup>46</sup> This strategy for active loading was applied to the liposomes made of PA/Chol/PEG-Chol (30/60/10 molar ratio). The encapsulation efficiency of DOX was calculated to be 84%, and the resulting drug to lipid ratio

was 0.06 (molar ratio). These parameters are comparable to those previously obtained with phospholipid-based liposomes.<sup>46, 61-63</sup> It should be pointed out that the reported trapping efficiency is very good since the drug to lipid ratio is expressed in molar terms and the investigated liposomes were formed from a monoalkylated amphiphile, in contrast to phospholipids, which bear two hydrophobic chains. The stability and the passive release of DOX-loaded liposomes were also examined. The results are summarized in Figure 5.8. It is shown that the non phospholipid liposomes displayed a very limited permeability to DOX; the drug slowly leaked out from the LUVs and only ~20% of encapsulated DOX was released after a three-month period. The stability of DOX-loaded PA/Chol/PEG-Chol LUVs was significantly improved compared to active-loaded phosphatidylcholine liposome containing 38 mol% of cholesterol and 5 mol% of PEG-lipid (PEG-DSPE or PEG-Chol). For those formulations, more than 30% of the encapsulated DOX was released within three days, in similar conditions.<sup>27</sup>

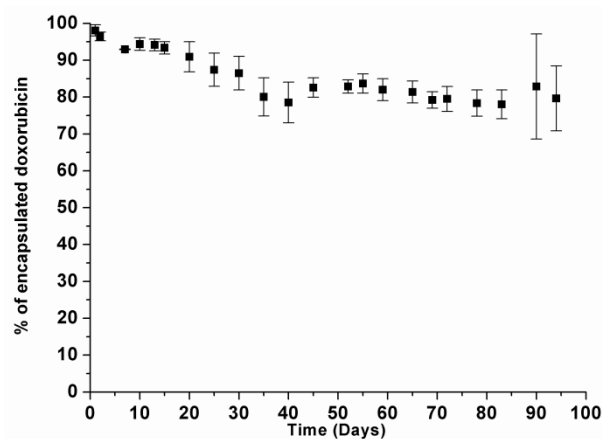


Figure 5.8. Passive leakage of actively loaded doxorubicin in PA/Chol/PEG-Chol 30/60/10 (molar ratio) LUVs, measured at room temperature, pH 8.4.

## 5.5 Discussion

The present study reveals that it is possible to introduce PEGylated cholesterol into non phospholipid liposomes prepared from palmitic acid and cholesterol. Up to 20 mol % of PEG-Chol can be included in the ternary system without significant phase separation.  $^2\text{H}$  NMR results show that all the palmitic acid molecules are included in the fluid lamellar phase while the diffusion coefficient of PEG-Chol indicates that PEG-Chol molecules are anchored to the liposomes. Moreover the cryo-EM analysis showed that spherical unilamellar vesicles dominated the samples for the PA/Chol mixtures that included 4 and 10 mol % of PEG-Chol. With 10 mol % PEG-Chol, different morphologies such as elongated, dumbbell-like and erythrocyte-like shapes were observed occasionally. According to the elastic model of vesicle shape,<sup>64, 65</sup> such form changes could be associated with an imbalance of the areas of the inner and outer leaflets of the bilayer. The higher curvature of the inner leaflet compared to that of the outer leaflet could lead to differences in the intermolecular interaction between interfacial PEG and/or to an uneven distribution of PEG between the two leaflets; these could be at the origin of the changes in morphology. These alterations were likely precursors of the more drastic transformations observed with larger PEG-Chol content. Beyond 20 mol % of PEG-Chol, an isotropic phase is formed (Figure 5.3, looking at PA- $d_{31}$ ) and the diffusion coefficient of PEG-Chol increases to the value obtained for PEG-Chol micelles (Figure 5.4). These results are likely due to the formation of mixed micelles of PEG-Chol with PA and likely cholesterol. It seems that the bilayer solubilization is complete and only the micellar form is observed when the mixture contains about 50 mol % of PEG-Chol. This behavior is reminiscent of the introduction of PEG-lipids in phospholipid bilayers. PEG2000-DSPE can be included in liposomes without altering their

structures when its proportion is less than 20 mol % for eggPC bilayers, and less than 10 mol % for DMPC ones.<sup>66</sup> It was also shown that up to 7 mol % of PEG1000-PE or PEG3000-PE could be inserted in DPPC bilayers without a phase separation.<sup>22</sup> Beyond 7 mol %, a progressive transformation from a lamellar to a mixed micellar phase was observed. The complete conversion to micelles was reached when the PEG-PE content was above 17 mol %. The incorporation of cholesterol ( $\geq 30$  mol %) in DPPC bilayers increased the cohesive strength of the bilayers and inhibited the phase separation in the presence of up to 20 mol % PEG1000-PE. Stable unilamellar vesicles could be prepared from diglycerol hexadecyl ether/Chol mixtures in the presence of 10 mol % PEG1000-Chol or 5 mol % PEG2000-Chol.<sup>30</sup> An increased proportion of interfacial polymers led to the formation of open disk-shaped aggregates that were the only observed structures when the PEG-lipid proportion reached 20 mol %. We conclude that a moderate proportion of PEG-Chol can be inserted in PA/Chol liposomes without significant morphological changes, in an analogous way to phospholipid liposomes.

It has been shown that PA/Chol system forms stable fluid bilayers only at high pH ( $\geq 7.5$ ) while lower pH favors the formation of solid phase cholesterol and palmitic acid.<sup>56</sup> It has been inferred that the protonation state of the carboxylic group dictates the bilayer stability through its modulation of the lipid mixing properties and the bilayer interface hydration. At lower pH, PA head group is protonated, favoring phase separation from cholesterol and reducing the hydration of the bilayer interface; as a consequence, the destabilization of the fluid lamellar phase is observed.<sup>34, 36</sup> In the present work, it is shown that the incorporation of PEG-Chol favors the formation of a lo phase at lower pH. For example, typical spectrum of cholesterol inserted in fluid bilayers was obtained at pH 5, 25 °C, when the PA-d<sub>31</sub>/Chol system included 7 mol % PEG-

Chol (Figure 5.2B). It is possible that the presence of PEG hydrophilic chains at the bilayer interface maintains a suitable degree of hydration of the bilayer, a parameter that is important for the stability of fluid bilayers.<sup>67, 68</sup> Furthermore, it has been shown that the presence of the interfacial PEG decreased the bilayer pH-sensitivity.<sup>69</sup> The apparent  $pK_a$  of PA in this case, is probably shifted to a lower value. This might be associated to the decrease of the concentration of protons at the interface. Consequently, a large proportion of PA may still sit in the unprotonated states, resulting in the formation of lamellar phases and a much reduced pH-sensitivity. The promotion of the fluid bilayer phase by the presence of PEG-Chol makes the extrusion of the ternary mixtures possible and the formation of LUVs even at low pH such as 5.0. It was proved impossible for PA/Chol system at such low pH.<sup>36</sup>

PEG-Chol-containing non phospholipid liposomes display a limited passive permeability compared to that generally observed for PEGylated phospholipid liposomes, as is shown in this paper for calcein as well as for DOX. This distinct impermeability is consistent with that previously reported for other similar systems prepared from a monoalkylated amphiphile and a sterol.<sup>33, 35</sup> This property has been associated with the high content of cholesterol leading to an increase in alkyl chain order, a thickening of the hydrophobic region of the bilayer,<sup>52, 70-72</sup> and a decreased permeability. The insertion of PEGylated cholesterol in the PA/Chol bilayers does not appear to have a significant effect on the passive permeability of the resulting LUVs. This observation is in good agreement with the absence of influence of PEG-Chol on the quadrupolar splittings of PA- $d_{31}$  in the  $^2\text{H}$  NMR spectra of PA- $d_{31}$ /Chol/PEG-Chol systems, the splittings being representative of the alkyl chain orientational order and consequently of the bilayer thickness. The pH-stimulated release from the PEG-coated non phospholipid liposomes was

however significantly decreased. Actually, practically no release could be triggered by decreasing the external pH to 5.5, in contrast to a pH-triggered release of about 20% for the naked PA/Chol liposomes (Figure 5.7). This result is consistent with the impact of interfacial PEG on the phase behavior of PA/Chol mixtures. As discussed above, the presence of interfacial PEG promotes the formation of a fluid lamellar phase at pH as low as 5. As a consequence, the solid–fluid transition of PA/Chol system observed for a pH variation from 5 to 8.4 is no longer detected in the presence of 10 mol % PEG and the system remains in the fluid lamellar phase over the whole pH range. This phenomenon appears to be common as a similar behavior was also reported for some PEG-coated phospholipid liposomes. For example, the inclusion of 1 or 5 mol % PEG-DSPE in pH-sensitive DOPE/oleic acid liposomes shifted the pH-triggered release curve towards more acidic regions and reduced the extent of the leakage that could be induced.<sup>69</sup> The presence of only 1 mol % PEG-DSPE in the formulation led to a decrease of release from > 90% without PEG to ~20%, when the pH was set to 5. Similarly the pH-sensitivity of cholesteryl hemisuccinate/DOPE liposomes was attenuated in the presence of PEG-PE.<sup>73</sup> The nearly complete release of the liposome content could be triggered at pH 5, while the inclusion of 2 mol % PEG-PE reduced the induced leakage to ~20%. Therefore, the presence of interfacial PEG changes the chemistry of the interface and it seems that it attenuates the pH-response of the functional groups such as the carboxylic group, leading to the reduction or even the loss of pH-responsiveness of the PEGylated liposomes.

Finally we examined the performance of PA/Chol/PEG-Chol liposomes for active loading of DOX. It is shown that DOX could be successfully loaded in the aqueous compartment of these LUVs with a conventional approach based on an ammonium sulfate gradient. A high drug

loading efficiency (84%) and a high drug to lipid ratio (0.06) were obtained, despite the much reduced bilayer permeability of these liposomes and the presence of interfacial PEG. The reported values are comparable to those reported for phospholipid liposomes.<sup>46</sup>

In conclusion, we described and characterized a novel ternary non phospholipid liposomes made of PA/Chol/PEG-Chol. It is shown that up to 20 mol % of PEG-Chol can be introduced in these non phospholipid sterol-rich liposomes without disturbing the lamellar phases. The presence of PEG, anchored using a cholesterol moiety, makes PA/Chol/PEG-Chol liposomes stable between pH 5 and 9.5. A very low permeability was obtained for encapsulated calcein and DOX. Active loading of DOX can be achieved by this ternary system. These distinctive properties suggest that PA/Chol/PEG-Chol liposomes possess an interesting potential as nanocarriers for delivery of drugs. Pharmacokinetics investigations of the circulation lifetime, the biodistribution and the targeting effects will be carried out in our future work.

## **5.6 Acknowledgements**

The authors thank the Natural Sciences and Engineering Research Council of Canada and the Fonds Québécois de la Recherche sur la Nature et les Technologies for the financial support. Z.-K. C is grateful to Université de Montréal and China Scholarship Council for his scholarship. We thank Cédric Malveau, Department of Chemistry, Université de Montréal, for his technical support during the NMR experiments.

## 5.7 References

1. Gregoriadis, G., Drug entrapment in liposomes. *FEBS Lett.* **1973**, *36*, 292-296.
2. Sawant, R. R.; Torchilin, V. P., Liposomes as 'smart' pharmaceutical nanocarriers. *Soft Matter* **2010**, *6*, 4026-4044.
3. Torchilin, V. P., Recent advances with liposomes as pharmaceutical carriers. *Nat. Rev. Drug Discov.* **2005**, *4*, 145-160.
4. Immordino, M. L.; Dosio, F.; Cattel, L., Stealth liposomes: review of the basic science, rationale, and clinical applications, existing and potential. *Int. J. Nanomed.* **2006**, *1*, 297-315.
5. Scherphof, G. L.; Dijkstra, J.; Spanjer, H. H.; Derksen, J. T. P.; Roerdink, F. H., Uptake and intracellular processing of targeted and nontargeted liposomes by rat kupffer cells *in vivo* and *in vitro*. *Ann. N.Y. Acad. Sci.* **1985**, *446*, 368-384.
6. Alving, C. R.; Wassef, N. M., Complement-dependent phagocytosis of liposomes: suppression by "stealth" lipids. *J. Liposome Res.* **1992**, *2*, 383-395.
7. Beaumier, P. L.; Hwang, K. J., Effects of liposome size on the degradation of bovine brain sphingomyelin cholesterol liposomes in the mouse liver. *Biochim. Biophys. Acta* **1983**, *731*, 23-30.
8. Damen, J.; Regts, J.; Scherphof, G., Transfer and exchange of phospholipid between small unilamellar liposomes and rat plasma high density lipoproteins dependence on cholesterol content and phospholipid composition. *Biochim. Biophys. Acta* **1981**, *665*, 538-545.
9. Patel, H. M.; Tuzel, N. S.; Ryman, B. E., Inhibitory effect of cholesterol on the uptake of liposomes by liver and spleen *Biochim. Biophys. Acta* **1983**, *761*, 142-151.
10. Roerdink, F. H.; Regts, J.; Handel, T.; Sullivan, S. M.; Baldeschwieler, J. D.; Scherphof, G. L., Effect of cholesterol on the uptake and intracellular degradation of liposomes by liver and spleen; a combined biochemical and  $\gamma$ -ray perturbed angular correlation study. *Biochim. Biophys. Acta* **1989**, *980*, 234-240.
11. Semple, S. C.; Chonn, A.; Cullis, P. R., Influence of cholesterol on the association of plasma proteins with liposomes. *Biochemistry* **1996**, *35*, 2521-2525.

12. Gabizon, A.; Papahadjopoulos, D., Liposome formulations with prolonged circulation time in blood and enhanced uptake by tumors. *Proc. Natl. Acad. Sci. U. S. A.* **1988**, *85*, 6949-6953.
13. Allen, T. M.; Hansen, C.; Rutledge, J., Liposomes with prolonged circulation times: factors affecting uptake by reticuloendothelial and other tissues. *Biochim. Biophys. Acta* **1989**, *981*, 27-35.
14. Maruyama, K.; Yuda, T.; Okamoto, A.; Ishikura, C.; Kojima, S.; Iwatsuru, M., Effect of molecular weight in amphipathic polyethyleneglycol on prolonging the circulation time of large unilamellar liposomes. *Chem. Pharm. Bull.* **1991**, *39*, 1620-1622.
15. Allen, T. M.; Hansen, C.; Martin, F.; Redemann, C.; Yauyoung, A., Liposomes containing synthetic lipid derivatives of poly (ethylene glycol) show prolonged circulation half-lives in vivo. *Biochim. Biophys. Acta* **1991**, *1066*, 29-36.
16. Drummond, D. C.; Meyer, O.; Hong, K.; Kirpotin, D. B.; Papahadjopoulos, D., Optimizing liposomes for delivery of chemotherapeutic agents to solid tumors. *Pharm. Rev.* **1999**, *51*, 691-743.
17. Rex, S.; Zuckermann, M. J.; Lafleur, M.; Silvius, J. R., Experimental and Monte Carlo simulation studies of the thermodynamics of polyethyleneglycol chains grafted to lipid bilayers. *Biophys. J.* **1998**, *75*, 2900-2914.
18. Allen, T. M., The use of glycolipids and hydrophilic polymers in avoiding rapid uptake of liposomes by the mononuclear phagocyte system. *Adv. Drug Deliv. Rev.* **1994**, *13*, 285-309.
19. Woodle, M. C., Surface-modified liposomes: assessment and characterization for increased stability and prolonged blood circulation. *Chem. Phys. Lipids* **1993**, *64*, 249-262.
20. Allen, T. M.; Mehra, T.; Hansen, C.; Chin, Y. C., Stealth liposomes an improved sustained release system for 1- $\beta$ -D-arabinofuranosylcytosine. *Cancer Res.* **1992**, *52*, 2431-2439.
21. Papahadjopoulos, D.; Allen, T. M.; Gabizon, A.; Mayhew, E.; Matthay, K.; Huang, S. K.; Lee, K. D.; Woodle, M. C.; Lasic, D. D.; Redemann, C.; Martin, F. J., Sterically stabilized liposomes: improvements in pharmacokinetics and antitumor therapeutic efficacy. *Proc. Natl. Acad. Sci. U. S. A.* **1991**, *88*, 11460-11464.
22. Bedu-Addo, F. K.; Huang, L., Interaction of PEG-phospholipid conjugates with phospholipid: implications in liposomal drug delivery. *Adv. Drug Deliv. Rev.* **1995**, *16*, 235-247.

23. Bedu-Addo, F. K.; Tang, P.; Xu, Y.; Huang, L., Effects of polyethyleneglycol chain length and phospholipid acyl chain composition on the interaction of polyethyleneglycol-phospholipid conjugates with phospholipid: implications in liposomal drug delivery. *Pharm. Res.* **1996**, *13*, 710-717.
24. Webb, M. S.; Saxon, D.; Wong, F. M. P.; Lim, H. J.; Wang, Z.; Bally, M. B.; Choi, L. S. L.; Cullis, P. R.; Mayer, L. D., Comparison of different hydrophobic anchors conjugated to poly(ethylene glycol): effects on the pharmacokinetics of liposomal vincristine. *Biochim. Biophys. Acta* **1998**, *1372*, 272-282.
25. Ishiwata, H.; Vertut-Doi, A.; Hirose, T.; Miyajima, K., Physical-chemistry characteristics and biodistribution of poly(ethylene glycol)-coated liposomes using poly(oxyethylene) cholesteryl ether. *Chem. Pharm. Bull.* **1995**, *43*, 1005-1011.
26. VertutDoi, A.; Ishiwata, H.; Miyajima, K., Binding and uptake of liposomes containing a poly(ethylene glycol) derivative of cholesterol (stealth liposomes) by the macrophage cell line J774: influence of PEG content and its molecular weight. *Biochim. Biophys. Acta* **1996**, *1278*, 19-28.
27. Zhao, X. B.; Muthusamy, N.; Byrd, J. C.; Lee, R. J., Cholesterol as a bilayer anchor for PEGylation and targeting ligand in folate-receptor-targeted liposomes. *J. Pharm. Sci.* **2007**, *96*, 2424-2435.
28. Yang, D. B.; Zhu, J. B.; Huang, Z. J.; Ren, H. X.; Zheng, Z. J., Synthesis and application of poly(ethylene glycol)-cholesterol (Chol-PEG(m)) conjugates in physicochemical characterization of nonionic surfactant vesicles. *Colloid Surf., B* **2008**, *63*, 192-199.
29. Sant, V. P.; Nagarsenker, M. S., Synthesis of monomethoxypolyethyleneglycol-cholesteryl ester and effect of its incorporation in liposomes. *AAPS Pharm. Sci. Tech.* **2011**, *12*, 1056-1063.
30. Beugin, S.; Edwards, K.; Karlsson, G.; Ollivon, M.; Lesieur, S., New sterically stabilized vesicles based on nonionic surfactant, cholesterol, and poly(ethylene glycol)-cholesterol conjugates. *Biophys. J.* **1998**, *74*, 3198-3210.
31. Miller, C. R.; Bondurant, B.; McLean, S. D.; McGovern, K. A.; O'Brien, D. F., Liposome-cell interactions in vitro: effect of liposome surface charge on the binding and endocytosis of conventional and sterically stabilized liposomes. *Biochemistry* **1998**, *37*, 12875-12883.

32. Parr, M. J.; Ansell, S. M.; Choi, L. S.; Cullis, P. R., Factors influencing the retention and chemical stability of poly(ethylene glycol)-lipid conjugates incorporated into large unilamellar vesicles. *Biochim. Biophys. Acta* **1994**, *1195*, 21-30.
33. Cui, Z.-K.; Bastiat, G.; Jin, C.; Keyvanloo, A.; Lafleur, M., Influence of the nature of the sterol on the behavior of palmitic acid/sterol mixtures and their derived liposomes. *Biochim. Biophys. Acta* **2010**, *1798*, 1144-1152.
34. Phoeung, T.; Aubron, P.; Rydzek, G.; Lafleur, M., pH-triggered release from nonphospholipid LUVs modulated by the pKa of the included fatty acid. *Langmuir* **2010**, *26*, 12769-12776.
35. Bastiat, G.; Oligier, P.; Karlsson, G.; Edwards, K.; Lafleur, M., Development of non-phospholipid liposomes containing a high cholesterol concentration. *Langmuir* **2007**, *23*, 7695-7699.
36. Bastiat, G.; Lafleur, M., Phase behavior of palmitic acid/cholesterol/cholesterol sulfate mixtures and properties of the derived liposomes. *J. Phys. Chem. B* **2007**, *111*, 10929-10937.
37. Phoeung, T.; Morfin Huber, L.; Lafleur, M., Cationic detergent/sterol mixtures can form fluid lamellar phases and stable unilamellar vesicles. *Langmuir* **2009**, *25*, 5778-5784.
38. Cui, Z.-K.; Bouisse, A.; Cottenye, N.; Lafleur, M., Formation of pH-sensitive cationic non phospholipid liposomes with monoalkylated primary amine and cholesterol. *Langmuir* **2012**, *28*, 13668-13674.
39. Cui, Z.-K.; Bastiat, G.; Lafleur, M., Formation of fluid lamellar phase and large unilamellar vesicles with octadecyl methyl sulfoxide/cholesterol mixtures. *Langmuir* **2010**, *26*, 12733-12739.
40. Thomas, A. M.; Kapanen, A. I.; Hare, J. I.; Ramsay, E.; Edwards, K.; Karlsson, G.; Bally, M. B., Development of a liposomal nanoparticle formulation of 5-Fluorouracil for parenteral administration: formulation design, pharmacokinetics and efficacy. *J. Control. Release* **2011**, *150*, 212-219.
41. Young, R. C.; Myers, R. F. O. C. E., The anthracycline antineoplastic drugs. *N. Engl. J. Med.* **1981**, *305*, 139-153.
42. Bouma, J.; Beijnen, J. H.; Bult, A.; Underberg, W. J. M., Anthracycline antitumour agents. A review of physicochemical, analytical and stability properties. *Pharm. Weekblad* **1986**, *8*, 109-133.

43. Gabizon, A.; Dagan, A.; Goren, D.; Barenholz, Y.; Fuks, Z., Liposomes as in vivo carriers of adriamycin: reduced cardiac uptake and preserved antitumor activity in mice. *Cancer Res.* **1982**, *42*, 4734-4739.
44. Harrington, K. J.; Syrigos, K. N.; Vile, R. G., Uposomally targeted cytotoxic drugs for the treatment of cancer. *J. Pharm. Pharmacol.* **2002**, *54*, 1573-1600.
45. Mayer, L. D.; Tai, L. C. L.; Ko, D. S. C.; Masin, D.; Ginsberg, R. S.; Cullis, P. R.; Bally, M. B., Influence of vesicle size, lipid composition, and drug-to-lipid ratio on the biological-activity of liposomal doxorubicin in mice *Cancer Res.* **1989**, *49*, 5922-5930.
46. Haran, G.; Cohen, R.; Bar, L. K.; Barenholz, Y., Transmembrane ammonium sulfate gradients in liposomes produce efficient and stable entrapment of amphipathic weak bases. *Biochim. Biophys. Acta* **1993**, *1151*, 201-215.
47. Tanner, J. E., Use of the stimulated echo in NMR diffusion studies. *J. Chem. Phys.* **1970**, *52*, 2523-2526.
48. Almgren, M.; Edwards, K.; Karlsson, G., Cryo transmission electron microscopy of liposomes and related structures. *Colloids Surf., A* **2000**, *174*, 3-21.
49. Allen, T. M., Calcein as a tool in liposome methodology. In *Liposome technology*, Gregoriadis, G., Ed. CRC Press: Boca Raton, FC, 1984; pp 177-182.
50. Benachir, T.; Lafleur, M., Study of vesicle leakage induced by melittin. *Biochim. Biophys. Acta* **1995**, *1235*, 452-460.
51. Paré, C.; Lafleur, M., Formation of liquid ordered lamellar phases in the palmitic acid/cholesterol system. *Langmuir* **2001**, *17*, 5587-5594.
52. Vist, M. R.; Davis, J. H., Phase equilibria of cholesterol/dipalmitoylphosphatidylcholine mixtures: <sup>2</sup>H nuclear magnetic resonance and differential scanning calorimetry. *Biochemistry* **1990**, *29*, 451-464.
53. Lafleur, M.; Cullis, P. R.; Bloom, M., Modulation of the orientational order profile of the lipid acyl chain in the L $\alpha$ -alpha phase. *Eur. Biophys. J.* **1990**, *19*, 55-62.
54. Davis, J. H., Deuterium magnetic resonance study of the gel and liquid crystalline phases of dipalmitoyl phosphatidylcholine. *Biophys. J.* **1979**, *27*, 339-358.
55. Henriksen, J.; Rowat, A. C.; Brief, E.; Hsueh, Y. W.; Thewalt, J. L.; Zuckermann, M. J.; Ipsen, J. H., Universal behavior of membranes with sterols. *Biophys. J.* **2006**, *90*, 1639-1649.

56. Ouimet, J.; Croft, S.; Pare, C.; Katsaras, J.; Lafleur, M., Modulation of the polymorphism of the palmitic acid/cholesterol system by the pH. *Langmuir* **2003**, *19*, 1089-1097.
57. Soderman, O.; Stilbs, P., NMR-studies of complex surfactant systems. *Prog. Nucl. Magn. Reson. Spectrosc.* **1994**, *26*, 445-482.
58. Leal, C.; Rognvaldsson, S.; Fossheim, S.; Nilssen, E. A.; Topgaard, D., Dynamic and structural aspects of PEGylated liposomes monitored by NMR. *J. Coll. Interf. Sci.* **2008**, *325*, 485-493.
59. El Jastimi, R.; Lafleur, M., A dual-probe fluorescence method to examine selective perturbation of membrane permeability by melittin. *Biospectroscopy* **1999**, *5*, 133-140.
60. Yoshida, A.; Hashizaki, K.; Yamauchi, H.; Sakai, H.; Yokoyama, S.; Abe, M., Effect of lipid with covalently attached poly(ethylene glycol) on the surface properties of liposomal bilayer membranes. *Langmuir* **1999**, *15*, 2333-2337.
61. Fritze, A.; Hens, F.; Kimpfler, A.; Schubert, R.; Peschka-Suss, R., Remote loading of doxorubicin into liposomes driven by a transmembrane phosphate gradient. *Biochim. Biophys. Acta* **2006**, *1758*, 1633-1640.
62. Mayer, L. D.; Bally, M. B.; Cullis, P. R., Strategies for optimizing liposomal doxorubicin. *J. Liposome Res.* **1990**, *1*, 463-480.
63. Amselem, S.; Cohen, R.; Druckmann, S.; Gabizon, A.; Abra, R. M.; Huang, A.; New, R.; Barnholz, Y., Preparation and characterization of liposomal doxorubicin for human use. *J. Liposome Res.* **1992**, *2*, 93-123.
64. Mui, B. L.-S.; Döbereiner, H.-G.; Madden, T. D.; Cullis, P. R., Influence of transbilayer area asymmetry on the morphology of large unilamellar vesicles. *Biophys. J.* **1995**, *69*, 930-941.
65. Lipowsky, R., The conformation of membranes. *Nature* **1991**, *349*, 475-481.
66. Sriwongsitanont, S.; Ueno, M., Physicochemical properties of PEG-grafted liposomes. *Chem. Phar. Bull.* **2002**, *50*, 1238-1244.
67. Tirosh, O.; Barenholz, Y.; Katzhendler, J.; Prievo, A., Hydration of polyethylene glycol-grafted liposomes. *Biophys. J.* **1998**, *74*, 1371-1379.
68. Volke, F.; Eisenblätter, S.; Galle, J.; Klose, G., Dynamic properties of water at phosphatidylcholine lipid-bilayer surfaces as seen by deuterium and pulsed field gradient proton NMR. *Chem. Phys. Lipids* **1994**, *70*, 121-131.

69. Hong, M. S.; Lim, S. J.; Oh, Y. K.; Kim, C. K., pH-sensitive, serum-stable and long-circulating liposomes as a new drug delivery system. *J. Pharm. Pharmacol.* **2002**, *54*, 51-58.
70. Thewalt, J. L.; Bloom, M., Phosphatidylcholine: cholesterol phase diagrams. *Biophys. J.* **1992**, *63*, 1176-1181.
71. Bloom, M.; Evans, E.; Mouritsen, O. G., Physical properties of the fluid lipid-bilayer component of cell membranes: a perspective. *Q. Rev. Biophys.* **1991**, *24*, 293-397.
72. Needham, D.; McIntosh, T. J.; Evans, E., Thermomechanical and transition properties of dimyristoylphosphatidylcholine/cholesterol bilayers. *Biochemistry* **1988**, *27*, 4668-4673.
73. Slepishkin, V. A.; Simoes, S.; Dazin, P.; Newman, M. S.; Guo, L. S.; deLima, M. C. P.; Duzgunes, N., Sterically stabilized pH-sensitive liposomes - intracellular delivery of aqueous contents and prolonged circulation in vivo. *J. Biol. Chem.* **1997**, *272*, 2382-2388.

## Chapter 6

### Conclusions and Future Perspectives

This work provided us with a deeper understanding of the prerequisites for the formation of lo lamellar phases by mixtures of monoalkylated amphiphiles and sterols, and on the properties of the derived Sterosomes. This study allowed us to design functionalized Sterosomes with desired properties for specific applications.

#### 6.1 New Sterosome formulations

In the present thesis, the Sterosome family was extended with several new formulations. Four different sterols (dihydrocholesterol, 7-dehydrocholesterol, stigmastanol, and stigmasterol), were found to form LUVs with PA. The resulting LUVs displayed different extent of permeability (Chapter 2). Complete neutral Sterosomes were first crafted with OMSO and Chol (Chapter 3). The designed dual functionalized Sterosomes with a positive surface charge, and pH-sensitivity were formulated with SA and Chol (Chapter 4). The last new formulation was the PA/Chol LUVs whose interface was modified with cholesterol-anchored PEG (Chapter 5).

## **6.2 Novel discovery and developments**

Prior to this thesis, a few Sterosome formulations with extremely low permeability had been reported, such as PA/Chol,<sup>1</sup> PA/Schol,<sup>2</sup> and CPC/Schol.<sup>3</sup> pH-sensitive Sterosomes were only formulated with PA and its derivatives.<sup>4</sup> In this thesis, we have extended the identification of molecular prerequisites, and gained a deeper understanding of intermolecular interactions leading to these self-assemblies, through the research on the new Sterosome formulations.

The nature of the sterols had significant effects on the formation of lo lamellar phases. All the sterols studied in this thesis were able to order the alkyl chains. However, sterols bearing a non-bulky alkyl tail chains led to a tighter chain packing in the bilayers.<sup>5</sup> This molecular feature played a more important role than the details of the ring network on the propensities to form lo lamellar phases, on the stability and the permeability of the resulting Sterosomes.<sup>5</sup> The half-time of calcein release was 20, 30, and 70 days for PA/stigmasterol, PA/stigmastanol, and PA/7-dehydrocholesterol, respectively.<sup>5</sup> This finding made the PA/sterol Sterosomes versatile from the passive release point of view; one can modulate the rate of passive leakage simply by changing the sterol in the mixture.

All the PA/sterol Sterosomes displayed similar pH-sensitivity.<sup>5</sup> No significant differences were observed from the different nature of the sterols, an additional evidence that the pH sensitivity is directly dictated by the protonation state of the carboxylic group, dictating the surface charge density. Negatively charged PA/sterol Sterosomes were stable, due to the electrostatic interactions favoring the lipid mixing and the suitable hydration of the interface.

Using a similar strategy, a primary amine group was introduced to form Sterosomes.<sup>6</sup> The protonated ammonium group provided the LUVs a positive charge and stability. pH-triggered release was achieved with the deprotonation of amine group, leading to a neutral surface.

The project of OMSO/Chol<sup>7</sup> mixture shed new light on understanding the intermolecular interactions within these self-assemblies. It was proposed that a strong hydrogen bond network involving the sulfoxide group, the hydroxyl group of cholesterol, and the surrounding water molecules promoted the mixing of the two neutral species, favored the hydration of the interface, and as a consequence, led to the formation of lo lamellar phase. It appeared, however, that H-bonds did not provide the same stability as interfacial charges and the lo bilayers were found to exist in a metastable state. This metastable phase, however, allowed extruding the mixture at room temperature to form LUVs. Surprisingly, the LUVs appeared to still exist even after the solidification of both species. The encapsulated calcein remained inside these “solid” LUVs for more than three months. A temperature–composition diagram was proposed to summarize the phase behavior of this neutral system (Figure 3.7).

Preliminary experiments were performed on the intravenous administration with the initial PA/Chol Sterosomes. Unfortunately, they were cleared very rapidly from the blood circulation despite the high content cholesterol in the formulation. Efforts have been devoted to develop this formulation to “stealth” Sterosomes, by anchoring PEG at the LUV interface using a cholesterol moiety. A systematic characterization was performed on these ternary mixtures. It is found that up to 20 mol % PEG-Chol can be introduced in the membrane without disturbing the bilayer structure. With the inclusion of 7 mol % PEG-Chol, stable lo phases are observed even at

low pH, contrasting with the phase separation observed for PA and Chol mixtures under the same conditions. The presence of PEG at the interface has no significant impact of the permeability, but inhibits the pH-sensitivity of the formulation. These phenomena are similar to those observed in phospholipid bilayers with PEG.<sup>8</sup> Active-loading of anti-cancer drug, DOX, is successful, despite the much reduced bilayer permeability of these liposomes and the presence of interfacial PEG. A high drug loading efficiency (84%) and a high drug to lipid ratio (0.06) have been obtained. These values are important for the application in drug delivery.

### **6.3 Suggestions for future work**

During this work, it was found that the presence of high valence ions affected the formation process of vesicles — a finding not included in the thesis. However, once the Sterosomes were formed, their influence on the liposome stability was drastically reduced or even disappeared. Up to now, the origin of their impact remains unclear, and therefore, it would be a very interesting project to examine the behavior of these non phospholipid liposomes in the presence of high valence ions. For example, one can study the affinity of different high valence ions, such as  $\text{PO}_4^{3-}$  and  $\text{SO}_4^{2-}$ , to various monoalkylated amphiphiles, sterols, and examine whether these ions induce phase separations that would be unfavorable to the formation of fluid lamellar self-assemblies.

The exchange of molecules in such condensed membranes is not characterized. The exchange of amphiphilic molecules between membranes, between a membrane and the monomers or the micelles in the milieu, and between leaflets, has an influence on the bilayer

structure and the functionality of biomembranes. Studies on the exchange of molecules in phospholipid vesicles have been carried out.<sup>9, 10</sup> However the impact of chain packing on these processes is not defined. It would be valuable contribution to study molecular exchange on our Sterosome systems as they are among the lamellar systems with the highest chain packing. These studies could highlight some physicochemical control of these dynamics and if it turns out to be significant, it would be interesting to investigate if it also plays a role in plasmic membranes.

The deformability and the viscoelasticity in biological membranes control many biological functions, e.g., the rather unique micromechanical properties of red blood cells allow them to go through capillaries.<sup>11</sup> It was shown that the inclusion of cholesterol had significant impact on the micromechanical properties of the membrane.<sup>12</sup> Generally, the more cholesterol in the membrane, the stiffer it becomes. Because of the high content of sterols in Sterosome membranes, it is of interest to explore the micromechanical properties of bilayers with such highly ordered chains.

In light of this work, other functionalized formulations can be designed and crafted. For example, photosensitive amphiphiles can be introduced in Sterosomes to provide nanocarriers with limited passive permeability and light-triggered release. Pharmacokinetics *in vivo* tests with PEGylated Sterosomes should be conducted to determine their circulation time in the blood stream, the permeability and biodistribution of encapsulated drugs. Some anti-cancer drugs, such as 5-FU,<sup>13</sup> could not be trapped efficiently in conventional phospholipid liposomes. Therefore, it is worthy to evaluate the retention of those challenging drugs in our Sterosomes.

From the application point of view, our Sterosomes could be valuable candidates as nanocarriers for active ingredients in many fields. The amphiphiles used in Sterosomes have a relatively low cost, and are more stable for storage compared to conventional phospholipids. Doxorubicin-loaded liposomes were the very first nanocarrier formulation approved by the US FDA and the European Medicines Agency (EMA) as cancer therapeutics. This formulation improved the quality of life of cancer patients. In an analogous way, our Sterosomes, with their distinct properties, may eventually be employed as active-ingredient carriers in many fields (Figure 6.1), including cosmetics, foods, textiles, etc. With future bioengineering application developments, Sterosomes may contribute to improve our live quality.

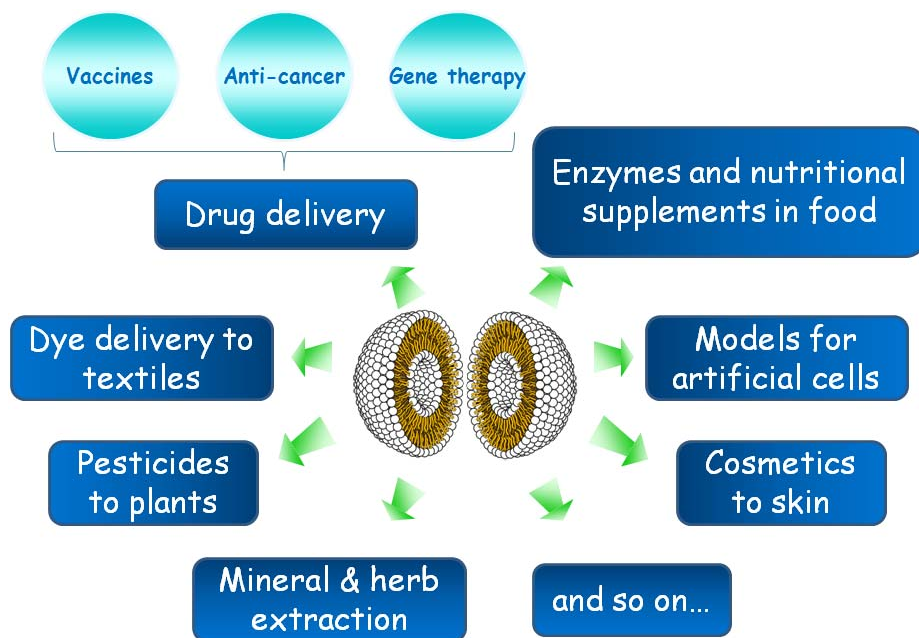


Figure 6.1. Sterosome potential applications in different fields.

## 6.4 References

1. Bastiat, G.; Oliger, P.; Karlsson, G.; Edwards, K.; Lafleur, M., Development of non-phospholipid liposomes containing a high cholesterol concentration. *Langmuir* **2007**, *23*, 7695-7699.
2. Bastiat, G.; Lafleur, M., Phase behavior of palmitic acid/cholesterol/cholesterol sulfate mixtures and properties of the derived liposomes. *J. Phys. Chem. B* **2007**, *111*, 10929-10937.
3. Phoeung, T.; Morfin Huber, L.; Lafleur, M., Cationic detergent/sterol mixtures can form fluid lamellar phases and stable unilamellar vesicles. *Langmuir* **2009**, *25*, 5778-5784.
4. Phoeung, T.; Aubron, P.; Rydzek, G.; Lafleur, M., pH-triggered release from nonphospholipid LUVs modulated by the pKa of the included fatty acid. *Langmuir* **2010**, *26*, 12769-12776.
5. Cui, Z.-K.; Bastiat, G.; Jin, C.; Keyvanloo, A.; Lafleur, M., Influence of the nature of the sterol on the behavior of palmitic acid/sterol mixtures and their derived liposomes. *Biochim. Biophys. Acta* **2010**, *1798*, 1144-1152.
6. Cui, Z.-K.; Bouisse, A.; Cottenye, N.; Lafleur, M., Formation of pH-sensitive cationic liposomes from a binary mixture of monoalkylated primary amine and cholesterol. *Langmuir* **2012**, *28*, 13668-13674.
7. Cui, Z.-K.; Bastiat, G.; Lafleur, M., Formation of fluid lamellar phase and large unilamellar vesicles with octadecyl methyl sulfoxide/cholesterol mixtures. *Langmuir* **2010**, *26*, 12733-12739.
8. Hong, M. S.; Lim, S. J.; Oh, Y. K.; Kim, C. K., pH-sensitive, serum-stable and long-circulating liposomes as a new drug delivery system. *J. Pharm. Pharmacol.* **2002**, *54*, 51-58.
9. Needham, D.; Zhelev, D. V., Lysolipid exchange with lipid vesicle membranes. *Ann. Biomed. Eng.* **1995**, *23*, 287-298.
10. Zhu, T.; Jiang, Z.; Ma, Y., Lipid exchange between membranes: Effects of membrane surface charge, composition, and curvature. *Colloids Surf., B* **2012**, *97*, 155-161.
11. Mohandas, N.; Chasis, J. A., Red blood cell deformability, membrane material properties and shape: regulation by transmembrane, skeletal and cytosolic proteins and lipids. *Semin. Hematol.* **1993**, *30*, 171-192.

12. Pan, J. J.; Tristram-Nagle, S.; Nagle, J. F., Effect of cholesterol on structural and mechanical properties of membranes depends on lipid chain saturation. *Phys. Rev. E* **2009**, *80*, 021931.
13. Thomas, A. M.; Kapanen, A. I.; Hare, J. I.; Ramsay, E.; Edwards, K.; Karlsson, G.; Bally, M. B., Development of a liposomal nanoparticle formulation of 5-Fluorouracil for parenteral administration: Formulation design, pharmacokinetics and efficacy. *J. Control. Release* **2011**, *150*, 212-219.